Chromatin architecture and the orchestration of gene expression: cell systems to explore epigenetic gene control

Brink, M.C.

Publication date
2009

Document Version
Final published version

Chromatin Architecture and the Orchestration of Gene Expression

Cell systems to explore epigenetic gene control

Maartje Carolien Brink

2009

CHROMATIN ARCHITECTURE AND THE ORCHESTRATION OF GENE EXPRESSION

CELL SYSTEMS TO EXPLORE EPIGENETIC GENE CONTROL

ACADEMISCH PROEFSCHRIFT

ter verkrijging van de graad van doctor
aan de Universiteit van Amsterdam
op gezag van de Rector Magnificus
prof. dr. D.C. van den Boom
ten overstaan van een door het college voor promoties ingestelde
commissie, in het openbaar te verdedigen in de Agnietenkapel

op donderdag 2 april 2009, te 10:00 uur

door

Maartje Carolien Brink

geboren te Chertsey, Verenigd Koninkrijk

Promotiecommissie

Promotor:	prof. dr. R. van Driel
Co-promotor:	dr. P. J. Verschure
Overige leden:	prof. dr. A. S. Belmont
	prof. dr. R. Versteeg
	prof. dr. C. J. van Noorden
	dr. W. Vermeulen
	dr. J. van der Vlag

Faculteit der Natuurwetenschappen, Wiskunde en Informatica

PhD thesis, University of Amsterdam
Cover image: Het Concertgebouw, Amsterdam (photograph by Leander Lammertink)
Printed by Ipskamp Drukkers B.V., Enschede

The printing of this thesis was financially supported by NWO (Nederlandse Organisatie voor Wetenschappelijk Onderzoek), J.E. Jurriaanse Stichting and SEN (Stichting tot Bevordering van de Electronenmicroscopie in Nederland).

The research described in this thesis was carried out at the Swammerdam Institute for Life Sciences, Nuclear Organisation Group, University of Amsterdam, Kruislaan 318, 1098 SM, Amsterdam, The Netherlands. This project was funded by the Netherlands Organisation for Scientific Research (NWO), Vernieuwingsimpuls VIDI (2003/03921/ALW/016.041.311).

"Back off, man. I'm a scientist."

Dr. Peter Venkman
(Ghostbusters, 1984)

Contents

Chapter 1

Introduction

Maartje C. Brink & Pernette J. Verschure

Introduction

The functional organization of nuclear architecture

The eukaryotic cell is faced with the challenge of packaging its genetic material in the nucleus while maintaining accessibility of its genes for DNA-associated processes. The answer that evolution has come up with is both elegant and effective: the genetic material is functionally organized as chromatin. Efficient folding of the about two meters of DNA inside the nucleus, which is only 10-20 μm in diameter, occurs by wrapping the DNA around an octamer of histone proteins, forming a 10 nm diameter fiber (Carter, 1978; Finch *et al.*, 1977; Kornberg, 1977; Luger *et al.*, 1997). Coiling of this fiber results in a compacted fiber of 30 nm diameter, which is folded further in an unknown way. The ensemble of DNA and proteins constituting chromatin plays an essential role in transcriptional regulation. Detailed understanding of the molecular systems that underlie the functional architecture of chromatin, both at the nucleosomal and the higher-order level (*i.e.* above the 30 nm fiber), remains elusive. Current research in this field is focused on uncovering the molecular mechanisms that are responsible for the dynamic higher-order structure of chromatin, controlling gene expression.

In order to orchestrate the level and timing of the expression of thousands of genes, the eukaryotic genome employs various methods of regulation. The most direct type of regulation is found at the DNA sequence level, by the interaction between transcription factors and regulatory sequences. Functionally related genes are sometimes clustered on the linear genome so they can be coregulated, as can be seen for the HoxB and β-globin loci for example (Chambeyron and Bickmore, 2004; Tolhuis *et al.*, 2002). Additionally, gene clusters of unrelated function were also identified on a genome-wide scale by integrating the human genome map with messenger RNA expression data (Caron *et al.*, 2001). The resulting human transcriptome map revealed the existence of genomic stretches of several mega basepairs containing functionally unrelated genes with similar levels of transcriptional activity. Regions of increased gene expression (ridges) and low gene expression (anti-ridges) were identified on the human genome (Lercher *et al.*, 2002; Versteeg *et al.*, 2003). Interestingly, insertion of a GFP reporter gene within a ridge resulted in an average fourfold upregulation of the GFP transcription compared to integration in an anti-ridge, demonstrating the importance of local genomic organization at the linear DNA sequence level (Gierman *et al.*, 2007).

Another form of gene regulation occurs at the level of the higher-order folding of chromatin, *i.e.* above the 30 nm fiber. On the basis of classic cytological studies, the genome can be divided into two major types of chromatin: compact and open chromatin, named heterochromatin and euchromatin, respectively. These types of chromatin are considered to reflect gene activity: the often gene-poor heterochromatin domains are generally compact and transcriptionally silent, while gene-rich

euchromatin consists of open, transcribed chromatin domains (Felsenfeld and Groudine, 2003). However, more recent data suggest that a more subtle discrimination between the functionality of compact and less compact chromatin domains should be made. Using sucrose gradient sedimentation, chromatin fibers were separated based on their compactness, demonstrating that transcriptionally active as well as inactive sites are found in both such compact and less compact isolated chromatin fibers (Gilbert *et al.*, 2004). In addition, Gilbert and colleagues (2004) found that less compact chromatin fibers are more gene dense than compact chromatin fibers. These *in vitro* results indicate that the distinction between heterochromatin and euchromatin is complex and probably based on more parameters than transcriptional activity alone.

An interesting feature of chromosome architecture is the existence of chromosome territories (CTs) in interphase nuclei (for a review, see Cremer and Cremer, 2001). According to fluorescent *in situ* hybridization (FISH) experiments, each chromosome occupies a distinct territory within the nucleus that was initially thought not to be intruded by other chromosomes (Cremer *et al.*, 1993). However, upon increasing resolution by imaging 150 nm thick cryosections (cryo-FISH) with the electron microscope, some intermingling between adjacent chromosomes was demonstrated (Branco and Pombo, 2006). CTs consist of domains of different degrees of compaction: 100-500 nm domains are surrounded by interchromatin areas containing little or no chromatin (Cremer *et al.*, 2004). Active transcription sites can be found throughout the CT near the surface of the compact subchromosomal domains (Fakan, 1994; Fakan and van Driel, 2007; Verschure *et al.*, 1999). An interesting finding is that, upon transcriptional activation, genomic loci may loop out, away from their CT (Mahy *et al.*, 2002a; Volpi *et al.*, 2000). A striking example of looping of transcriptionally active genes was found for the HoxB locus (Chambeyron and Bickmore, 2004). Here, induction of the genes within the cluster caused sequential looping out of the CT, in the same order as their transcriptional activation. Furthermore, introduction of the human β-globin locus control region (LCR) into a gene-dense region of the mouse genome caused transcriptional upregulation combined with more frequent positioning away from the CT (Noordermeer *et al.*, 2008). These findings argue that transcription occurs near the surface of the compact chromatin domains, possibly on chromatin that loops out into the interchromatin domain. It should be noted however, that looping is not necessary to enable transcription of a chromatin fiber, since transcriptionally active genes can also be situated inside a CT (Mahy *et al.*, 2002b; Verschure *et al.*, 1999).

The spatial organization of chromatin in the nucleus may also play a role in gene regulation. For instance, in some cell types gene-poor chromatin is clustered at the periphery of the cell nucleus. This has been illustrated by FISH experiments, demonstrating that in human primary lymphocytes and lymphoblasts, the gene-poor chromosome 18 is positioned more to the periphery of the nucleus than the gene-rich chromosome 19 (Croft *et al.*, 1999). Furthermore, Goetze *et al.* (2007a) demonstrated

in five different human cell lines that certain gene-rich, highly expressed ridges are generally located more towards the nuclear interior than certain gene-sparse, low expressed anti-ridges of the same chromosomes. This radial positioning of chromosomal (sub)domains leads to compartmentalization of the nucleus, resulting in a gene-rich, transcriptionally active interior. However, radial positioning of chromosomes according to gene density seems to be restricted to specific cell types. In human skin fibroblasts for instance, chromosome size rather than gene content dictates radial positioning (Bolzer *et al.*, 2005). Approaching the issue of radial positioning from a different perspective, Guelen *et al.* (2008) identified genomic regions that are naturally recruited to the nuclear periphery in human lung fibroblasts, using the DNA adenine methyltransferase (Dam) ID technique. The authors demonstrated that these lamina-associated genomic domains are generally gene poor and depleted of RNAPII, allowing little transcriptional activity (Guelen *et al.*, 2008). Taken together, these data suggest a model in which gene-poor inactive chromatin is located more towards the periphery of the nucleus in some cell types, whereas transcriptionally active chromatin is more concentrated in the center of the nucleus.

Whether positioning of genes near the nuclear periphery is caused or influenced by the transcriptional status, has been addressed in several recent studies using a bacterial lactose (lac) operator integrated into mammalian chromatin (Robinett *et al.*, 1996). Because of the high affinity of the bacterial lac repressor (lacR) for the lac operator (lacO), proteins fused to the lacR can be effectively targeted to an integrated lacO repeat (Robinett *et al.*, 1996). By fusing lacR to a lamin-interacting protein, a lacO locus could be targeted to the nuclear lamina (Finlan *et al.*, 2008; Kumaran and Spector, 2008; Reddy *et al.*, 2008). Finlan *et al.* (2008) demonstrated that transcription of some, but not all, of the endogenous genes located in or near the targeted site was suppressed. Yet another study showed that after targeting of a chromosome arm containing a lacO repeat and a reporter gene to the nuclear periphery, transcription of the reporter gene could be induced (Kumaran and Spector, 2008). These data indicate that the nuclear domain close to the lamina, *i.e.* the nuclear periphery, is primarily a region harbouring repressed genes, but that gene expression can be induced, suggesting a complex functional relationship between nuclear localization and gene regulation. Taken together, it has become clear that the spatial organization of chromatin in the nucleus is functionally linked to the transcriptional status of chromatin, although the molecular mechanisms remain to be uncovered.

Epigenetic regulation: the orchestration of gene expression

The insight that not only the genetic code but also other factors, such as chromatin architecture, influence transcriptional activity has led to many questions regarding the extent and mechanisms of this regulation. The field of epigenetics focuses on identifying these factors and unraveling their mechanistic role in genome regulation. Over the past decade a large number of studies has furthered our understanding of

epigenetic gene regulation and a view has emerged in which chromatin is the key player. As reviewed by Taverna and colleagues (2007), histone- and DNA-modifying proteins can heritably change gene expression by covalently adding or removing methyl groups on DNA and/or a variety of chemical groups on the histone proteins of chromatin, most notably phosphate, methyl, ubiquitin and acetyl groups. The interplay of histone modifications in controlling genome activity is often referred to as the 'histone code' (Jenuwein and Allis, 2001; Turner, 2007). The histone code is thought to mark parts of the genome as eligible for transcription or for repression. Exactly how this is encoded is still largely unknown, but two models are currently considered (Taverna *et al.*, 2007). The first is a 'direct' model in which specific histone modifications, including phosphorylation and acetylation, change the positive histone charge thereby disturbing interactions with the negatively charged phosphate groups of DNA. These altered interactions induce conformational changes in chromatin structure, rendering it more compatible with transcription. The second 'effector-mediated' model depends on the existence of effector proteins that translate the histone code into meaningful downstream events. For instance, specific methylated sites of histones are recognized by proteins containing a chromodomain, such as heterochromatin protein 1 (HP1; Bannister *et al.*, 2001). Acetylated sites are recognized by bromodomains and several phosphorylated sites by 14-3-3 proteins (Kouzarides, 2007). These effector proteins can in turn recruit transcription factors and/or chromatin remodeling complexes, affecting changes in transcription.

However, the histone code functions in a more complex way than a simple standard conversion from an epigenetic mark to the gene expression state. For instance, the location of the modification in the promoter or coding region of a gene exerts a different effect on the transcriptional state. Histone 3 lysine 9 methylation has a negative effect on transcription when present at the promoter region, but when present throughout the coding region of genes it is associated with transcriptional elongation through the recruitment of HP1γ (Vakoc *et al.*, 2005). The same epigenetic mark may therefore lead to a different response, depending on its location.

Furthermore, the abundance of available histone modifications presents the possibility for a vast array of transcriptional responses as a result of epigenetic cross-talk. For instance, opposing histone modifications may be present at the same time on a single regulatory site. The existence of these so-called bivalent chromatin domains, containing both active and repressive marks simultaneously, forms a particularly challenging puzzle (Azuara *et al.*, 2006; Bernstein *et al.*, 2006). The enrichment of these opposing histone modifications in mouse embryonic stem cells is present on chromatin regions that are mostly silent. Upon differentiation, the cells preserve only one of the two histone modifications and change gene expression levels accordingly, dependent on the cell type (Bernstein *et al.*, 2006). Supposedly, the function of these opposing histone modifications is to poise the genetic locus, preparing it for transcription, but not yet activating it.

One approach to unraveling the complex interplay between epigenetic marks is through the characterization of the proteins that interact with chromatin. By interfering with the protein of interest, its effect on epigenetic modifications, chromatin structure and transcriptional status can be deduced. For example, HP1 protein function was inhibited by means of a dominant-negative approach to characterize the function of HP1 in maintaining heterochromatin structure. HP1 binds to histone H3 methylated at lysine 9, present in silent chromatin such as mouse chromocenters. By over-expressing a chromodomain-deficient HP1 mutant, we depleted HP1 from pericentromeric heterochromatin (*i.e.* mouse chromocenters; Mateos-Langerak *et al.*, 2007; chapter 4 of this thesis). Remarkably, in the absence of functional HP1 pericentromeric heterochromatin domains retained their condensed chromatin structure, demonstrating that heterochromatin maintenance is independent of the binding of HP1 (Mateos-Langerak *et al.*, 2007).

By studying the effects of both gene knock-out and over-expression, important discoveries have also been made recently for methyl-CpG-binding protein 2 (MeCP2). MeCP2 has long been considered a transcriptional silencer, because of its affinity for methylated DNA (a mark for silent chromatin) and recruitment of HDAC silencing complexes (Meehan *et al.*, 1992; Nan *et al.*, 1997; Nan *et al.*, 1998b). However, a recent report studied gene expression patterns after up- or downregulation of MeCP2 in the mouse hypothalamus (Chahrour *et al.*, 2008). Surprisingly, ~85% of the genes that bound over-expressed MeCP2 were upregulated. Conversely, knockout of the MeCP2 gene caused these genes to be downregulated, suggesting a role in transcriptional activation for MeCP2. These results are in line with our finding that the targeting of MeCP2 to compact chromatin domains results in decondensation (chapter 2 of this thesis).

A true advance in the study of epigenetic regulators and their *in vivo* effects on chromatin was made with the introduction of engineered targeting systems. Such systems consist of protein-binding arrays that associate with DNA-binding proteins with a high affinity. Fluorescent tagging of the DNA-binding protein allows one to visualize the genomic binding array in living cells. Moreover, these systems can be exploited to demonstrate the effect of binding of epigenetic regulatory proteins on the compaction state of the integrated chromosomal array. The initial targeting system, devised in mammalian cells, contained a highly amplified chromosomal domain consisting of a stretch of bacterial lac operator (lacO) repeats that bind a chimeric fluorescent lac repressor (lacR) protein with high affinity (Robinett *et al.*, 1996; figure 1). Subsequent studies established the value of this tool, demonstrating that the *in vivo* targeting of the lacR-tagged viral activation domain VP16 to a lacO array results in the decondensation of the chromosomal array and its movement to the interior of the nucleus (Tumbar and Belmont, 2001; Tumbar *et al.*, 1999). Targeting of the lacR-tagged epigenetic silencer HP1 to the chromosomal array produced an opposite effect; lacO chromatin condensed locally, concomittant with the recruitment of histone

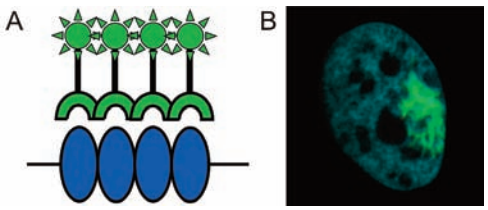

Figure 1. The engineered lac operator/lac repressor targeting system. (A) Schematic representation of the lac operator/lac repressor targeting system. Integrated lacO repeats (blue) are recognized and bound by the lacR-EGFP fusion protein (green). (B) A eukaryotic cell with an amplified lacO array that has been targeted by lacR-EGFP. The three-dimensional structure of chromatin is visible due to its fluorescent tagging.

methyltransferase SETDB1 and the enhancement of trimethylation of histone H3 lysine 9 in that domain (Brink *et al.*, 2006; Verschure *et al.*, 2005; chapter 3 of this thesis). The lacO/lacR technology has been further developed over the years, adding inducibility of the lacR fusion protein and incorporation of a fluorescent reporter gene and MS2 repeats for measurements of transcript concentration *in vivo*, further expanding its usefulness (Janicki *et al.*, 2004; Tsukamoto *et al.*, 2000). Studies using engineered lacO/lacR systems are described in chapters 2, 3 and 5 of this thesis.

In conclusion, eukaryotic gene regulation is achieved at several levels. A multitude of studies have established various correlations between chromatin organization, *e.g.* higher-order folding of the chromatin fiber and positioning of chromosomal domains within the nucleus, and gene expression. However, whether the level of gene expression is a cause or consequence of chromatin organization is still unclear. The use of engineered targeting systems allows us to manipulate and visualize changes at the chromatin level in relation to changes in gene expression and hence systematically unravel cause-and-effect relationships. Uncovering these details will advance our understanding of the principles of genome biology.

Thesis outline

The objective of the studies described in this thesis was to define causal relationships between reputed epigenetic chromatin silencers, chromatin structure and changes in gene expression. We have used several approaches to achieve this aim.

In **chapter 2** and **3** we have utilized an amplified lacO array targeting system in Chinese Hamster Ovary cells. Targeting the gene silencer MeCP2 (**chapter 2**) we observed, contrary to our expectations, that chromatin of the lacO-containing amplified chromosome region is decondensed upon MeCP2 binding. This decondensation requires the C-terminal domain of MeCP2. While HP1α and HP1β remain bound to the lacO, HP1γ is depleted after MeCP2 binding. Interestingly, transcriptional silencing is maintained, despite the induced chromatin decondensation.

Chapter 3 examines targeting of a truncated HP1α or HP1β protein, lacking its chromodomain, which normally mediates binding to histone H3 methylated at lysine 9. Like full-length HP1, local binding of chromodomain-deficient HP1 results in heterochromatinization of the amplified chromosome region as shown by three-

dimensional quantitative measurements of chromatin structure, elevated levels of H3K9me3 and recruitment of endogenous HP1α and HP1β (Brink *et al.*, 2006). These results suggest that recruitment of protein factors by the chromoshadow and hinge domain is sufficient to induce heterochromatinization.

In **chapter 4** we present the results of depletion of HP1 from heterochromatin by a dominant-negative approach (Mateos-Langerak *et al.*, 2007). We utilize the self-binding properties of HP1 through its chromoshadow domain. By over-expressing truncated HP1 without its chromodomain, we inhibit the binding of full-length HP1 to its chromatin binding sites, depleting HP1 from mouse chromocenters. Pericentromeric heterochromatin domains remain intact after HP1 displacement, demonstrating that HP1 is not essential to heterochromatin maintenance.

In **chapter 5** we describe the setting up of an advanced chromatin targeting system in human cells and discuss its benefits and points for improvement. A key feature of this engineered system is its single-copy integration into predefined well-characterized genomic locations in different functional domains. This enables us to study the effect of the genomic environment on chromatin structure and on gene expression of a reporter gene. Furthermore, two different small arrays that are incorporated in the engineered construct can be used to simultaneously target different regulatory factors, providing information about their functional interactions and their effect on gene expression. Pilot studies demonstrate the potential of our novel engineered targeting system.

Finally, **chapter 6** is a perspective in which we discuss novel approaches to describe and analyze eukaryotic gene networks. Among others, this should give insight into the role of epigenetics in gene networks.

Chapter 2

MeCP2 revisited: Chromatin Decondensation and the Displacement of HP1γ without Transcriptional Activation

Maartje C. Brink, Diewertje G. E. Piebes, Martijn S. Luijsterburg, Roel van Driel & Pernette J. Verschure

In preparation

Abstract

Methyl-CpG-binding protein 2 (MeCP2) is a chromatin-binding protein involved in the DNA methylation pathway and has been characterized both as a repressor and as a potential activator of transcription. MeCP2 was shown to bind methylated DNA and the epigenetic silencer HP1 and to cause the *in vitro* compaction of chromatin and the *in vivo* formation of repressive chromatin loops. Here we show that, remarkably, the *in vivo* binding of lac repressor-tagged MeCP2 causes extensive decondensation of a lac operator-containing chromosomal domain. The C-terminus of MeCP2 is required for the observed chromatin decondensation, excluding involvement of the methyl-binding and transcriptional-repression domain. MeCP2-induced chromatin decondensation occurs throughout interphase in the absence of changes in CpG methylation. Strikingly, targeted MeCP2 does not activate the transcription of genes embedded in the decondensed chromosomal domain and, in agreement, causes the repression of a luciferase reporter gene *in vivo*. Targeting of MeCP2 triggers the release of HP1γ from the array, but not of HP1α and HP1β. Moreover, over-expression of MeCP2 induces an overall increase of HP1γ mobility. We propose a novel role for MeCP2 in reorganizing chromatin structure in order to facilitate changes in gene expression.

Introduction

The spatial organization of chromatin plays a critical role in the control of eukaryotic gene expression (reviewed by Goetze *et al.*, 2007b). Both the radial positioning of chromatin within the eukaryotic nucleus and folding of the chromatin fiber into more or less condensed states are functionally linked to transcriptional regulation. Establishing the causal relationship between the three-dimensional (3D) chromatin structure and gene activity is an important step towards clarifying the molecular mechanisms underlying eukaryotic gene control. The 3D-chromatin structure is regulated by epigenetic marks, including histone modifications, histone variants and DNA methylation (Chambeyron and Bickmore, 2004; Tumbar *et al.*, 1999). A variety of regulatory proteins are able to specifically bind epigenetic marks and translate these marks to changes in gene expression (Taverna *et al.*, 2007). The interplay between the various epigenetic factors results in an intricate pattern of gene regulation. Previously, we showed that *in vivo* targeting of HP1 to an amplified lac operator-containing chromosomal domain caused local condensation of chromatin structure and recruitment of histone methyltransferase SETDB1, concomitant with methylation of histone 3 at lysine 9 (Verschure *et al.*, 2005). Increasing evidence points towards cross-talk between HP1 and methyl-CpG-binding

proteins. For instance, upon myogenic differentiation the level of methyl-CpG-binding proteins increases, inducing chromocenter clustering concomitant with the relocalization of HP1 to heterochromatin, in particular of the HP1γ isoform (Agarwal *et al.*, 2007; Brero *et al.*, 2005). Additionally, all three HP1 isoforms were found to co-precipitate with methyl-CpG-binding protein 2 (MeCP2; Agarwal *et al.*, 2007).

In the present study, we demonstrate that the *in vivo* targeting of MeCP2 caused extensive chromatin decondensation requiring the C-terminal part of MeCP2. MeCP2-induced chromatin decondensation occurred throughout interphase in the absence of transcriptional activation or changes in CpG methylation. We demonstrate an intricate interplay between MeCP2 and HP1 proteins by showing that MeCP2 promotes eviction of HP1γ from chromatin, but not of HP1α or HP1β. We propose that MeCP2-induced chromatin decondensation reflects a poised status, preparing chromatin for further transcriptional regulation.

Materials and methods

Construction of plasmids

Full-length rat MeCP2 was produced by PCR and cloned into the AscI site of p3'SS-EGFP-dimer lac repressor (Robinett *et al.*, 1996). cDNA of the MeCP2 point mutation R133C (Yusufzai and Wolffe, 2000) was similarly procured. For fusion at the N-terminus of EGFP-lacR, we produced the complete MeCP2 and separate functional domains by PCR, extended with *XbaI* and *XhoI* restriction sites, and cloned these into the identical sites of p3'SS-EGFP-dimer lac repressor. mCherry-lacR and mCherry-lacR-MeCP2 were created by excising EGFP from EGFP-lacR or EGFP-lacR-MeCP2 with *Xba*I and *BsrGI* followed by insertion of mCherry, cut with *NheI* and *BsrGI*.

Cell culture and transfection

The AO3_1 and RRE_B1 cell line are derivatives of CHO DG44, with a condensed or decondensed integration of lac operator repeats and flanking DNA, respectively (Li *et al.*, 1998; Robinett *et al.*, 1996). Cells were regularly cultured in Ham's F-12 without thymidine and hypoxanthine, supplemented with triple dialyzed FBS (Perbio) and 0.1 μM MTX for AO3_1 or 10 μM MTX for RRE_B1 cells, never allowing confluency to reach over 90% or less than 30%. Osteosarcoma cells (U2OS) and NIH/3T3 mouse fibroblasts were cultured in Dulbecco minimal essential medium containing 10% fetal bovine serum. All cells were cultured at 37°C in a 5% CO_2 atmosphere. Cells were transfected at 80% confluency on cover slips coated with Alcian Blue. Alternatively, for live cell experiments, cells were transfected in 35 mm glass bottom dishes (MatTek) at 80% confluency. Transfection was performed with Lipofectamine 2000 according to the manufacturer's protocol. After 24-48 hours, cells were imaged directly or first washed in PBS, fixed in 4% paraformaldehyde for 15 minutes at 4°C and embedded in Vectashield (Brunschwig, Burlingame, CA) with DAPI (4′,6′-diamidino-2-phenylindole; Vector Laboratories, Burlingame, CA). The luciferase reporter gene assay was performed as described elsewhere (Bunker and Kingston, 1996; Verschure *et al.*, 2005).

Immunolabeling and fluorescent *in situ* hybridization

For immunolabeling, cells were permeabilized after fixation with 0.5% (w/v) Triton X-100 in PBS for 5 minutes and incubated in PBS containing 100 mM glycine for 10 minutes. Subsequently, cells were incubated at 4°C overnight with primary antibodies diluted in PBS containing 0.5% (w/v) bovine serum albumin and 0.1% (w/v) gelatin (PBG; Sigma, St. Louis, MO). The following primary antibodies were used:

rabbit anti-H3K9me2 (Upstate, Milton Keynes, United Kingdom; Nakayama *et al.*, 2001), rabbit anti-H3K9me3 (Cowell *et al.*, 2002), rabbit anti-SETDB1 (Schultz *et al.*, 2002), anti-EZH2 and anti-EED (Hamer *et al.*, 2002), rabbit anti-TFIIH p62 subunit (SantaCruz Biotech), mouse anti-SC35 (Abcam; Fu and Maniatis, 1990), mouse anti-histone H1 (Imgen), goat anti-hBrahma (N-19; Santa Cruz Biotechnology), rabbit anti-H3K4me2 (Upstate), rabbit anti-H4K16ac and rabbit anti-H3K27me2 (Upstate). For labeling of DNA methylation, we incorporated a 30-minute denaturation step of 2 M HCl at 37°C and blocked with 10% BSA for 15 minutes, preceding the primary antibody incubation with mouse anti-5mC (Eurogentec) and rabbit anti-lacR, diluted in saline buffer supplemented with 0.5% BSA, 0.1% gelatin and 0.05% tween-20. Primary antibody recognition was achieved by donkey anti-mouse conjugated to biotin and Streptavidin-FITC for anti-5mC and by donkey anti-Rabbit Cy3 for anti-lacR. Fluorescent *in situ* hybridization was performed largely as described elsewhere (Cremer *et al.*, 2001). Denaturation was carried out at 78°C in SSC (0.15 M NaCl, 0.015 M sodium citrate) containing 50% formamide and 10% dextran sulfate. Hybridization was allowed to proceed overnight at 37°C. Posthybridization washes were carried out with 2×SSC/50% formamide at 45°C. All incubations for probe detection were performed at room temperature in 4×SSC containing 5% (w/v) non-fat dried milk.

Run-on transcription labeling

For transcription labeling, BrUTP was incorporated into nascent RNA as described previously (van Royen *et al.*, 2007; Verschure *et al.*, 1999; Wansink *et al.*, 1993). Briefly, cells were permeabilized in glycerol buffer (20 mM Tris HCl, 0.5 mM $MgCl_2$, 0.5 mM EGTA, 25% glycerol and 1 mM PMSF) supplemented with 0.05% Triton X-100, 5 μM DTT and 20 U/ml RNAsin for 3 minutes. BrUTP incorporation was performed for 10 minutes at RT in synthesis buffer (100 mM Tris HCl, 5 mM $MgCl_2$, 0.5 mM EGTA, 200 mM KCl, 50% glycerol, 0.05 mM SAM, 20 U/ml RNAsin, and 0.5 mM PMSF) supplemented with 0.5 mM ATP, CTP, GTP, and BrUTP (Sigma-Aldrich). Cells were fixed and labeled as described above. BrUTP was immunolabeled overnight with rat anti-BrdU (Seralab) diluted 1:500 in PBG at 4°C. Primary antibody detection was followed by biotin-conjugated donkey anti–rat IgG (Jackson ImmunoResearch Laboratories) 1:300 and Cy3-conjugated streptavidin (Jackson ImmunoResearch Laboratories) 1:250.

Image analysis

All cells were imaged using a Zeiss LSM 510 (Zeiss, Jena, Germany) confocal laser scanning microscope equipped with a 63x/1.4 oil immersion objective. We used multitrack scanning, employing a UV laser (364 nm), an argon laser (488 and 514 nm) and a helium neon laser (543 nm) to excite DAPI staining and green and red fluorochromes. Emitted fluorescence was detected with BP 385-470, BP 505-550 and 560 LP filters. Three-dimensional (3D) images were scanned at 512 by 512 pixels using 200 nm axial and 60 nm lateral sampling rates. Images were averaged 4 times. For FLIP and FRAP experiments, microscopes were equipped with an objective heater and cells were examined in microscopy medium (137 mM NaCl, 5.4 mM KCl, 1.8 mM $CaCl_2$, 0.8 mM $MgSO_4$, 20 mM D-glucose and 20 mM HEPES) at 37°C. Surface factor measurements were performed using the Huygens system 2 software package (Scientific Volume Imaging, Hilversum, The Netherlands), as described previously (Verschure *et al.*, 2005). Briefly, the surface factor is calculated as the ratio between the smallest possible surface area of the volume occupied by the array and the actual surface area. A surface factor of 1 therefore represents a perfectly spherical structure, whereas a lower value is assigned to a more furrowed structure. All surface factors were assembled in a histogram (binning 5). The threshold value was set at 0.6, assigning the decondensed chromatin state to all operator arrays with a surface factor lower than 0.6.

Fluorescence Recovery after Photobleaching (FRAP)

FRAP analysis was used to measure the mobility of EGFP-lacR, EGFP-lacR-MeCP2, EGFP-lacR-R133C, C-terminus-EGFP-lacR and MeCP2-EGFP at the lac operator array as described previously (Houtsmuller *et al.*, 1999; Luijsterburg *et al.*, 2007). Briefly, a square of 512x512 pixels was imaged at 2.56 μs per frame, zoom 14 (1 pixel is 0.02x0.02 μm). After 3 images, a strip of 275x150 pixels, encompassing half the lac operator array was bleached by applying 4 scans at maximal 488 and 514 nm laser intensity (AOTF 100%, total time 1.9 s) and the fluorescence recovery was acquired by scanning at least 60 images at a 5-second interval (1x average/frame). For FRAP of EGFP-HP1γ in- and outside of the array, images were taken at 512x512 pixels (0.04x0.04 μm), 1.60 μs per frame, zoom 7. After 10 images, a square of 56x56 pixels was bleached for 10 scans (total time = 1.1 s) and recovery was measured for at least 60 images at a 2-second time interval. The data was normalized to the original intensity before the bleach pulse by using the equation:

$I_{FRAP} = (I_{strip\ t=t} - I_{background\ t=t}) / (I_{strip\ t=0} - I_{background\ t=0})$, where $I_{strip\ t=t}$ and $I_{strip\ t=0}$ represent the intensity within the strip at t=t and the intensity before the bleach pulse (t=0), respectively. For graphical representation, recovery plots were normalized between 0 and 1.

Fluorescence Loss in Photobleaching (FLIP)
FLIP analysis was used to measure the residence time of EGFP-HP1γ on chromatin (Hoogstraten *et al.*, 2002; Luijsterburg *et al.*, 2007). Images of 512x512 pixels were acquired with a scan time of 1.60 µs (1x average/frame) at zoom 7 (1 pixel is 0.04x0.04 µm). After 10 images, a region of 275x150 pixels, occupying an area of 1/3 of the nucleus (excluding the lac operator array), was continuously bleached with maximal 488 nm and 514 nm laser intensity (AOTF 100%). EGFP-HP1γ fluorescence was monitored with low laser intensity for at least 80 images with a 2-second time interval between images. The loss of fluorescence in the unbleached part of the nucleus was quantified. All values were background corrected and normalized to 1 by using the equation: $I_{FLIP} = (I_{spot\ t=t} - I_{background\ t=t}) / (I_{spot\ t=0} - I_{background\ t=0})$. FLIP and FRAP curves were fitted with Igor Pro 5.00 software according to the equation: $y_0 + A_1 \exp(-inv\ Tau_1 x) + A_2 \exp(-inv\ Tau_2 x)$, with $\chi^2 < 0.06$.

Results

MeCP2 fusion proteins localize at mouse chromocenters

To study the effect of MeCP2 binding to chromatin *in vivo*, we fused rat MeCP2 to a fluorescently tagged lacR (EGFP-lacR), enabling targeting and visualization of MeCP2 to an amplified lacO array in living cells (Li *et al.*, 1998). MeCP2 contains a methyl binding domain (MBD), a transcription repression domain (TRD) and a poorly characterized C-terminal domain (Nan *et al.*, 1997; Nan *et al.*, 1993; Nan *et al.*, 1998b). We tagged both full-length MeCP2, as well as the individual domains MBD, TRD, MBD-TRD and the C-terminus of MeCP2, to EGFP-lacR as depicted in figure 1A. In addition, we constructed an EGFP-lacR-tagged version of an MeCP2 point mutation in the MBD domain, R133C, which leads to the development of Rett Syndrome (Ballestar *et al.*, 2000).

MeCP2 naturally resides at heterochromatic sites, such as mouse pericentromeric heterochromatin repeats (chromocenters; Lewis *et al.*, 1992). To demonstrate that our fusion proteins behave similarly to wild-type MeCP2, we assayed their localization in mouse fibroblasts. The MeCP2 domains MBD, MBD-TRD, TRD and point mutant R133C fusion proteins localized to chromocenters similar to full-length MeCP2 (figure 1B-F, H). The EGFP-lacR-tagged C-terminus was homogeneously distributed throughout the nucleus as was the EGFP-lacR control protein (figure 1G and I). The EGFP-lacR-tagged C-terminus lacks the domains associated with methylated DNA and repressor complexes, as found in the MBD, TRD and R133C fusion proteins, and is therefore more likely to display a distribution without enrichment at the chromocenters. These results confirm that all MeCP2-derived fusion proteins except the EGFP-lacR-tagged C-terminus, have a nuclear distribution similar to wild-type MeCP2.

MeCP2 targeting causes local chromatin decondensation

To study the influence of MeCP2 binding on higher-order chromatin structure we targeted the MeCP2-containing lacR fusion proteins in CHO DG44 cell lines containing a highly amplified chromosomal array (of approximately 90 Mb), consisting of tandem lacO repeats interspersed with the DHFR gene. The amplified chromosomal region appeared as either a condensed heterochromatic or an unusually extended fibrillar conformation, in cell line AO3_1 and RRE_B1 respectively (Li *et al.*, 1998; Robinett *et al.*, 1996). Targeting of either N- or C-terminally lacR-tagged MeCP2 induced extensive large-scale decondensation of the amplified chromosomal array in both the AO3_1 and RRE_B1 cell line (figure 2 and data not shown). FISH labeling with a lacO probe confirmed that the fluorescent MeCP2-targeted decondensed structure overlapped completely with the decondensed lacO chromosomal array (figure 3).

The observed decondensation typically occurred in only part (~40%) of the transfected population. To investigate whether MeCP2-induced decondensation is cell-cycle dependent, we transfected AO3_1 cells with EGFP-lacR-MeCP2 and mCherry-tagged proliferating cell nuclear antigen (PCNA). PCNA forms a distinct pattern of replication foci during S-phase and can be used as a marker for cell-cycle stage (Leonhardt *et al.*, 2000). Both condensed and decondensed configurations of the amplified chromosomal arrays upon MeCP2 targeting were observed in cells within S-phase (containing PCNA foci) as well as cells outside of S-phase (not containing PCNA foci; figure 4). Our results show that targeting of EGFP-lacR-MeCP2 results in an extensive decondensation of the amplified chromosomal region in living cells, independent of cell-cycle stage.

The C-terminus of MeCP2 is responsible for chromatin decondensation

To identify the domain of MeCP2 that is essential for the observed decondensation, we targeted individual MeCP2 domains or the Rett-mutant R133C to the amplified chromosomal array in AO3_1 cells. Targeting of lacR-tagged fusion proteins expressing the MBD, the TRD or both these domains, did not clearly decondense the array (figure 5C-E), though occasionally a slightly enlarged array was observed. Conversely, upon targeting of the lacR-tagged C-terminus of MeCP2 or the point mutation R133C, we did observe clear chromatin decondensation, albeit to a lesser extent than full-length MeCP2 (figure 5A, B).

To quantify the degree of decondensation of the array, we collected confocal image stacks of lacO chromatin structures that were the result of targeting full-length MeCP2 proteins or partial MeCP2 domains and measured the extent of decondensation of the chromosomal array, as scored by the parameter 'surface factor' (see materials and methods and de Leeuw *et al.*, 2006; Goetze *et al.*, 2007a; Verschure *et al.*, 2005). The surface factor of ~30 nuclei was plotted in a histogram for each targeted protein,

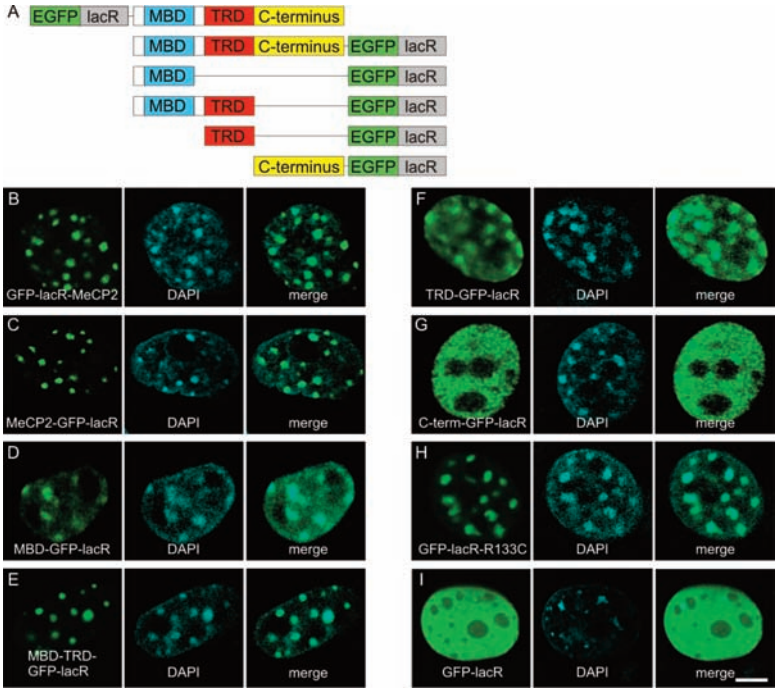

Figure 1. Nuclear distribution of EGFP-lacR-tagged MeCP2 domains in mouse fibroblasts. MeCP2 partial domains were fused in frame to EGFP-lacR and expressed in NIH/3T3 cells. (A) Schematic representation of MeCP2 constructs. (B-I) Cells were fixed, DAPI stained and 3D images were recorded. The images shown represent individual optical sections. The green signal shows the targeting to the chromosomal array of EGFP-lacR-MeCP2 (B), MeCP2-EGFP-lacR (C), MBD-EGFP-lacR (D), MBDTRD-EGFP-lacR (E), TRD-EGFP-lacR (F), C-terminus-EGFP-lacR (G), EGFP-lacR-R133C (H) or EGFP-lacR control (I), the blue signal shows DAPI staining. Nuclei are on the same scale, bar = 5 μm.

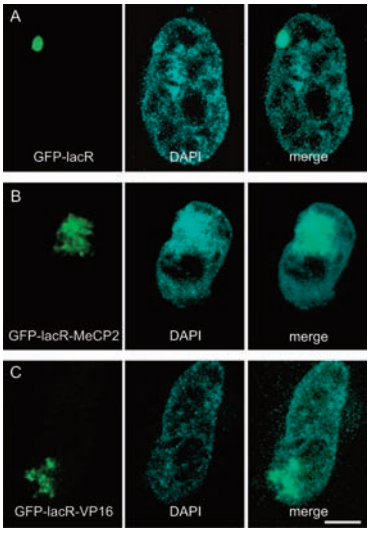

Figure 2. MeCP2 causes chromatin decondensation. AO3_1 cells containing an integrated lac operator domain were transfected with EGFP lacR (control) (A), with EGFP-lacR-MeCP2 (B) or EGFP-lacR-VP16 (C). Cells were fixed, DAPI stained and 3D images were recorded. The green signal shows the targeting of EGFP-lacR with or without full-length MeCP2 at the chromosomal array, the blue signal shows DAPI staining. The images shown represent individual optical sections. Nuclei are on the same scale, bar = 5 μm.

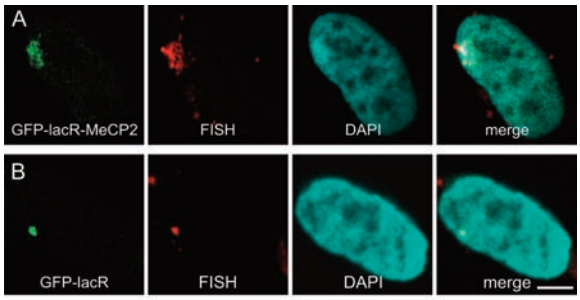

Figure 3. MeCP2-decondensed array contains chromatin. AO3_1 cells were transfected with EGFP-lacR-tagged MeCP2 or the EGFP-lacR control and hybridized with a fluorescently-labeled lac operator DNA probe. Cells were fixed, DAPI stained and 3D images were recorded. The green signal shows the targeting of EGFP-lacR-MeCP2 (A) or of EGFP-lacR (B) to the chromosomal array, the red signal the FISH-labeled lac operator-containing chromosomal array, the blue signal shows DAPI staining. The images shown represent individual optical sections. Bar = 5 μm.

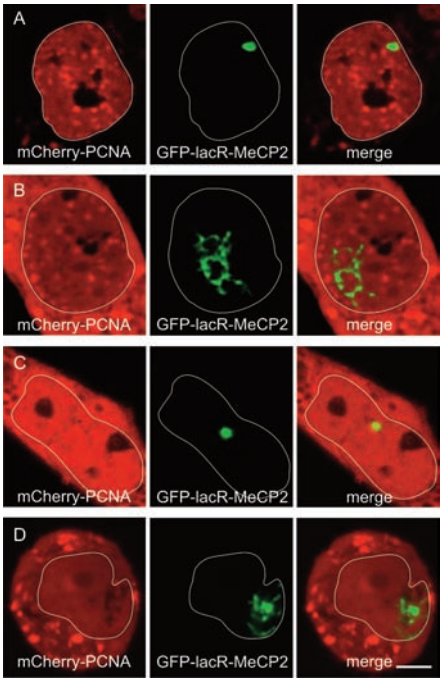

Figure 4. Decondensation is independent of cell-cycle stage. AO3_1 cells were cotransfected with EGFP-lacR-MeCP2 and mCherry-PCNA. Cells were fixed, DAPI stained and 3D images were recorded. The position of the nucleus is indicated by the white line. The green signal shows the targeting of EGFP-lacR-tagged MeCP2 at the chromosomal array, the red signal shows mCherry-PCNA. The images shown represent individual optical sections. Nuclei are on the same scale, bar = 5 μm.

displaying a bimodal distribution that reflects cell nuclei containing either a condensed or a decondensed chromosomal array. The ratio of the two distributions provides information on what fraction of cells contains decondensed arrays. Figure 5F depicts the percentage of nuclei containing decondensed arrays for all targeted proteins. Compared to the decondensation induced by lacR-MeCP2 according to the surface factor, lacR-tagged VP16, MeCP2 (N-terminal), C-terminus and R133C were not significantly different (one-tailed Mann Whitney test, $P<0.05$), causing similar levels of decondensation. In contrast the lacR control and lacR-tagged MBD, TRD and MBDTRD did not cause decondensation and were significantly different to lacR-MeCP2. These quantitative results mirrored our visual observations: the degree of decondensation of the chromosomal array was most pronounced in the cells targeted by fusion proteins containing an intact C-terminus of MeCP2. We conclude that the C-terminal domain of MeCP2 plays a pivotal role in MeCP2-induced chromatin decondensation.

Untargeted MeCP2 causes decondensation of the amplified chromosomal array

To determine whether decondensation of the MeCP2-targeted chromosomal array was a result of fusion of MeCP2 to the lacR, we expressed fluorescent MeCP2 without a lacR tag in AO3_1 cells. Untargeted MeCP2-mRFP (*i.e.* not fused to the lacR) localized at the amplified lacO array, both in EGFP-lacR control and in EGFP-lacR-MeCP2 transfected cells (Figure 6A, B). Furthermore, MeCP2-mRFP caused decondensation at the amplified array in the lacR-expressing cells, albeit to a lesser extent than in the lacR-targeted MeCP2 cells. To consolidate our microscopic observations, we quantified the extent of decondensation in MeCP2-mRFP-expressing cells by measuring the surface factor of the chromosomal array. In the MeCP2-mRFP-expressing cells the surface factor differs significantly from that in lacR-targeted control cells ($P<0.01$), however decondensation induced by untargeted MeCP2 also differs significantly from the extensive decondensation induced by targeted lacR-MeCP2. The percentage of cells with a decondensed array is shown in figure 5F. Untargeted MeCP2 decondenses the amplified lacO chromatin to a much smaller extent than lacR-targeted MeCP2 both in volume of the array (as measured by the surface factor) and in percentage of cells in which the effect is observed (figures 2B, 5F and 6A). We considered the possibility that differences in residence times between untargeted MeCP2 and lacR-targeted MeCP2 were responsible for causing different degrees of chromatin decondensation. In order to determine residence times of untargeted and targeted MeCP2, we performed FRAP (Fluorescence Recovery After Photobleaching) analysis. Bleaching was performed on a region covering one third of the lacO array followed by monitoring fluorescence recovery of the various EGFP-tagged proteins. Figure 6C shows that in control cells, EGFP-lacR was nearly fully immobilized at the amplified lacO array: we detected almost no recovery of fluorescence after the bleach pulse during the detection period. In cells expressing lacR-MeCP2, the immobilization of the lacR-tagged MeCP2 was even more pronounced. Similar results were obtained for lacR-tagged R133C and lacR-tagged C-terminus (data not shown). In contrast, untargeted MeCP2 was mobile at the amplified lacO array with a $t_{1/2}$ of ~24s (mono-exponential fit). These results illustrate that lacR-fused MeCP2 or partial MeCP2 domains are tightly bound to the array by the lacR-lacO interactions and do not exchange on a time-scale of minutes in contrast to MeCP2 without a lacR-tag. It is tempting to speculate that the residence time of molecules bound at the array, influenced by differences in affinity and available binding sites, determines the degree of chromatin decondensation.

MeCP2 induces the displacement of HP1γ

A potential interaction between MeCP2 and the HP1 proteins was recently identified by co-immunoprecipitation of MeCP2 and HP1γ from mouse cells (Agarwal *et al.*, 2007). Co-transfections of mCherry-lacR-tagged MeCP2 and EGFP-tagged HP1α, HP1β or HP1γ in AO3_1 cells showed that the three HP1 isoforms are enriched at the

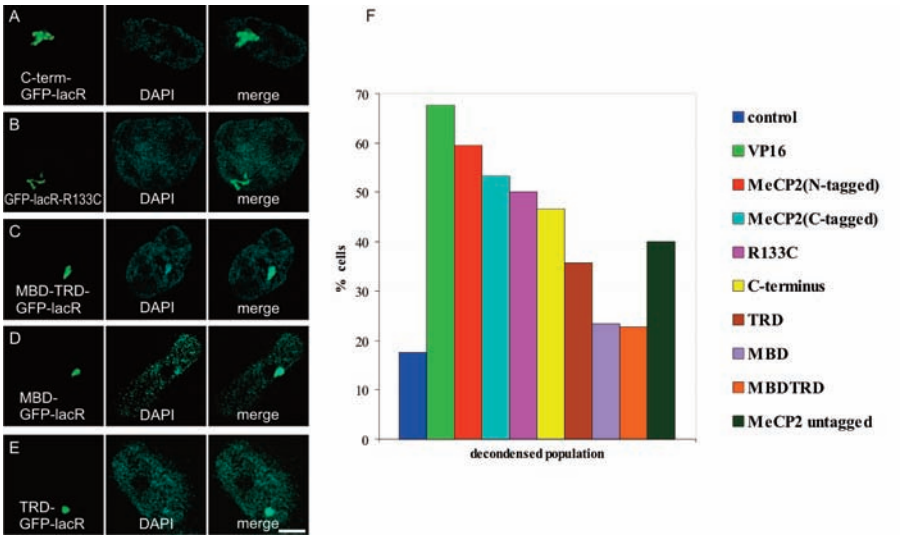

Figure 5. The MeCP2 C-terminal domain is responsible for chromatin decondensation. MeCP2 partial domains were fused to EGFP-lacR and expressed in AO3_1 cells. Cells were fixed, DAPI-stained and imaged in 3D. Image analysis software identified the array within each nucleus and calculated the corresponding surface factors. Targeting of the EGFP-lacR-tagged C-terminal domain (A), R133C (B), MBDTRD (C), MBD (D) and TRD (E) at the amplified array. The green signal shows the targeting of EGFP-lacR or EGFP-lacR-tagged MeCP2 domains at the chromosomal array, the blue signal shows DAPI staining. The images shown represent individual optical sections. Nuclei in panels A-E are on the same scale. Bar = 5 μm. (F) Plotting of the surface factor distributions revealed the fraction of the amplified arrays in condensed state. The histogram shows the percentage of cells that have a decondensed array upon targeting by all EGFP-lacR-tagged proteins and upon expression of untagged MeCP2.

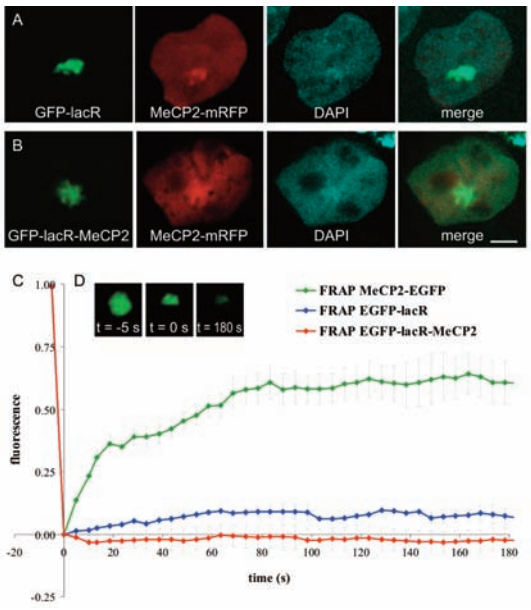

Figure 6. Untargeted MeCP2 localizes to and decondenses the lac operator array. AO3_1 cells were co-transfected with MeCP2-mRFP and either EGFP-lacR or EGFP-lacR-MeCP2. A bleach pulse was administered, bleaching half of the lac operator array. Subsequent fluorescence recovery was measured during 3 minutes. 3D-projection of transfected AO3_1 nucleus co-transfected with untargeted MeCP2-mRFP and EGFP-lacR (A) or optical section of AO3_1 nucleus co-transfected with MeCP2-mRFP and EGFP-lacR-MeCP2 (B). The green signal shows the targeting of EGFP-lacR or EGFP-lacR-tagged full-length MeCP2 at the chromosomal array, the red signal shows the expressed MeCP2-mRFP. Bar = 5 μm. (C) FRAP curves of untargeted MeCP2-EGFP, control EGFP-lacR and EGFP-lacR-MeCP2 fusion proteins. Inset (D) shows the lac-operator array targeted by EGFP-lacR before, immediately after and 3 minutes after the bleach pulse.

chromosomal array (visualized by the mCherry-lacR protein) in the absence of MeCP2 targeting (figure 7A, C and E). Strikingly, HP1γ accumulation at the amplified array was lost after targeting lacR-tagged MeCP2, both at the condensed and the decondensed arrays (figure 7B and data not shown). Conversely, HP1α and β remained bound after MeCP2 targeting (figure 7D, F). These results show that targeting of MeCP2 interferes with the binding of HP1γ at the amplified array, but not with that of HP1α and HP1β.

To quantify the effect of MeCP2 on HP1γ binding to the amplified array, we determined HP1γ mobility using FRAP. A small square of the nucleus of an EGFP-HP1γ-transfected cell was bleached either in- or outside of the amplified region, visualized by mCherry-lacR, and subsequent fluorescent recovery was measured (figure 7G). Fitting of the two FRAP curves identified two HP1γ populations of different mobility both in- and outside of the array. Outside of the amplified array, the largest fraction (~90%) of the HP1γ population displayed fast mobility ($t_{1/2}$ = 1.4 s), likely representing freely diffusing HP1γ. Approximately 10% of the protein pool displayed slower exchange and was considered chromatin-bound HP1γ ($t_{1/2}$ = 12.0 s). Measurements in the amplified domain revealed a marked shift in the distribution of the freely diffusing versus chromatin-bound HP1γ populations. At the amplified array only 57% of the HP1γ population displayed high mobility whereas 43% of the protein pool showed reduced mobility, indicating efficient accumulation of HP1γ at the amplified array in the absence of MeCP2 targeting.

Next, we performed FLIP (Fluorescence Loss In Photobleaching) of HP1γ in the presence of lacR or lacR-MeCP2, by continuously bleaching part of the nucleus outside of the amplified domain and performing simultaneous measurements on the loss of fluorescence in the rest of the nucleus (figure 7H). Fitting of the FLIP curves identified two HP1γ pools; one highly mobile, freely diffusing population and a less mobile, bound population. The lacR-transfected control cells displayed free diffusion for 71% of the HP1γ proteins ($t_{1/2}$ = 3.1 s). Strikingly, the proportion of the freely diffusing HP1γ population went up to 97% ($t_{1/2}$ = 1.5 s) after targeting of lacR-tagged MeCP2. Moreover, in the presence of untargeted MeCP2, we measured an increase in unbound HP1γ (94%), similar to that in lacR-MeCP2 transfected cells. These results confirm that MeCP2 effectively antagonizes direct or indirect binding of HP1γ to chromatin.

Localization of MeCP2-associated factors upon MeCP2 targeting

Apart from the eviction of HP1γ upon MeCP2 targeting, we were unable to detect local accumulation or displacement of several tested factors (see table 1 and materials and methods). We did not detect the activating factors CREB1 or TFIIB that were shown to interact with MeCP2 (Chahrour *et al.*, 2008; Kaludov and Wolffe, 2000). Other factors and epigenetic marks associated with transcription (RNAPII, H3K4 dimethylation and H4K16 acetylation), were not enhanced after MeCP2 binding. The chromatin-remodeling complex SWI/SNF has been suggested to interact *in vivo* with

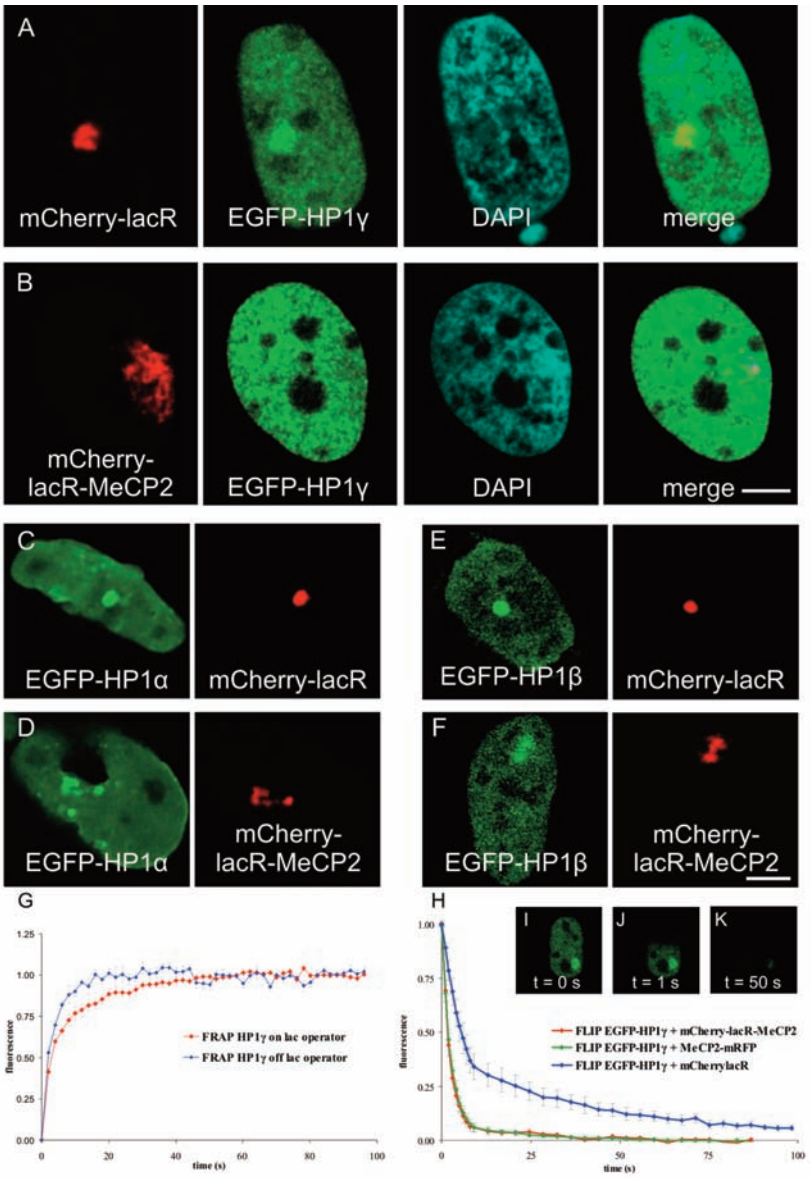

Figure 7. MeCP2 interferes with HP1γ binding. Optical sections of AO3_1 nucleus transfected with mCherry-lacR and HP1γ (A), HP1α (C) or HP1β (E) or mCherry-lacR-MeCP2 and HP1γ (B), HP1α (D) or HP1β (F). The red signal shows the targeting of mCherry-lacR or mCherry-lacR-MeCP2 at the chromosomal array, the green signal shows the expressed EGFP-tagged HP1 isoforms. Nuclei in A-B and in C-F are on the same scale. Bars are 5 μm. (G) FRAP curve of HP1γ in- and outside of the array. (H) FLIP curves of HP1γ in the presence of mCherry-lacR-MeCP2, MeCP2-mRFP or mCherry-lacR. The insets (I-K) show an EGFP-HP1γ and mCherry-lacR-expressing cell of which half of the nucleus is continuously bleached (only green channel is shown). FLIP was measured in the unbleached half of the nucleus.

Table 1. Localization of MeCP2-associated factors at the amplified array with and without EGFP-lacR-MeCP2 targeting. Various factors were assayed for their presence at the amplified lacO-containing array by immunolabeling or co-transfection, upon either EGFP-lacR (control) or EGFP-lacR-MeCP2 targeting. Localization at the array is indicated by: (+) present, (+/-) sometimes present or (-) absent.

labeling	**control**	**MeCP2**
H3K9me2	+/-	+/-
H3K9me3	+/-	+/-
H1	+/-	+/-
EZH2	+/-	+/-
EED	-	-
p62 (TFIIH)	-	-
hBrahma	-	-
H3K4me2	-	-
H4K16ac	-	-
H3K27me2	-	-
SC35	-	-
SETDB1	-	-
mCpG	+	+
transfection	**control**	**MeCP2**
H1	+/-	+/-
RNAPII	-	-
TFIIH	-	-
CREB	-	-
Dnmt1	-	-
Dnmt3b	-	-
HP1α	+	+
HP1β	+	+
HP1γ	+	-

MeCP2 through its catalytic subunit Brahma, though other reports did not detect such an interaction (Harikrishnan *et al.*, 2005; Hu *et al.*, 2006; Wang, 2003). We did not detect enhanced accumulation of Brahma after MeCP2 targeting. Additionally, MeCP2 has been shown to compete with histone H1 for chromatin binding sites (Nan *et al.*, 1997; Nikitina *et al.*, 2007a). Eviction of H1 from chromatin by MeCP2 could explain changes in chromatin structure, however we did not observe any changes in H1 distribution upon MeCP2 targeting. The C-terminus of MeCP2 is able to bind RNA splicing factors (Buschdorf and Stratling, 2004). We considered the possibility that lacR-MeCP2 relocalizes chromatin to SC35 domains or speckles, nuclear bodies enriched in mRNA splicing factors (Lamond and Spector, 2003). Antibody labeling of SC35 identified no co-localization between SC35 domains and the MeCP2-decondensed chromatin array. MeCP2 was originally described as a protein that binds to methylated DNA (Lewis *et al.*, 1992). Therefore, we examined DNA methylation levels at the amplified chromosomal array in those cells showing extensive decondensation of the array upon lacR-MeCP2 targeting. We visualized the *in situ* DNA methylation levels using 5-methylcytosine immunolabeling, which allows analysis at the single-cell level. Methylated CpGs were concentrated at the amplified array both in lacR-MeCP2-targeted and in lacR-targeted control cells (figure 8A and B), illustrating that the observed chromatin decondensation is not related to a change in DNA methylation.

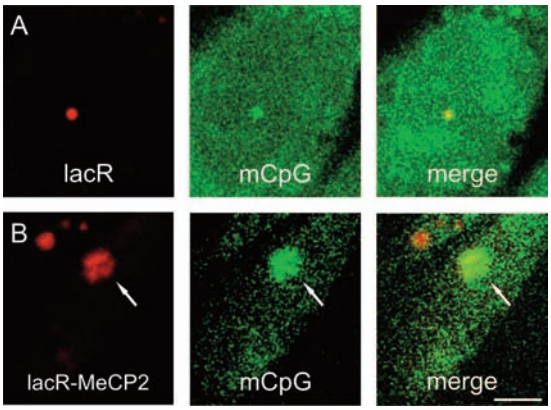

Figure 8. DNA methylation. AO3_1 cells were transfected with mCherry-lacR (A) or mCherry-lacR-MeCP2 (B) and immunolabeled for the presence of lacR and methylated CpGs after denaturation. Cells were fixed, DAPI stained and 3D images were recorded. The red signal shows labeling of mCherry-lacR or mCherry-lacR-tagged MeCP2 at the chromosomal array, the green signal shows 5-methyl-cytosine labeling. Arrows indicate the array. The images shown represent individual optical sections. Nuclei are on the same scale. Bar = 5 µm.

Targeted MeCP2 maintains transcriptional repression *in vivo*

Wild-type MeCP2 acts as a transcriptional repressor, both *in vitro* and *in vivo* (Nan *et al.*, 1997; Nan *et al.*, 1998a). To confirm that MeCP2 maintains its repressive characteristics upon decondensing the amplified chromosomal domain, we performed BrUTP labeling of nascent RNA. This approach allows us to identify changes in the amount of transcripts originating from the chromosomal array in individual cells that display decondensation upon MeCP2 targeting. BrUTP incorporation into newly synthesized RNA was performed on AO3_1 cells transfected with lacR-MeCP2 or with the lacR control. We observed no visible increase of BrUTP-labeled transcript levels at the decondensed amplified chromosomal array upon MeCP2 targeting compared to

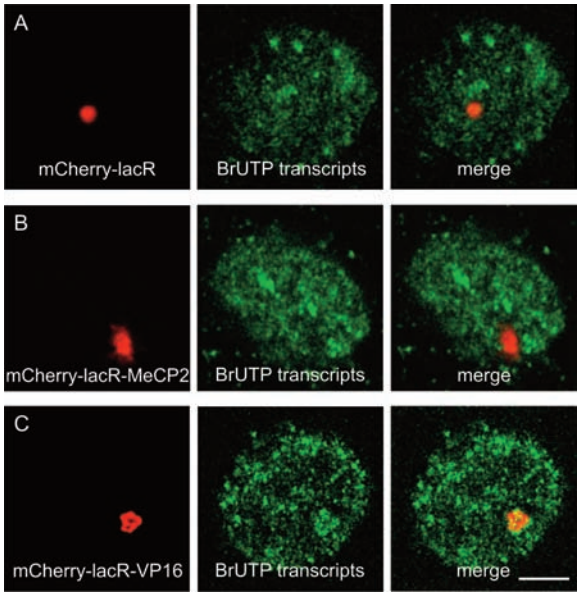

Figure 9. MeCP2 maintains transcriptional silencing at the decondensed lac operator array. AO3_1 cells were transfected with mCherry-lacR (A), mCherry-lacR-MeCP2 (B) or mCherry-lacR-VP16 (C). Cells were permeabilized and incubated with BrUTP for 10 minutes, fixed and stained by immunolabeling. 3D images were recorded. The red signal shows the targeting of mCherry-lacR or mCherry-lacR-tagged MeCP2 or VP16 at the chromosomal array, the green signal shows the nascent RNA. The images shown represent individual optical sections. Nuclei are on the same scale. Bar = 5 µm.

transcript levels at the array in lacR-targeted cells (figure 9A and B). We did observe a considerable increase in BrUTP-labeled transcripts at the chromosomal domain after targeting lacR-VP16, correlated with chromatin decondensation (figure 9C and shown previously by Tumbar *et al.*, 1999). To prove that targeted MeCP2 and other constructs used in this study repress gene expression, we measured the gene expression levels of a luciferase reporter gene fused to 8 lacO copies, upon lacR targeting of MeCP2 (Verschure *et al.*, 2005). The reporter construct was transiently expressed in U2OS cells, together with lacR-tagged MeCP2, R133C or partial MeCP2 domains. MeCP2, R133C and the MBDTRD domain of MeCP2 significantly inhibited luciferase expression compared to the lacR control (60-70%). Interestingly, in contrast to the other MeCP2-derived fusion proteins, the tagged C-terminus only caused repression to a moderate extent (~10%). Taken together, these results demonstrate that the lacR-tagged MeCP2 protein is able to repress gene activity of a transiently expressed luciferase reporter gene. We show that decondensation of the amplified chromosomal array upon MeCP2 targeting does not correlate with gene activation.

Discussion

Regulation of mammalian gene expression is a tightly controlled process. Mistakes in the orchestration of the thousands of genes can have far-reaching consequences, such as the manifestation of various developmental disorders or cancer. For example, mutations in the epigenetic regulator MeCP2 cause the developmental disorder known as Rett Syndrome (Amir *et al.*, 1999). Yet, it remains unclear how MeCP2, a protein embedded in the DNA methylation pathway, influences epigenetic regulation. In previous studies we have shown that targeting of silencing proteins, such as HP1, to an amplified chromosomal array condenses higher-order chromatin structure (Brink *et al.*, 2006; Verschure *et al.*, 2005). These findings are in agreement with the general notion that silencing proteins associate with condensed chromatin.

Here, we provide evidence that the relationship between gene activity and spatial chromatin organization is not straightforward. We show that targeting of MeCP2 to a lacO-containing amplified chromosomal domain induces decondensation of this heterochromatic structure without gene activation. We present evidence that the C-terminus of MeCP2 mediates the observed chromatin decondensation and that MeCP2-induced chromatin decondensation is correlated with the release of bound HP1γ, but not of HP1α and of HP1β.

MeCP2 decondenses chromatin *in vivo*

We demonstrate that the C-terminal domain of MeCP2 is capable of decondensing chromatin, excluding involvement of the MBD and TRD in restructuring chromatin. In previous *in vitro* studies, the C-terminal domain of MeCP2 was shown to bind chromatin and suggested to play a role in restructuring chromatin architecture by

inducing, contrary to our observations, chromatin compaction (Georgel *et al.*, 2003; Nikitina *et al.*, 2007b). However, *in vitro* reconstituted nucleosomal arrays lack higher-order chromatin structure that is present in the interphase nucleus of living cells, probably invoking a different response to the binding of MeCP2. The observed MeCP2-induced *in vivo* chromatin decondensation suggests that polymer cross-linking is not a major activity of MeCP2 in living cells. In mouse myoblasts, over-expression of MeCP2 resulted in chromatin compaction by the clustering of chromocenters during myogenic differentiation, an effect dependent on the MBD of MeCP2 (Brero *et al.*, 2005), whereas in this study chromatin decondensation is achieved by the C-terminal MeCP2 domain. An explanation for the discrepancy between our data and the findings by Brero and colleagues likely relates to the type of chromatin investigated (mouse chromocenters contain specialized repetitive DNA, such as *Alu* and satellite repeats) and the type of MeCP2 domain that is involved, *i.e.* the MBD or the C-terminal domain.

Chromatin restructuring by MeCP2 is independent of transcriptional activation
We show that transcription remains repressed after targeting of MeCP2, despite the fact that the amplified chromatin domain is extensively decondensed, similar to the decondensed chromatin structure induced by targeting the viral activator VP16 (Tumbar *et al.*, 1999). Accordingly, we found no evidence for the presence of activating factors CREB1 or TFIIB that have been previously associated with MeCP2 (Chahrour *et al.*, 2008; Kaludov and Wolffe, 2000). Also RNAPII and epigenetic marks associated with transcriptional competence, *i.e.* H3K4 dimethylation and H4K16 acetylation, were not enhanced upon MeCP2 targeting, confirming that MeCP2-induced decondensation occurs independent of transcription. These observations illustrate a deviation from the canonical model in which condensed chromatin is considered silent and decondensed chromatin is considered active. In concordance with our findings, analysis of the transcriptional activity of sucrose-gradient-isolated chromatin fibers revealed that both transcriptionally active and inactive sites occur in compact as well as in less compact chromatin fibers (Gilbert *et al.*, 2004).

Similar to the epigenetic silencer HP1 which binds to both active and inactive chromatin according to ChIP and DamID (de Wit *et al.*, 2007; Vakoc *et al.*, 2005), MeCP2 has been found associated with both active and inactive neuronal promoters (Yasui *et al.*, 2007). One report argued that MeCP2 can switch the gene expression state to either repression or activation (Chahrour *et al.*, 2008). In light of such a proposed function for MeCP2, the opening up of chromatin by MeCP2 observed in this study could reflect an indeterminate state in which the targeted locus is poised for transcription. Examples of changes in chromatin structure preceding a transcriptional activation have been reported previously for the HoxB and MHC locus (Chambeyron and Bickmore, 2004; Volpi *et al.*, 2000). We propose that by unfolding chromatin structure, MeCP2 switches chromatin from a transcriptionally restrictive to a permissive state. In this scenario, the recruitment of additional activating or repressive factors subsequently decides the transcriptional fate of genes embedded within the permissive chromatin.

MeCP2 and DNA methylation

Several studies hint at a relationship between DNA methylation levels, the presence of methyl-CpG-binding proteins and changes in chromatin structure. In the absence of DNA methylation in mouse embryonic stem cells lacking Dnmt3a and 3b, a genome-wide increase in H3K9me3 and histone acetylation as well as chromocenter clustering is observed (Gilbert *et al.*, 2007). On the other hand, during myogenic differentiation, over-expression of methyl-CpG-binding proteins induced increased DNA methylation levels and chromocenter clustering, independent of the H3K9 histone methylation pathway and requiring the MBD domain of MeCP2 (Brero *et al.*, 2005). Our data do not implicate a role for DNA methylation in the MeCP2-induced chromatin restructuring, which is not surprising considering that the C-terminal domain and not the MBD of MeCP2 is the prominent domain involved in decondensation. These findings demonstrate that the causal relationship between MeCP2, DNA methylation levels and changes in chromatin structure are still unclear.

Eviction of HP1γ upon MeCP2 binding

Interestingly, we find that MeCP2 inhibits HP1γ binding at the chromosomal array. Our FRAP analysis shows that HP1γ is retained at the array in the absence of MeCP2 targeting, possibly due to the heterochromatic nature of the amplified array. Indeed, we measure similar kinetics of HP1γ at the array as previously measured at heterochromatic sites in mouse cells (Cheutin *et al.*, 2003; Schmiedeberg *et al.*, 2004). Surprisingly, MeCP2 binding triggers the release of HP1γ, reflected by the loss of local HP1γ accumulation at the amplified array after MeCP2 targeting and by the globally altered HP1γ mobility upon MeCP2 over-expression. Strikingly, HP1α and β, which are essential for HP1γ recruitment to heterochromatic sites, are still present at the amplified domain (Dialynas *et al.*, 2007). Possibly, MeCP2 inhibits HP1γ binding by steric hindrance or by structurally changing the substrate through chromatin decondensation. Displacement of HP1γ was previously observed preceding transcriptional activation at a luciferase reporter gene integrated in breast cancer cells (Vicent *et al.*, 2008). Here, a hormonal signaling cascade leads to phosphorylation of H3S10, displacement of HP1γ and subsequent ATP-dependent chromatin remodeling, providing an open chromatin structure as 'landing platform' for the transcription machinery (Vicent *et al.*, 2008). It is tempting to speculate that the eviction of HP1γ and decondensation of the chromosomal array after MeCP2 binding are part of a mechanism to prepare chromatin for transcriptional changes.

Our results show that MeCP2 is an architectural protein that has the ability to unfold condensed chromatin, while maintaining transcriptional silencing. We propose that MeCP2 is a versatile protein that affects higher-order chromatin structure in order to prepare genomic domains for changes in gene expression.

Acknowledgements

We thank Wim de Leeuw for help on the operation of the Huygens software, Suzanne Kooistra for performing the luciferase reporter assay measurements and Federico Tessadori for critical reading of the manuscript. Plasmids MeCP2-mRFP and MeCP2-EGFP were received from C. Cardoso (Berlin, Germany), EGFP-HP1 plasmids from P. Hemmerich (Jena, Germany; Schmiedeberg *et al.*, 2004), EGFP-TFIIB from Danyang Chen (Sui Huang Lab, Chicago, USA), EGFP-RNAPII from W. Vermeulen (Rotterdam, the Netherlands), EGFP-CREB1 from H. Eldar-Finkelman (Tel Aviv, Israel), mCherry-PCNA from C. Dinant (Rotterdam, the Netherlands; Dinant *et al.*, 2007) and EGFP-H1 from N.P. Dantuma (Karolinska Institutet, Stockholm). This work was supported by the Netherlands Organisation for Scientific Research (NWO, project number VIDI2003/03921/ALW/016.041.311).

Chapter 3

Truncated HP1 lacking a functional chromodomain induces heterochromatinization upon *in vivo* targeting

Maartje C. Brink, Yme van der Velden, Wim de Leeuw, Julio Mateos-Langerak, Andrew S. Belmont, Roel van Driel & Pernette J. Verschure

Adapted from Histochem Cell Biol, 125:53-61 (2006)

Abstract

Packaging of the eukaryotic genome into higher-order chromatin structures is tightly related to gene expression. Pericentromeric heterochromatin is typified by accumulations of heterochromatin protein 1 (HP1), methylation of histone H3 at lysine 9 (MeH3K9) and global histone deacetylation. HP1 interacts with chromatin by binding to MeH3K9 through the chromodomain (CD). HP1 dimerizes with itself and binds a variety of proteins through its chromoshadow domain. We have analyzed at the single-cell level whether HP1 lacking its functional CD is able to induce heterochromatinization *in vivo*. We used a lac operator-array-based system in mammalian cells to target EGFP-lac repressor-tagged truncated HP1α and HP1β to a lac operator-containing gene-amplified chromosome region in living cells. After targeting truncated HP1α or HP1β we observe enhanced tri-MeH3K9 and recruitment of endogenous HP1α and HP1β to the chromosome region. We show that CD-less HP1α can induce chromatin condensation, whereas the effect of truncated HP1β is less pronounced. Our results demonstrate that after lac repressor-mediated targeting, HP1α and HP1β without a functional CD are able to induce heterochromatinization.

Introduction

In the eukaryotic nucleus, various levels of chromatin packaging can be discerned (Horn and Peterson, 2002). The condensation state of chromatin is a key aspect of epigenetic gene control. Different chromatin condensation states are related to the presence or absence of proteins involved in the regulation of gene expression (reviewed in Lachner and Jenuwein, 2002). Pericentromeric heterochromatin, for instance, is typified by the accumulations of heterochromatin protein 1 (HP1), methylation of histone H3 at lysine 9 (MeH3K9) and global histone deacetylation (reviewed in Dillon, 2004; Maison and Almouzni, 2004). The molecular mechanisms underlying the structural and functional aspects of heterochromatin are still unresolved.

In mammals, three isoforms of HP1 have been identified, HP1α, HP1β and HP1γ, showing different subnuclear distributions. HP1α is primarily found in pericentromeric heterochromatin. HP1β and to a much lesser extent HP1γ are also present in pericentromeric heterochromatin (Cowell *et al.*, 2002; Horsley *et al.*, 1996; Li *et al.*, 2003; Minc *et al.*, 1999; Wreggett *et al.*, 1994). HP1 proteins have emerged as key structural and regulatory components for the assembly of compact chromatin (Maison and Almouzni, 2004). HP1 consists of a chromodomain (CD) at the amino terminus and a chromoshadow domain (CSD) at the carboxy terminus, separated by a hinge domain (HD). The CD recognizes MeH3K9, mediating binding to chromatin (Bannister *et al.*, 2001; Cowell *et al.*, 2002; Jacobs and Khorasanizadeh, 2002; Jacobs

et al., 2001; Lachner *et al.*, 2001; Nielsen *et al.*, 2002). The CSD interacts with a consensus peptide that is present in a number of proteins, including the CSD of HP1 itself, thereby targeting proteins to heterochromatin and forming HP1 dimers (Thiru *et al.*, 2004). The conserved CD and CSD are essential for the function of HP1. The HD of HP1 is less well characterized; a few studies indicate that it plays a direct role in HP1 function (Meehan *et al.*, 2003).

Recently, we showed that targeting of intact HP1α and HP1β is sufficient to induce large-scale chromatin compaction, enhanced tri-MeH3K9 and recruitment of proteins involved in heterochromatinization (Verschure *et al.*, 2005). In the present study, we investigate whether HP1 that lacks a functional CD is able to induce heterochromatinization. Our results demonstrate that when HP1α or HP1β without a functional CD is targeted to chromatin, it is able to induce heterochromatinization.

Materials and methods

Construction of plasmids

A plasmid expressing the enhanced green fluorescent protein (EGFP)-dimer lac repressor-simian virus 40 nuclear localization signal (NLS) fusion protein under control of the F9-1 promoter, called p3'SS-EGFP-dimer lac repressor was used as the basis for these studies (Tumbar *et al.*, 1999). This plasmid was modified as described previously to generate EGFP-lacR-*AscI*-NLS (NYE4; Nye *et al.*, 2002). HP1α and HP1β correspond to full sequences of the human HP1. Both human HP1α and HP1β have only a minor amino acid difference from the Chinese hamster HP1α and HP1β (for HP1β one amino acid difference in the hinge domain and for HP1α one amino acid difference in the CD, two in the HD and two outside of the domains). HP1α-Δ(2-39) and HP1β-Δ(2-40) have deletions of amino acids 2 to 39 and 2 to 40 in HP1α and HP1β, respectively. These proteins lack a large part of the CD, including V21 (HP1α) and V23 (HP1β), which are required for MeH3K9 binding (Bannister *et al.*, 2001; Lachner *et al.*, 2001; Platero *et al.*, 1995). Full-length HP1α and HP1β as well as HP1α-Δ(2-39) and HP1β-Δ(2-40) fragments were PCR amplified using primers that contain *AscI* sites in frame. The PCR products were digested with *AscI* and ligated into the *AscI*-digested EGFP-lacR-*AscI*-NLS (NYE4) vector to create full-length HP1α and HP1β as well as HP1α-Δ(2-39) and HP1β-Δ(2-40) C-terminal in-frame fusions with the EGFP-lacR-*AscI*-NLS (NYE4) vector. All regions of constructs that had undergone PCR were sequenced to ensure fidelity.

Cell culture and transfection assay

We used the CHO-derived cell line RRE_B1, which contains large amplified genomic domains (several tens of mega basepairs) consisting of arrays of lac operator binding sites, in an extended, often fibrillar conformation, suggesting a euchromatin-like structure (Robinett *et al.*, 1996a). The *in situ* appearance of the RRE_B1 cell line as visualized with the light microscope is described in detail in Verschure *et al.* (2005). Cells were cultured in F12 Ham's media without hypoxanthine or thymidine supplemented by 10% dialyzed fetal bovine serum (HyClone Labs, Logan, Utah, USA) and 10 μM methotrexate at 37°C in a 5% CO_2 atmosphere. Transient transfections were performed with FuGENE6 reagent (Roche, Indianapolis, IN, USA) according to the manufacturer's instructions, using 500 ng of DNA and 6 μl FuGENE6 reagent per milliliter of culture medium using cells growing on coverslips. Fresh medium was added 24 hours after transfection. After 48 hours, cells were rinsed with phosphate buffered saline (PBS) and used for immunofluorescent labeling.

Immunofluorescent labeling

Immunofluorescent labeling was performed as described previously (Verschure *et al.*, 2002). Briefly, cells were fixed for 10 minutes at 4°C in 2% (w/v) formaldehyde in PBS. After fixation, cells were permeabilized

with 0.5% (w/v) Triton-X 100 in PBS for 5 minutes and incubated in PBS containing 100 mM glycine for 10 minutes. Subsequently, cells were incubated for 1 hour at 37°C with the primary antibodies diluted in PBG: PBS containing 0.5% (w/v) bovine serum albumin (BSA) and 0.1% (w/v) gelatin (Sigma, St Louis USA). The following primary antibodies were used: rabbit anti-tri-MeH3K9 (Nakayama *et al.*, 2001), mouse anti-HP1α and anti-HP1β (Euromedex; Mundolsheim France; Nielsen *et al.*, 2001). After several washes with PBS, cells were incubated with the appropriate secondary antibodies, using Cy3-conjugated donkey anti-rabbit antibody or Cy3-conjugated donkey anti-mouse antibody (Jackson, West Grove, PA, USA). Secondary antibodies were diluted in PBG. Incubations were performed for 1 hour at room temperature. Cells were then rinsed with PBS at room temperature and DNA staining was performed with 0.4 μg/ml DAPI 33258 (Sigma) in PBS. Slides were mounted in Vectashield (Brunschwig, Burlingame, CA, USA), stored at 4°C and analyzed within 24 hours. As a control, the primary antibody was omitted.

Confocal scanning laser microscopy
All experiments were performed at least twice in duplicate. Images were recorded using a Zeiss LSM 510 (Zeiss, Jena, Germany) confocal laser scanning microscope, equipped with a 100x/1.23 NA oil immersion objective. We used an argon laser at 488 nm in combination with a helium neon laser at 543 nm to excite green and red fluorochromes simultaneously. Emitted fluorescence was detected with a 505-530 nm bandpass filter for the green signal and a 560 nm longpass filter for the red signal. Three-dimensional (3D) images were scanned as 512x512x32 voxel images (sampling rate: 49 nm lateral and 208 nm axial).

Image analysis
For a semi-quantitative analysis of the spatial relationship between the relative spatial distributions of components in dually labeled cells, line scans were made. The signal intensities of the two labels are plotted along a line through the nucleus. The line scan method provides a rapid and straightforward way to determine to what extent two components colocalize. To quantitatively analyze changes in large-scale chromatin structure, we applied 3D-image-analysis tools as described in a previous study (Verschure *et al.*, 2005). Briefly, 3D images of the amplified chromosome region were acquired and attributes of the 3D structure were determined. A region of interest, *i.e.* the EGFP-labeled chromosome region, is defined. The images were Gaussian filtered to reduce noise with a size of 20 pixels (σ = 250 nm). For each set we record the intensity gradient over the chromatin region. The distribution of the intensity gradient is plotted in a box-plot. The second and third quartiles of the observed values are within the box, the median value is shown by the thick horizontal line, the vertical small lines show the first and fourth quartile of the observed values. We used the Wilcoxon non-parametric test to calculate the *P*-value giving the probability that two populations are different from each other.

Results

Experimental approach

To investigate the ability of HP1 lacking a functional CD to induce heterochromatinization, we used the CHO cell line RRE_B1. This cell line contains a large amplified chromatin region consisting of arrays of lac operator binding sites (Robinett *et al.*, 1996). When visualized *in vivo* by binding of EGFP-tagged lac repressor (lacR), the amplified region occupies a large nuclear area and displays an open chromatin structure, suggesting a euchromatin-like state (Robinett *et al.*, 1996). These cells constitute a useful system to investigate euchromatin/heterochromatin transitions. In a previous study, we have shown that targeting of full-length HP1α or HP1β to the lac operator arrays induced chromatin compaction, enhanced tri-MeH3K9 and the recruitment of endogenous HP1 and the histone methyltransferase SETDB1

(Verschure *et al.*, 2005). These results demonstrated that HP1 binding is sufficient to trigger heterochromatinization.

DNA constructs were made encoding truncated human HP1α and HP1β, lacking the C-terminal part of their CD, tagged with EGFP-lacR: EGFP-lacR-HP1α-Δ(2-39) and EGFP-lacR-HP1β-Δ(2-40). Two controls were used: (1) similar constructs that code for full-length wild-type HP1α and HP1β instead of the truncated protein and (2) a construct coding for EGFP-lacR. Proteins coded by all constructs bind to the amplified chromatin region via their lacR domain. As expected, after transient transfection in cells without lacR-binding sites, CD-less HP1 does not accumulate in pericentromeric heterochromatin, since it lacks the binding site for MeH3K9 (data not shown). In contrast, EGFP-lacR full-length HP1 does accumulate in pericentromeric domains (Verschure *et al.*, 2005). These findings agree with the notion that the CD is responsible for localization of HP1α and HP1β in pericentromeric heterochromatin through MeH3K9 binding (Bannister *et al.*, 2001; Cheutin *et al.*, 2003; Jacobs *et al.*, 2001; Lachner *et al.*, 2001; Nakayama *et al.*, 2001; Nielsen *et al.*, 2002).

To analyze whether targeting of truncated HP1 results in changes in the chromatin structure we measured three different parameters: (1) tri-MeH3K9 using immunofluorescent labeling with an anti-tri-MeH3K9-specific antibody, (2) accumulation of endogenous HP1α or HP1β and (3) changes in *in vivo* 3D chromatin structure of the EGFP-marked amplified chromatin domain, imaged by confocal microscopy followed by quantitative image analysis.

Histone H3 lysine 9 methylation

MeH3K9 creates a binding site for the CD of HP1, whereas the CSD interacts with a variety of proteins, including HP1 itself (Aasland and Stewart, 1995; Bannister *et al.*, 2001; Cowell *et al.*, 2002; Jacobs and Khorasanizadeh, 2002; Jacobs *et al.*, 2001; Lachner *et al.*, 2001; Lechner *et al.*, 2005; Nielsen *et al.*, 2002; Smothers and Henikoff, 2001; Thiru *et al.*, 2004). Recently, we showed that lacR-mediated targeting of full-length HP1α or HP1β results in strong heterochromatinization, including an increase of tri-MeH3K9 and recruitment of HP1 and a histone methyltransferase (Verschure *et al.*, 2005). Figure 1 shows that in cells transfected with EGFP-LacR-HP1α-Δ(2-39) or EGFP-LacR-HP1β-Δ(2-40) the level of tri-MeH3K9 is considerably increased in the amplified chromatin domain. In addition, tri-MeH3K9 is present diffusely throughout the nucleus. Line scans confirm that enhanced methylation levels colocalize with the binding of CD-less HP1 to the chromatin array. This phenomenon is observed in all the cells transfected with either full-length (Verschure *et al.*, 2005) or truncated HP1α or HP1β (figure 1). In control cells transfected with EGFP-lacR the methylation level is not changed (figure 1A-D). These observations show that CD-less HP1 is able to recruit a histone methyltransferase directly or indirectly , similar to wild-type HP1.

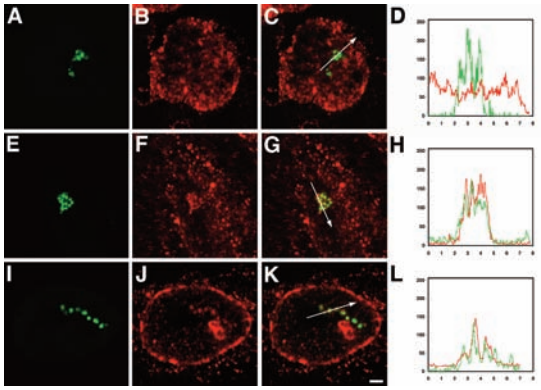

Figure 1. Enhanced tri-MeH3K9 at the amplified chromosome region. RRE_B1 cells transfected with EGFP-lacR (as a control) (A-D), EGFP-lacR-HP1α-Δ(2-39) (E-H) or EGFP-lacR-HP1β-Δ(2-40) (I-L), were immunofluorescently labeled with an antibody against tri-MeH3K9 after 48 hours. The green signal shows the EGFP-tagged chromosomal array and the red signal marks the distribution of the immunolabeled tri-MeH3K9. Three-dimensional images were recorded. Images shown are individual mid-nuclear optical sections. Figure D, H and L show line scans through the nuclei shown in A-C, E-G and I-K, respectively. The position of the line scans is shown by the white arrow. Nuclei in A-C, E-G and I-K are the same scale; bar represents 2 μm.

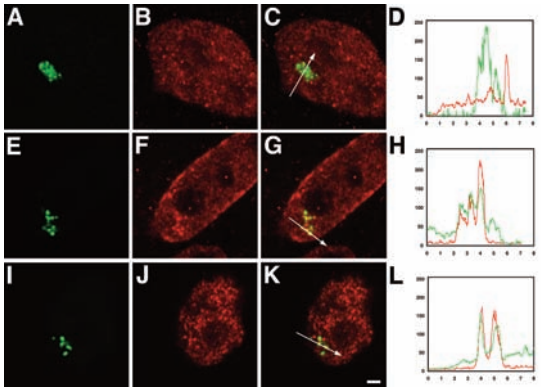

Figure 2. Recruitment of endogenous HP1 at the amplified chromosome region. RRE_B1 cells transfected with EGFP-lacR (A-D), EGFP-lacR-HP1α-Δ(2-39) (E-H) or EGFP-lacR-HP1β-Δ(2-40) (I-L) were immunofluorescently labeled after 48 hours with an antibody against HP1β (A-D) and (E-H) or against HP1α (I-L). Three-dimensional images were recorded. Images shown are individual mid-nuclear optical sections. The green signal shows the EGFP-lacR-tagged chromosomal array and the red signal marks the distribution of the immunolabeled endogenous HP1 proteins. Figure D, H and L show line scans through the nuclei shown in A-C, E-G and I-K, respectively. The position of the line scans is shown by the white arrow. Nuclei in A-C, E-G and I-K are the same scale; bar represents 2 μm.

Recruitment of endogenous HP1

LacR-mediated targeting of wild-type HP1α or HP1β results in local accumulation of endogenous HP1α and HP1β at the chromatin array. Here we analyze whether targeting of HP1 without a functional CD has the same effect. Cells transfected with EGFP-LacR-HP1α-Δ(2-39) were fluorescently labeled with an antibody against HP1β, and cells transfected with EGFP-LacR-HP1β-Δ(2-40) with an antibody specific for HP1α. Figure 2 shows that both the truncated proteins are able to recruit a considerable amount of endogenous HP1 to the amplified chromatin domains. Line scans confirm that endogenous HP1 accumulates at the sites where the CD-less HP1 protein is bound

(figure 2). In control cells transfected with EGFP-lacR the distribution of endogenous HP1 is not changed (figure 2A-D). These results indicate that targeting of HP1 without the CD domain enables the recruitment of endogenous HP1.

Large-scale chromatin structure

In a recent study, we showed that lacR-mediated binding of wild-type HP1 induces considerable chromatin compaction (Verschure *et al.*, 2005). Figure 3 shows that HP1 without a functional CD is also able to induce a similar condensation of chromatin, as can be visualized by confocal microscopy of the EGFP-tagged amplified chromatin domain. In many cells targeting of truncated HP1 induces condensation of the amplified chromatin regions in a cluster or chain of highly condensed spherical chromatin domains. There is significant variability in the appearance of the chromatin domains in a population of otherwise identical cells for full-length HP1 (Verschure *et al.*, 2005), for CD-less HP1 and for control cells (figure 3). Therefore, we carried out a quantitative analysis of the change in compaction of the chromatin structure of the array. As a measure for the degree of compaction we used a parameter that quantifies the discreteness of the individual subdomains in the amplified chromatin domain (Verschure *et al.*, 2005). In control cells transfected with EGFP-lacR, such subdomains are poorly discernable (figure 3A). In contrast, after HP1-induced chromatin condensation (either wild-type or truncated HP1), the individual domains can be clearly discerned (figure 3B-E). As a quantitative parameter we measured the gradient of the EGFP signal over such chromatin subdomains. The analysis was carried out on 3D images using novel image-analysis software as described in greater detail by Verschure *et al.* (2005). For each experiment several tens of cells were analyzed (*n*-values are shown in table 1).

Results are summarized in figure 4 and table 1. Figure 4 shows the median value (thick horizontal line) of the observed values, the second and third quartiles (open box) and the first and fourth quartiles of the detected values (thin vertical lines). The results confirm the large cell-to-cell variation observed earlier (Verschure *et al.*, 2005). Statistical analysis (Wilcoxon test; table 1) shows that CD-less HP1α induces significant chromatin condensation, similar to wild-type HP1α and HP1β. Although condensed chromatin is seen in a number of cells transfected with EGFP-LacR-HP1β-Δ(2-40), the difference with the control cell population (transfected with EGFP-lacR) is statistically not significant. This suggests that CD-less HP1α is more effective in condensing chromatin than CD-less HP1β. In contrast, both truncated proteins are similarly effective in inducing enhanced tri-MeH3K9 and in recruiting endogenous HP1 according to light-microscopy evaluation (figures 1 and 2). Unexpectedly, our results also show that the effect of chromatin condensation after targeting full-length HP1α is more pronounced than the effect of full-length HP1β. Apparently, both wild-type HP1α and CD-less HP1α are more effective than their HP1β counterparts.

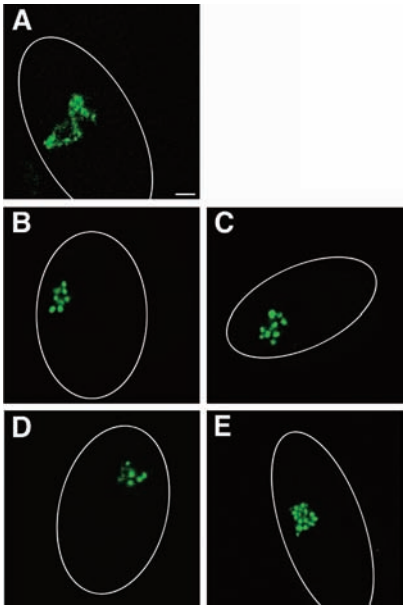

Figure 3. Local chromatin compaction of the amplified chromosome region. RRE_B1 cells were transfected with EGFP-lacR-HP1α, EGFP-lacR-HP1β, EGFP-lacR-HP1α-Δ(2-39) or EGFP-LacR-HP1β-Δ(2-40) fusion constructs or with EGFP-lacR as a control. Three-dimensional images were collected 48 hours after transfection. Images shown represent individual mid-nuclear optical sections illustrating the EGFP signal of the amplified chromosome region. The chromosomal array in a control nucleus transfected with EGFP-lacR (A) has the appearance of an extended fibrillar structure. After HP1α (B) or HP1β (C) targeting, the amplified chromosome region is compacted to a cluster of distinct spherical subdomains. After targeting of HP1α-Δ(2-39) (D) or HP1β-Δ(2-40) (E) similar compaction of the large-scale chromatin structure was observed. The approximate position of the nuclear envelope is shown by the white line. Nuclei in A-E are the same scale; bar represents 0.9 μm.

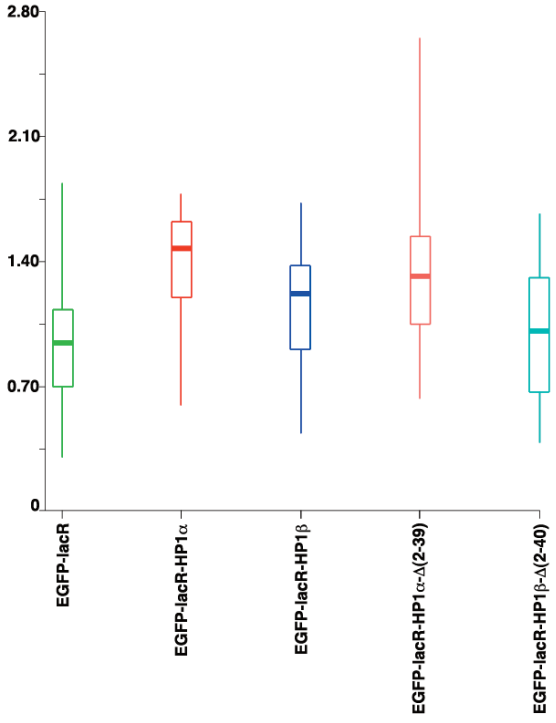

Figure 4. Quantitative analysis of the change in chromatin structure. Three-dimensional images of RRE_B1 cells transfected with EGFP-lacR-HP1α, EGFP-lacR-HP1β, EGFP-lacR-HP1α-Δ(2-39),EGFP-lacR-HP1β-Δ(2-40) or EGFP-lacR as a control were acquired 48 hours after transfection. We measured the gradient of the EGFP-signal intensity over the amplified chromosome region. The results are shown as a box-plot of the measured values for cells transfected with EGFP-lacR (green), EGFP-lacR-HP1α (dark red), EGFP-lacR-HP1β (dark blue), EGFP-lacR-HP1α-Δ(2-39) (orange) and EGFP-lacR-HP1β-Δ(2-40) (light blue). The second and third quartiles of the observed values are within the box (open box), the median value is shown by the thick horizontal line, the vertical small lines show the first and fourth quartiles of the observed values.

Discussion

Heterochromatin is a specialized chromatin state that is typically condensed, late replicating, and displays a diminished gene activity. The HP1 protein family is involved in the formation of heterochromatin. The observation that HP1 specifically binds to MeH3K9 via its chromodomain (CD), directly links these proteins to epigenetic gene-control mechanisms (Lachner and Jenuwein, 2002). In the present study we analyze *in vivo* and at the single-cell level whether HP1 that lacks a functional CD can induce heterochromatinization. We use three parameters to assess euchromatin/heterochromatin transitions: (1) enhanced tri-MeH3K9, (2) recruitment of endogenous HP1α and HP1β, and (3) condensation of chromatin. Results show that CD-less HP1α and HP1β are able to cause tri-MeH3K9 and recruitment of endogenous HP1α and HP1β. Targeting of truncated HP1α induces chromatin compaction, similar to what is observed after targeting full-length HP1α and HP1β (Verschure *et al.*, 2005). The effect of truncated HP1β is less pronounced. Our data demonstrate that both CD-less HP1α and CD-less HP1β are able to induce heterochromatinization, CD-less HP1α being more effective than CD-less HP1β.

Table 1

Populations analyzed	number of cells	*P*-value	significant
Control – wild-type HP1α	57 - 27	< 0.0001	yes
Control – wild-type HP1β	57 - 53	0.001	yes
Control – CD-less HP1α	57 - 27	< 0.0001	yes
Control – CD-less HP1β	57 - 29	0.29	no
Wild-type HP1α – wild-type HP1β	27 - 53	0.0008	yes

Table 1. Statistical evaluation of the structural analysis. Statistical evaluation of the differences in chromatin structure after targeting EGFP-lacR-tagged constructs; differences between control cells transfected with EGFP-lacR and cells transfected with EGFP-lacR-HP1α, EGFP-lacR-HP1β, EGFP-LacR-HP1α-Δ(2-39) or EGFP-LacR-HP1β-Δ(2-40) (rows 1 through 4) and between EGFP-lacR-HP1α and EGFP-lacR-HP1β (row 5). Shown are the *P*-values determined in a Wilcoxon statistical test, indicating the probabilities that two populations (column 1) are different, the number of cells that were analyzed (column 2) and the interpretation in terms of significance of the difference, choosing a cut-off value of P=0.05 (column 3 and 4).

Comparison of HP1α and HP1β

In the present study, we compared the effect of targeting HP1α with that of HP1β (both wild-type and CD-less HP1 proteins) on heterochromatinization of an amplified chromatin region. Results show that the effect of chromatin condensation after targeting full-length HP1α is more pronounced than that of full-length HP1β. Similarly, CD-less HP1α is more effective in inducing chromatin compaction than truncated HP1β. In contrast, both proteins are similarly effective in inducing enhanced tri-MeH3K9 and in recruiting endogenous HP1. The cause of this difference between HP1α and HP1β in their ability to induce chromatin compaction is unclear. The amino

acid sequence of both proteins differs only marginally (Minc *et al.*, 1999). In the present study, we used human HP1 in Chinese hamster cells, but there is only a minor amino acid difference between human HP1α and HP1β and Chinese hamster HP1α and HP1β (see materials and methods). Therefore, it is unlikely that the difference in effect between HP1α and HP1β is related to less efficient binding of the human HP1 in Chinese hamster cells. The difference in effect between HP1α and HP1β is probably related to the fact that HP1α and HP1β have distinct nuclear and mitotic distributions and differ in cell cycle-related phosphorylation (Minc *et al.*, 1999). HP1α is phosphorylated throughout the cell cycle, whereas HP1β remains unphosphorylated. HP1α and HP1β are predominantly located in centromeric heterochromatin. A third member of the HP1 family, HP1γ is found in euchromatin and to a much lesser extent in heterochromatin. In a recent study, using a dominant-negative approach by over-expressing truncated HP1 lacking a functional CD, we show that endogenous HP1α or HP1β are lost from mouse chromocenters without changing their condensed chromatin structure (Mateos-Langerak *et al.*, 2007; chapter 4 of this thesis). Together, these observations indicate that full-length HP1α and HP1β as well as CD-less HP1α and HP1β are sufficient to induce heterochromatinization, but are not necessarily required to maintain the condensed state.

Three HP1 domains

The CD of HP1 recognizes MeH3K9 and is essential for the association of HP1 with heterochromatin. HP1 can form homodimers and bind a variety of other proteins through its CSD (Aasland and Stewart, 1995; Bannister *et al.*, 2001; Cowell *et al.*, 2002; Jacobs and Khorasanizadeh, 2002; Jacobs *et al.*, 2001; Lachner *et al.*, 2001; Lechner *et al.*, 2005; Nielsen *et al.*, 2002; Smothers and Henikoff, 2001; Thiru *et al.*, 2004). It is known from *in vitro* studies that HP1 also binds to DNA and linker histones through its HD (Meehan *et al.*, 2003). Furthermore, the HD is involved in targeting HP1 to heterochromatin through an RNA binding activity (Muchardt *et al.*, 2002).

It is generally assumed that the interaction of HP1 with MeH3K9 facilitates the formation of heterochromatin and represses gene activity (Lachner *et al.*, 2001). Our results show that when HP1 without a functional CD is targeted to chromatin, here via the lac repressor/lac operator interaction, its ability to induce heterochromatin is maintained. This indicates that the CSD and HD are sufficient to recruit and bind the protein factors required for the heterochromatinization process. Interestingly in this context, Stewart *et al.* (2005) recently showed that H3K9 methylation and HP1 can also act independently. Probably, incorporation of HP1 into heterochromatin is a multi-step process, involving interactions with histone methyltransferases, binding to MeH3K9 and possibly stabilization by RNA components (Maison and Almouzni, 2004; Muchardt *et al.*, 2002). Our data suggest that the complex process of heterochromatin formation does not require the CD domain if HP1 is bound to chromatin in a CD-independent manner.

Acknowledgements

We are grateful to dr. P. B. Singh, for kindly providing us with the antibodies used in the present study. Confocal microscopy was performed at the Centre for Advanced Microscopy, we gratefully thank dr. E. M. M. Manders for expert assistance. This work was supported by the Netherlands Organisation for Scientific Research (NWO; project number VIDI2003/03921/ALW/016.041.311).

Chapter 4

Pericentromeric heterochromatin domains are maintained without accumulation of HP1

Julio Mateos-Langerak, Maartje C. Brink, Martijn S. Luijsterburg, Ineke van der Kraan, Roel van Driel & Pernette J. Verschure

Adapted from Mol Biol Cell, 18:1464-71 (2007)

Abstract

The heterochromatin protein 1 (HP1) family is thought to be an important structural component of heterochromatin. HP1 proteins bind via their chromodomain to nucleosomes methylated at lysine 9 of histone H3 (H3K9me). To investigate the role of HP1 in maintaining heterochromatin structure we used a dominant-negative approach by expressing truncated HP1α or HP1β proteins lacking a functional chromodomain. Expression of these truncated HP1 proteins individually or in combination resulted in a strong reduction of the accumulation of HP1α, HP1β and HP1γ in pericentromeric heterochromatin domains in mouse 3T3 fibroblasts. The expression levels of HP1 did not change. The apparent displacement of HP1α, HP1β and HP1γ from pericentromeric heterochromatin did not result in visible changes in the structure of pericentromeric heterochromatin domains, as visualized by DAPI staining and immunofluorescent labeling of H3K9me. Our results show that the accumulation of HP1α, HP1β and HP1γ at pericentromeric heterochromatin domains is not required to maintain DAPI-stained pericentromeric heterochromatin domains and the methylated state of histone H3 at lysine 9 in such heterochromatin domains.

Introduction

The HP1 (heterochromatin protein 1) gene was first discovered in Drosophila melanogaster as a mutant suppressing position-effect variegation, a phenomenon in which a gene adjacent to a heterochromatin domain shows a mosaic expression pattern (Eissenberg *et al.*, 1990; Festenstein *et al.*, 1999; James and Elgin, 1986). Since then, a variety of HP1 homologues has been found in many eukaryotes (Li *et al.*, 2002). There are at least three HP1 proteins in mammals. HP1α and HP1β are present in heterochromatic regions, whereas HP1γ has been found either exclusively in euchromatin or in both euchromatin and heterochromatin (Cheutin *et al.*, 2003; Horsley *et al.*, 1996; Minc *et al.*, 1999; Minc *et al.*, 2000; Wreggett *et al.*, 1994). HP1 proteins are thought to have a role in gene regulation in a broad range of eukaryotes: from fission yeast to mammals (Hediger and Gasser, 2006; Hiragami and Festenstein, 2005).

The HP1 gene products are proteins of ~180 amino acids, containing two protein-binding domains linked by a flexible hinge region. The chromodomain (CD) located at the N-terminal side of the hinge region specifically binds histone H3 methylated at lysine 9 (H3K9me; Bannister *et al.*, 2001; Jacobs and Khorasanizadeh, 2002; Lachner *et al.*, 2001), which is a marker for heterochromatin and is related to gene silencing (Cowell *et al.*, 2002; Sims *et al.*, 2003). HP1 is able to repress gene activity when artificially targeted to a site near a reporter gene (van der Vlag *et al.*, 2000). The

C-terminal part of HP1 contains the chromoshadow domain (CSD), which is partially homologous to the CD (Aasland and Stewart, 1995; Sims *et al.*, 2003). The CSD binds to a consensus peptide that is present in a number of proteins, including the CSD of HP1 itself, thereby targeting proteins to heterochromatin and forming HP1 dimers (Brasher *et al.*, 2000; Li *et al.*, 2002; Nielsen *et al.*, 2001; Smothers and Henikoff, 2000; Thiru *et al.*, 2004). Finally, HP1 can bind RNA, probably through its hinge region. RNA binding is important for the binding of the protein to pericentromeric heterochromatin (Muchardt *et al.*, 2002). HP1 proteins are assumed to have a structural role in defining the condensed heterochromatin state. HP1 dimers may bridge nucleosomes in heterochromatin via H3K9me, resulting in a compact chromatin structure (Jenuwein, 2001; Lachner and Jenuwein, 2002; Nielsen *et al.*, 2001; Singh and Georgatos, 2002). However, there is no direct evidence that HP1 is an essential component of heterochromatin (Singh and Georgatos, 2002). In mouse fibroblasts, pericentromeric heterochromatin constitutes conspicuous nuclear domains that can be visualized by DAPI staining. HP1 proteins are highly accumulated in these domains. A large fraction of the HP1 in heterochromatin domains rapidly exchanges with nucleoplasmic HP1, whereas a small fraction exchanges slowly, as shown by FRAP and FCS studies (Cheutin *et al.*, 2003; Festenstein *et al.*, 2003; Schmiedeberg *et al.*, 2004).

In this study we investigate whether HP1 accumulation is essential for maintaining pericentromeric heterochromatin domains that can be visualized by DAPI staining in mouse fibroblasts. Using a dominant-negative approach in which truncated forms of HP1α and HP1β that lack a functional chromodomain are over-expressed, we show that the apparent displacement of HP1α, HP1β and HP1γ from pericentromeric heterochromatin does not result in visible changes in large-scale chromatin structure of DAPI-stained heterochromatin domains and in H3K9me levels of such domains. Results indicate that the accumulation of HP1α, HP1β or HP1γ at pericentromeric heterochromatin is not required to maintain DAPI-stained pericentromeric heterochromatin domains and the methylated state of histone H3 at lysine 9 in such heterochromatin domains.

Materials and Methods

DNA constructs

HP1α and HP1β denote the full-length sequences of the human HP1s. HP1α-Δ(2-39) and HP1β-Δ(2-40) have deletions of amino acids 2 to 39 and 2 to 40 in HP1α and HP1β, respectively. These proteins lack a large part of the chromodomain, including V21 (HP1α) and V23 (HP1β), which are required for MeH3K9 binding (Bannister *et al.*, 2001; Lachner *et al.*, 2001; Platero *et al.*, 1995). HP1α, HP1β, HP1α-Δ(2-39) and HP1β-Δ(2-40) fragments were PCR-amplified and cloned into a tetracycline-inducible vector (pUHD10-3; Gossen and Bujard, 1992) at the N-terminal end of an inserted flag-tag. The truncated HP1β-Δ(2-40) DNA fragment was digested with *EcoRI* and *BamHI* and inserted into pmCherry-C1 (Shaner *et al.*, 2004) resulting in pmCherry-HP1β-Δ(2-40). EGFP-tagged HP1β was kindly provided by drs L. Schmiedeberg and

P. Hemmerich (Schmiedeberg *et al.*, 2004).

Cell culture and transfection
NIH/3T3 mouse fibroblasts were cultured in DMEM supplemented with 10% tetracycline-free fetal bovine serum (BD Biosciences, Clontech, San Jose, CA, USA) in a 5% CO_2 atmosphere. Cells were grown on cover slips coated with Alcian blue 8GS (Fluka, Buchs, Switzerland). Cells were transfected using FuGENE6 (Roche, Basel, Switzerland) by adding 0.5 µg DNA of each plasmid and 6 µl of FuGene6 reagent per milliliter culture medium. Fibroblasts were cotransfected with pUHD15-1, containing the tTA gene, necessary for the Tet-ON system (Gossen and Bujard, 1992). We used pEGFP-C1 (BD Biosciences-Clontech) for expressing enhanced green fluorescent protein (EGFP). NIH/3T3 cells stably expressing EGFP-tagged HP1β were selected using 800 µg/ml G418. A low-expressing cell population was sorted by FACS analysis. Cells expressing EGFP-HP1β were transiently transfected with pmCherry-HP1β-Δ(2-40) and analyzed between 24 and 48 hours after transfection.

Immunolabeling and DAPI staining
Cells growing on cover slips were washed twice with PBS and fixed with 2% formaldehyde for 15 minutes at RT and permeabilized with 0.5% (w/v) Triton X-100 in PBS for 5 minutes. Residual aldehyde groups were blocked for 10 minutes with 0.1 M glycine PBS at RT. Incubation with primary antibodies in PBG (0.5% (w/v) BSA, 0.1% (w/v) gelatin in PBS) was performed for 2 hours at RT and with the secondary antibodies for 1 hour in the same buffer at RT. DAPI staining was carried out by incubation for 5 minutes in 0.4 µg/ml DAPI in PBS.

Antibodies
To detect flag-tagged proteins we used rabbit anti-flag and mouse anti-flag M2 (Sigma-Aldrich, Zwijndrecht, The Netherlands). To detect HP1α mouse anti-HP1α (MaHP1α; Euromedex, Mundolsheim, France; Nielsen *et al.*, 1999) and rabbit anti-HP1α (RaHP1α; Kourmouli *et al.*, 2000) were used. For detection of HP1β we used mouse anti-HP1β (MaHP1β; Euromedex; Nielsen *et al.*, 1999) and rat anti-HP1β (RaaHP1β; Wreggett *et al.*, 1994). We used mouse anti-HP1γ (MaHP1γ; Euromedex; Nielsen *et al.*, 1999) to detect HP1γ. RaHP1α and RaaHP1β were kindly provided by Dr. P. B. Singh. All anti-HP1 antibodies recognize human as well as murine HP1. For *in situ* labeling of H3K9me we used rabbit anti-trimethylated H3K9 (RaH3K9me3; Cowell *et al.*, 2002), also provided by Dr. P. B. Singh, rabbit anti-dimethylated H3K9 (RaH3K9me2; Upstate, Milton Keynes, UK; Nakayama *et al.*, 2001), and rabbit anti-branched (4x) methylated peptide-H3K9 (RaH3K9me-branched; Maison *et al.*, 2002) provided by Dr. T. Jenuwein. As secondary antibodies we used donkey anti-rabbit IgG(H+L)-Cy5, donkey anti-rabbit IgG(H+L)-Cy3, donkey anti-mouse IgG(H+L)-Cy3, donkey anti-mouse IgG(H+L)-FITC, donkey anti-rabbit IgG(H+L)-FITC and donkey anti-rat IgG-FITC (Jackson ImmunoResearch Laboratories, West Grove, PA, USA).

Microscopy and image analysis
Images were recorded with a Zeiss LSM 510 confocal laser scanning microscope equipped with C-Apochromat 63x/1.2 water immersion lenses (Carl Zeiss Jena GmbH, Jena, Germany). All tracks were recorded separately to reduce cross-talk. Three or more midnuclear confocal sections (0.5-1 µm apart) were recorded for every image. We made line scans in the *x-y* plane. Figures were composed in Adobe PhotoShop v. 7.0 (Adobe Systems, San Jose, CA, USA). For quantitative image analysis, maximum intensity projections of the imaged cells (represented in the Supplementary Figure S1) were generated. Average signal intensity was measured for every channel over circular areas of 1.5 μm^2. These circles were placed over five DAPI-dense chromatin regions and five non-DAPI-dense chromatin regions in transfected and non-transfected control cells. The ratio between transfected (dn) and non-transfected cells (wt) for the DAPI, as well as the endogenous HP1 signal, was calculated in individual images as the ratio between the differences between average intensity in DAPI-dense heterochromatic chromatin regions (HC) and non-DAPI-dense euchromatic regions (EC) according to the following: $(HC\text{-}EC)_{dn}/(HC\text{-}EC)_{wt}$.

To quantify the levels of EGFP-tagged HP1β in living cells before and after pmCherry-HP1β-Δ(2-40) expression, we imaged the cells on a Zeiss Axiovert 200M widefield fluorescence microscope, equipped with a 100x Plan-Apochromat (1.4 NA) oil immersion lens (Zeiss, Oberkochen, Germany) and a Cairn Xenon Arc lamp with monochromator (Cairn research, Kent, UK). The objective was temperature-controlled with an objective heater and cells were examined in microscopy medium (137 mM NaCl, 5.4 mM KCl, 1.8 mM $CaCl_2$, 0.8 mM $MgSO_4$, 20 mM D-glucose and 20 mM HEPES) at 37°C. Images were recorded with a cooled

CCD camera (Coolsnap HQ, Roper Scientific, Tucson, AZ, USA). A 375-490 excitation filter, 490 long-pass dichroic mirror and 525-40 band-pass emission filter were used for EGFP imaging (monochromator: 470 nm ± 20 nm). A 375-580 excitation filter, 585 long-pass dichroic mirror and 620-60 band-pass emission filter was used for mCherry imaging (monochromator: 550 nm ± 20 nm). The average pixel intensity in the nucleus of the imaged EGFP-HP1β-expressing cells was quantified using Metamorph software (Molecular Devices Corporation, Sunnyvale, CA). The distribution of pixel intensities (ranging from 0-1600) of 50 cells of each population (transfected and non-transfected) was plotted in a histogram (32 bins with a width of 50).

Results

Approach

We used a dominant-negative approach to analyze the role of HP1 in maintaining pericentromeric heterochromatin in the interphase mouse nucleus. Human HP1α and HP1β were cloned as full-length FLAG-tagged proteins (HP1α-flag and HP1β-flag) and as FLAG-tagged truncated proteins (HP1α-Δ(2-39)-flag and HP1β-Δ(2-40)-flag) that lack most of the CD, which is essential for binding to H3K9me (Bannister *et al.*, 2001; Lachner *et al.*, 2001; Platero *et al.*, 1995). To identify transfected cells, a FLAG-tag was positioned at the C-terminal end of all constructs. We used 3T3 mouse fibroblasts, which have large pericentromeric heterochromatin domains that are easily visible after DAPI staining. Cells were co-transfected with the tetracycline-inducible vector pUHD15-1 and the wild-type or mutant HP1 construct in the absence of tetracycline or doxycycline. Expression of all transfected proteins (full-length and truncated HP1) was detectable 12 hours after transfection using an anti-flag antibody (data not shown). After 24 hours, cells with high expression levels were analyzed for HP1 localization and DAPI-stained heterochromatin domains.

Immunofluorescent labeling, using mouse anti-flag (figure 1) and rabbit anti-flag antibodies (data not shown), showed that the transfected wild-type HP1α-flag and HP1β-flag proteins are targeted to the DAPI-stained heterochromatin domains in the nucleus, as shown by others (Cheutin *et al.*, 2003; Horsley *et al.*, 1996; Minc *et al.*, 1999; Wreggett *et al.*, 1994). The same anti-flag antibodies showed that HP1α-Δ(2-39)-flag and HP1β-Δ(2-40)-flag proteins are localized in the nucleus. As expected, HP1α-Δ(2-39)-flag and HP1β-Δ(2-40)-flag did not accumulate in the DAPI-dense areas, since they lack the CD (figure 2, red and cyan channels). In most of these cells the anti-flag signal is homogeneously distributed in the nucleus, whereas in some cells the anti-flag signal is more concentrated at the periphery of the cell nucleus. Our results agree with the notion that the CD is required for localization of HP1α and HP1β in DAPI-stained pericentromeric heterochromatin through H3K9me binding (Bannister *et al.*, 2001; Cowell *et al.*, 2002; Jacobs and Khorasanizadeh, 2002; Lachner *et al.*, 2001).

Truncated HP1α and HP1β displace endogenous HP1α, HP1β and HP1γ from pericentromeric heterochromatin

Endogenous HP1α, HP1β and HP1γ in non-transfected cells are located in the nucleus and accumulate in DAPI-dense pericentromeric heterochromatin domains (figure 2, S1; Cheutin *et al.*, 2003; Horsley *et al.*, 1996; Minc *et al.*, 1999; Minc *et al.*, 2000; Wreggett *et al.*, 1994). To establish whether truncated HP1 displaces the endogenous protein from heterochromatin domains, cells were transfected with HP1α-Δ(2-39)-flag (figure 2A, B, figure S1), or HP1β-Δ(2-40)-flag (figure 2C-E, figure S1). After 24 hours, cells were fixed and fluorescently labeled with antibodies against flag-tagged transfected proteins (figure 2, red channel and figure S1) and with antibodies against HP1α, HP1β or HP1γ (figure 2, green channel and figure S1) and stained with DAPI (figure 2, cyan channel and figure S1). For detection of HP1α we used two different antibodies, *i.e.* a mouse anti-HP1α monoclonal antibody (MaHP1α; figure S1B and F) and a rabbit anti-HP1α polyclonal antibody (RaHP1α; figure 2A, 2C and S1) that gave identical results. Cells expressing HP1α-Δ(2-39)-flag showed a strong increase in labeling intensity by MaHP1α but not by RaHP1α labeling. This indicates that MaHP1α recognizes the transfected HP1α-Δ(2-39)-flag protein, whereas RaHP1α does not. For detection of endogenous HP1β we used a mouse anti-HP1β monoclonal antibody (MaHP1β; figure S1) and a rat anti-HP1β monoclonal antibody (RaaHP1β; figure 2B, 2D, S1). Both anti-HP1β antibodies did not recognize the mutant HP1β-Δ(2-40)-flag protein. To detect HP1γ we used a monoclonal mouse anti-HP1γ (MaHP1γ; figure 2E, S1). The specificity of all antibodies has been tested elsewhere (see references in the materials and methods section). As a control we analyzed non-transfected cells in the same preparation to relate HP1 accumulation at pericentromeric heterochromatin in control cells to the amount of HP1 in these domains in transfected cells. To allow semi-quantitative assessment of the co-localization and intensity of the different labels, line scans were made in the *x*-*y* plane through intense DAPI domains in transfected (figure 2 A2, B2, C2, D2 and E2) and in non-transfected control cells (figure 2 A1, B1, C1, D1 and E1).

In cells transfected with HP1α-Δ(2-39)-flag, HP1α labeling with RaHP1α showed a dispersed distribution of the HP1α antigen throughout the nucleus, lacking accumulation in the DAPI-stained pericentromeric regions (figure 2A, S1). Labeling with MaHP1α also showed no accumulation of HP1α in DAPI-dense domains in HP1α-Δ(2-39)-flag transfected cells, compared to non-transfected control cells (figure S1). This indicates that endogenous HP1α is displaced from the DAPI-stained pericentromeric heterochromatin domains by the truncated protein. Strikingly, in HP1α-Δ(2-39)-flag transfected cells, HP1β labeling with RaaHP1β (figure 2B, S1) or MaHP1β (figure S1) also showed no accumulation of endogenous HP1β in DAPI-stained chromocenters. These results show that truncated HP1α displaces endogenous HP1α and HP1β from DAPI-stained pericentromeric heterochromatin.

In HP1β-Δ(2-40)-flag transfected cells, HP1β did not accumulate in the DAPI-

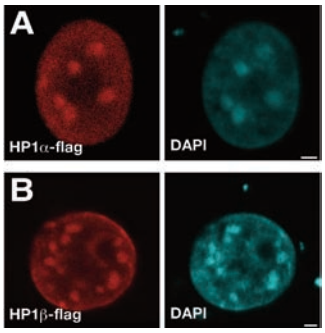

Figure 1. Distribution of transfected full-length HP1α-flag and HP1β-flag in mouse fibroblasts. Cells transfected with HP1α-flag (A) and HP1β-flag (B) were fluorescently immunolabeled 24 hours after transfection. The red signal (mouse anti-flag) shows the distribution of transfected HP1α-flag (A) and HP1β-flag (B). The cyan channel shows the DAPI staining. Bars represent 2 µm. Individual midnuclear optical sections are shown.

Figure 2. See next page for legend.

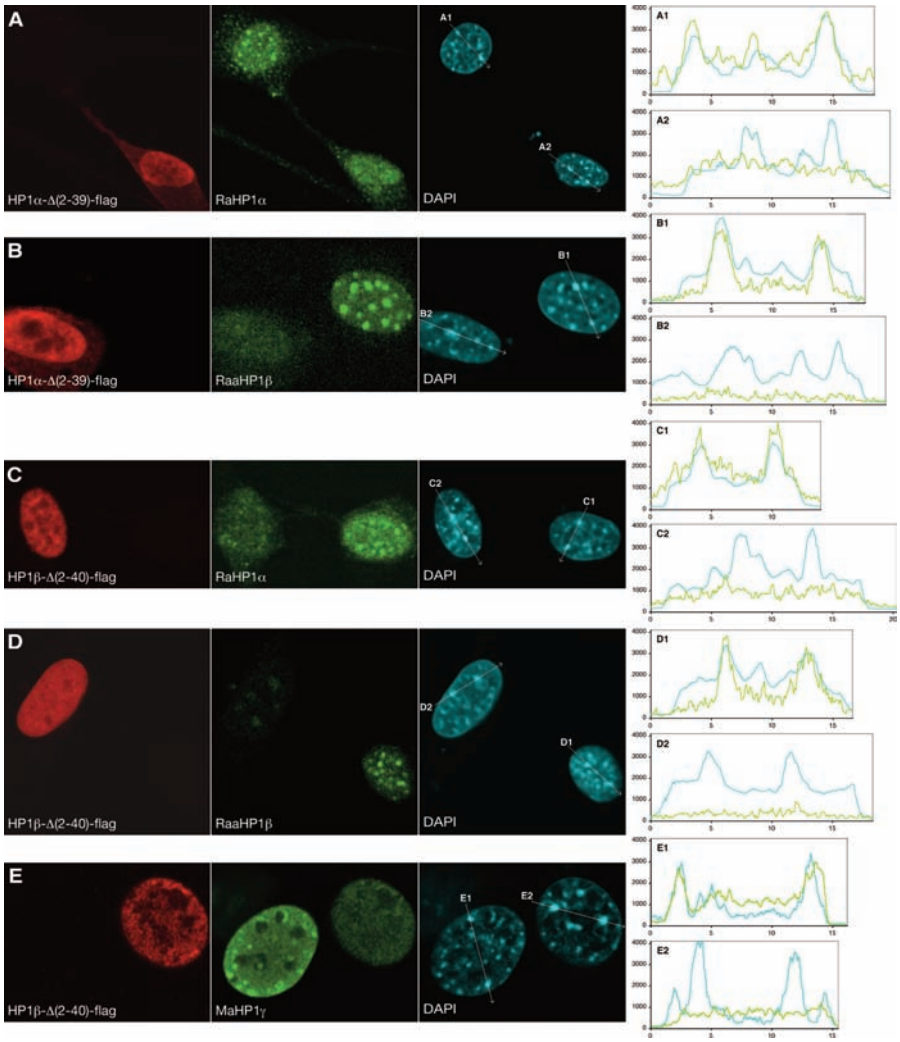

Figure 2. Spatial distribution of transfected truncated HP1, endogenous HP1 and DAPI-stained heterochromatin domains. Cells transfected with HP1α-Δ(2-39)-flag (A and B) and HP1β-Δ(2-40)-flag (C-E) were fluorescently labeled 24 hours after transfection. The red signal (Maflag in A-D and Raflag in E) shows the transfected HP1α-Δ(2-39)-flag (A and B) and HP1β-Δ(2-40)-flag (C-E). The green signal shows the distribution of endogenous HP1α, HP1β and HP1γ after labeling with RaHP1α (A and C), RaaHP1β (B and D) and MaHP1γ (E). The cyan signal shows the DAPI staining. On the right, intensity profiles along the lines shown in the DAPI images show endogenous HP1α, HP1β and HP1γ (green line) and DAPI staining (cyan line). A1, B1, C1, D1 and E1 are line scans in control cells and A2, B2, C2, D2 and E2 in transfected cells. The *x*-axis shows the distance in μm; the *y*-axis represents signal intensity in arbitrary units. Individual midnuclear optical sections are shown.

stained pericentromeric domains and was dispersed throughout the nucleoplasm, as shown by labeling with two different antibodies, *i.e.* RaaHP1β (figure 2D, S1) and MaHP1β (figure S1). Moreover, in HP1β-Δ(2-40)-flag transfected cells RaHP1α (figure 2C, S1), MaHP1α (figure S1) and MaHP1γ (figure 2E, S1) labeling did not show any accumulation of HP1α and HP1γ in DAPI-stained pericentromeric domains. To verify that the displacement of endogenous HP1 is not a consequence of the transfection procedure, fibroblasts were transfected with a plasmid containing only the enhanced green fluorescent protein (eGFP) gene and were subsequently immunofluorescently labeled with MaHP1α and MaHP1β. No changes in the distribution or intensity of endogenous HP1 were observed, compared to non-transfected cells (data not shown). Therefore, it is unlikely that the observed changes in HP1 distribution after expression of the mutant HP1 proteins are an artifact of the transfection procedure.

In addition to the analysis of endogenous HP1 levels in fixed cells using anti-HP1 antibodies, we analyzed the dominant-negative effect of transfecting cells with truncated HP1 in living cells. To this end we created a mouse fibroblast cell line stably expressing EGFP-tagged HP1β. In these EGFP-HP1β-expressing cells, HP1β was found to accumulate in DAPI-stained pericentromeric heterochromatin domains and to occur diffusely throughout the nucleoplasm (figure 3A). Transfection of these EGFP-HP1β-expressing cells with mCherry-tagged HP1β-Δ(2-40) resulted in a homogeneous nuclear distribution of both the truncated and the wild-type HP1β proteins (figure 3B, C). These results confirm the antibody labeling data in figures 2, 5 and S1, showing that truncated HP1 protein that lacks a functional CD displaces full-length HP1 from the DAPI-dense nuclear domains.

To examine whether expression of truncated HP1β-Δ(2-40) results in a decrease of the HP1β concentration, we determined the expression level of cells stably expressing EGFP-HP1β with and without transfection with mCherry-HP1β-Δ(2-40) (figure 3). The fluorescence intensity of EGFP-HP1β integrated over the nucleus was determined 24 hours after transfection in cells expressing high levels of mCherry-HP1β-Δ(2-40) (based on the red signal) and in untransfected cells. The distribution of EGFP-HP1β fluorescence measured in transfected and non-transfected cells was fitted with a Gaussian distribution yielding average EGFP-HP1β fluorescence intensities of 161 ± 26 and 162 ± 40 for non-transfected and transfected cells, respectively. These results

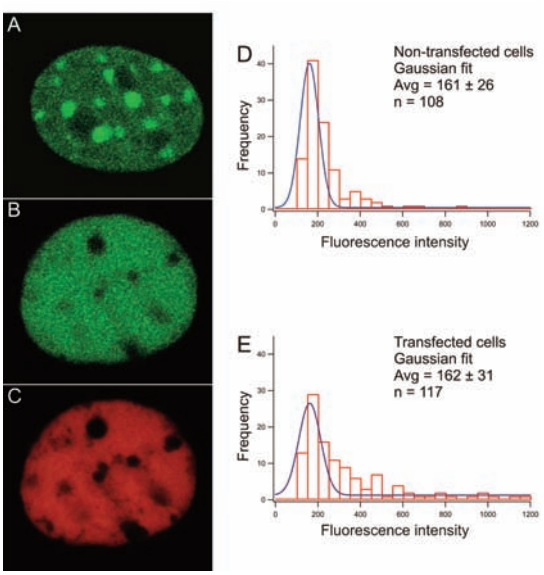

Figure 3. Spatial distribution of EGFP-tagged HP1β in cells transfected with or without mCherry-HP1β-Δ(2-40). Cells stably expressing EGFP-tagged HP1β show that HP1 is accumulated in pericentromeric heterochromatin domains (A). EGFP-tagged HP1β-expressing cells were transfected with mCherry-tagged HP1β-Δ(2-40) (B and C). The green signal shows the EGFP-tagged HP1β (B). The red signal shows the transfected mCherry-tagged HP1β-Δ(2-40) (C). The fluorescence intensity of EGFP-HP1β in cells transfected with mCherry-tagged HP1β-Δ(2-40) was compared to non-transfected cells. A histogram of the Gaussian distribution of the EGFP-HP1β fluorescence intensity in transfected (E) and non-transfected cells (D) is shown. The *x*-axis represents the average fluorescence intensity in arbitrary units; the *y*-axis shows the number of cells.

show that expression of truncated HP1β does not change the cellular concentration of full-length EGFP-HP1β (figure 3D, E). These results show that truncated HP1α and truncated HP1β protein, which lack a functional CD, not only expel their full-length HP1 counterpart from the DAPI-stained pericentromeric heterochromatin domains, but also the two other HP1 homologues. This suggests that the three HP1 homologues interact in heterochromatin.

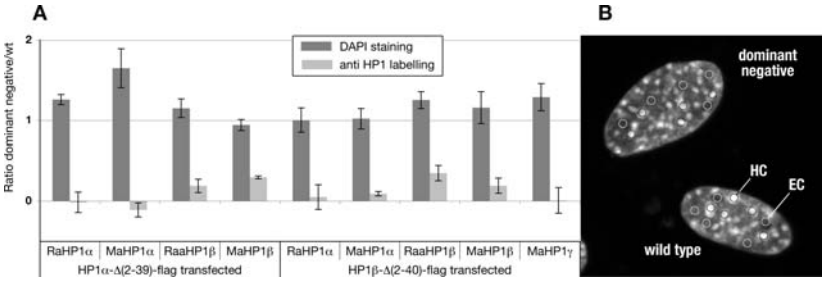

Figure 4. Quantitative analysis of the spatial distribution of transfected truncated HP1, endogenous HP1 and DAPI-stained heterochromatin domains. Maximum intensity projections of the imaged cells (see figure S1) were generated. The average signal intensity was measured for every channel over circular areas of 1.5 μm^2. These circles were placed over five DAPI-dense chromatin regions and five non-DAPI-dense chromatin regions in transfected and non-transfected cells (B). The ratio between cells transfected with HP1α-Δ(2-39)-flag or HP1β-Δ(2-40)-flag versus non-transfected control cells, for the DAPI signal (dark grey bars) as well as for the endogenous HP1 signal (light grey bars) was calculated. This was done in individual images as the ratio of the differences between average intensity in DAPI-dense chromatin regions (HC) and non-DAPI-dense euchromatic chromatin regions (EC) in transfected (dn) and non-transfected cells (wt): $(HC\text{-}EC)_{dn}/(HC\text{-}EC)_{wt}$ (A). The error bars represent the standard error between the different images.

Loss of HP1α and HP1β from heterochromatin does not result in changes in large-scale heterochromatin structure

We performed a quantitative analysis of the relative amount of DAPI staining and endogenous HP1 levels in cells transfected with HP1α-Δ(2-39)-flag or HP1β-Δ(2-40)-flag and in untransfected control cells. Results demonstrate that there is no change in DAPI staining after transfection with either HP1α-Δ(2-39)-flag or HP1β-Δ(2-40)-flag. The ratio of DAPI stain in transfected versus non-transfected cells is close to unity (figure 4). In contrast, the ratio for the HP1 signal, using different antibodies (*i.e.* RaHP1α, MaHP1α, RaaHP1β, MaHP1β and MaHP1γ) is close to zero (figure 4). These measurements show in a quantitative manner that, after expression of HP1 that lacks the chromodomain, most of the endogenous HP1 is relocated from DAPI-dense chromatin regions to the nucleoplasm, whereas the DAPI staining remains unchanged.

To analyze whether the loss of HP1α and HP1β from DAPI-stained pericentromeric heterochromatin domains is correlated with a decrease in H3K9me level, we analyzed the distribution of H3K9me 24 hours after transfection with HP1α-Δ(2-39)-flag, HP1β-Δ(2-40)-flag, or with both simultaneously. We labeled H3K9me with three different antibodies: RaH3K9me2, RaH3K9me3 and RaH3K9me-branched. The RaH3K9me-branched antibody is described to have a high affinity for H3K9me3, to significantly cross-react with di- and trimethylation of several other H3 lysine positions, and to decorate pericentromeric heterochromatin and the inactive X-chromosome (Maison *et al.*, 2002; Perez-Burgos *et al.*, 2004; figure 5B, D). No detectable change in H3K9me labeling was observed with the RaH3K9me3 and RaH3K9me-branched antibodies 24 hours after transfection with either HP1α-Δ(2-39)-flag (figure 5A, B), HP1β-Δ(2-40)-flag (figure 5C, D), or with HP1α-Δ(2-39)-flag and HP1β-Δ(2-40)-flag simultaneously (data not shown). Similarly, no change in the dimethylation level of H3K9 was observed (figure 5E). The same results were obtained 48 hours after transfection, using RaH3K9me2, RaH3K9me3 and RaH3K9me-branched antibodies (data not shown). These results show that, although all three endogenous HP1 proteins are, to a large degree, displaced from DAPI-stained pericentromeric heterochromatin domains by HP1α-Δ(2-39)-flag or HP1β-Δ(2-40)-flag, this does not result in a visible reduction of H3K9me levels in these domains.

We showed that the overall structure, size and nuclear distribution of DAPI-stained pericentromeric heterochromatin domains remained unaffected as the three HP1 proteins are displaced (figures 2, 5, S1). These observations demonstrate that the visible accumulation of HP1α, HP1β and HP1γ is not essential for maintaining pericentromeric heterochromatin structure as visualized by DAPI staining and by immunofluorescent labeling of H3K9me2, H3K9me3 or H3K9me-branched.

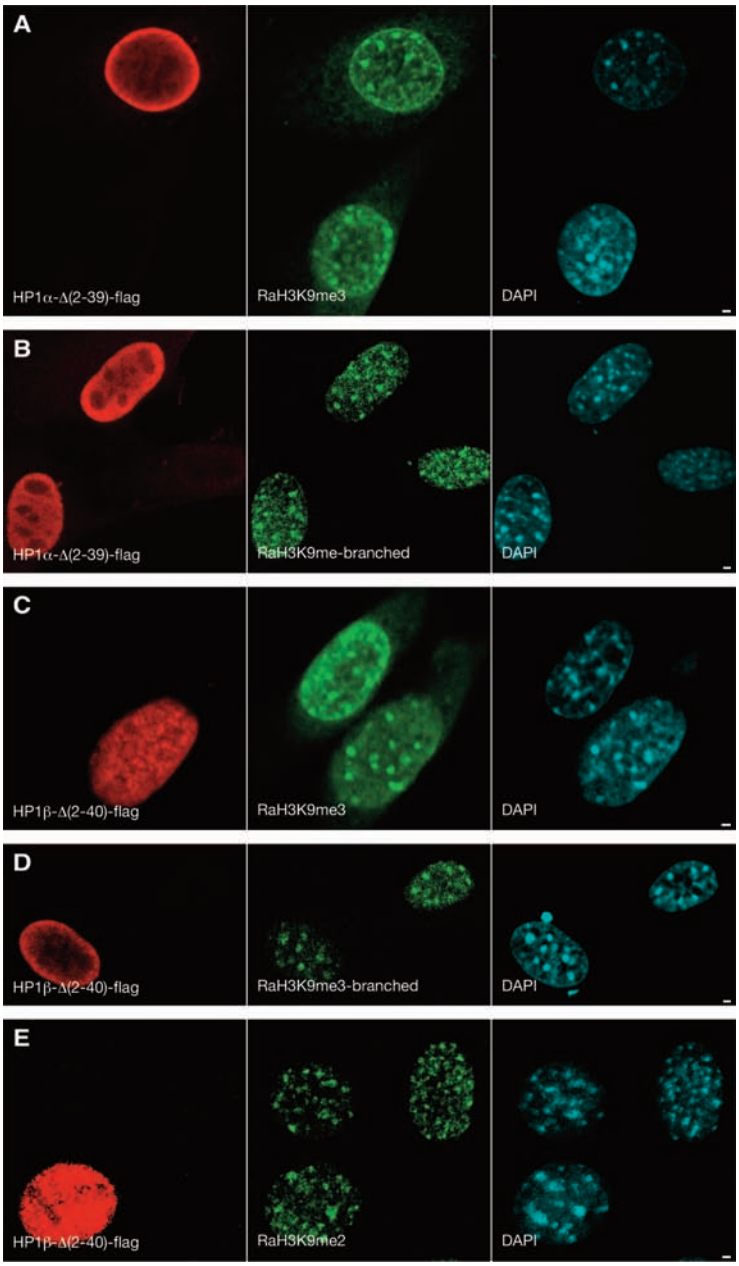

Figure 5. Spatial distribution of H3K9me in cells transfected with truncated HP1α and HP1β. Cells transfected with HP1α-Δ(2-39)-flag (A and B) and HP1β-Δ(2-40)-flag (C-E) were fluorescently labeled 24 hours after transfection. The red signal (mouse anti-flag) shows the transfected HP1α-Δ(2-39)-flag (A and B) and HP1β-Δ(2-40)-flag (C-E). The green signal shows distribution of H3K9me detected by either RaH3K9me3 (A and C), RaH3K9mebranched (B and D), or RaH3K9me2 (E). The cyan signal represents DAPI staining. Bars represent 2 μm. Individual midnuclear optical sections are shown.

Discussion

HP1 is thought to play an important role in heterochromatin organization and the control of gene expression (Hediger and Gasser, 2006; Hiragami and Festenstein, 2005). This involves the specific binding of the CD to H3K9me, dimerization via its CSD and recruitment of a variety of proteins that specifically interact via HP1 with H3K9me-rich chromatin domains (Brasher *et al.*, 2000; Cowell *et al.*, 2002; Jenuwein, 2001; Lachner and Jenuwein, 2002; Nielsen *et al.*, 2001; Singh and Georgatos, 2002; Thiru *et al.*, 2004). HP1 dimerizes through its CSD and may bridge two H3K9me-containing nucleosomes, inducing a higher-order packing of heterochromatin (Jenuwein, 2001; Lachner and Jenuwein, 2002; Nielsen *et al.*, 2001; Singh and Georgatos, 2002; Thiru *et al.*, 2004). It has also been proposed that HP1 dimers bind to methylated K9 and K27 on a single histone H3 tail, instead of binding to methylated K9 on nearby nucleosomes (Jacobs and Khorasanizadeh, 2002). HP1 may also play a role in the maintenance of the heterochromatin state through cell division, via its interactions with chromatin assembly factor 1 (CAF1), H3K9 methyltransferase Suv39 and the DNA methyltransferases Dnmt1 and Dnmt3a (reviewed in Maison and Almouzni, 2004). In this study we used a dominant-negative approach to interfere with HP1 function to obtain insight into the role of HP1α, HP1β and HP1γ in maintaining DAPI-stained pericentromeric heterochromatin domains in mouse fibroblasts.

Expressing truncated HP1α and HP1β, lacking a functional CD, resulted in displacement of the endogenous HP1α, HP1β and HP1γ from the visible DAPI-stained pericentromeric heterochromatin domains (figure 2). It did not result in a significant decrease in full-length HP1 expression (figure 3). Remarkably, loss of HP1 did not result in a visible change in the structure of pericentromeric heterochromatin domains, as visualized by DAPI staining, and did not result in a visible change in the methylation state of H3K9 (figures 2, 4, 5, S1). It is known that the CD is responsible for specific binding of HP1 to H3K9me in heterochromatin (Bannister *et al.*, 2001; Cheutin *et al.*, 2003; Cowell *et al.*, 2002; Jacobs and Khorasanizadeh, 2002; Lachner *et al.*, 2001). Therefore, as expected, HP1 lacking a CD did not accumulate in DAPI-stained heterochromatin domains (figure 2, S1), in contrast to wild-type HP1α-flag and HP1β-flag, which did accumulate in these domains (figure 1). Evidently, interaction of the CD of the endogenous HP1 with H3K9me is not sufficient to keep the proteins associated with DAPI-stained heterochromatin domains. Most likely, the truncated polypeptides sequester endogenous proteins that are necessary to stabilize the interaction of HP1 with H3K9me. Because expression of each of the truncated proteins individually resulted in the apparent displacement of HP1α, HP1β and HP1γ from DAPI-stained pericentromeric heterochromatin, it is likely that these three HP1 proteins interact directly or indirectly *in vivo*.

Our results are consistent with studies showing that the CD is necessary but not sufficient for HP1 to bind H3K9me-containing nucleosomes (Smothers and Henikoff,

2001; Thiru *et al.*, 2004) and that HP1β as a monomeric protein is not stably associated with pericentromeric heterochromatin (Thiru *et al.*, 2004). Our data show that when most endogenous HP1 is displaced from DAPI-dense heterochromatin, the level and distribution of tri- and dimethylated H3K9me remains unchanged. This demonstrates that accumulation of HP1α, HP1β and HP1γ is not required for keeping histone H3K9 in its methylated state in DAPI-stained heterochromatin domains. In this context, labeling with the H3K9me-branched antibody as well as HP1α accumulation at pericentromeric heterochromatin were lost after incubation with RNAse and after culturing in the presence of a histone deacetylase inhibitor (Maison *et al.*, 2002; Muchardt *et al.*, 2002). Besides, Gilbert *et al.* (2003) reported that during differentiation of chicken erythrocytes HP1 is completely lost, whereas there is only a modest reduction in H3K9me. Obviously, maintaining H3K9me levels does not require the continuous presence of HP1 proteins.

Interestingly, Peters *et al.* (2001) presented evidence that DAPI-dense domains, where HP1 accumulates, remain present in cells that fully lack the histone methyltransferases Suv39h1 and 2. In these cells heterochromatin domains do not contain H3K9me. From these and our results it can be concluded that HP1 binding and H3K9me are independent processes and are not required simultaneously for heterochromatin stability. Recently, we showed that *in vivo* targeting of HP1α or HP1β to an amplified chromosomal region, causes local chromatin condensation, enhanced trimethylated H3K9me and recruitment of histone methyltransferases (Verschure *et al.*, 2005). Targeting of the HP1 lacking a functional CD also caused heterochromatinization of the amplified chromosome region (Brink *et al.*, 2006; chapter 3 of this thesis). These results show that normal binding of HP1 through its CD domain, as well as artificial binding of HP1 without a CD through the lac operator/lac repressor interaction, is sufficient to trigger heterochromatin formation. The present studies indicate that HP1 is not required for maintaining the DAPI-stained heterochromatin domains.

HP1 in heterochromatin is remarkably dynamic and exchanges rapidly with its soluble pool (Cheutin *et al.*, 2003; Festenstein *et al.*, 2003; Schmiedeberg *et al.*, 2004). HP1 is bound in heterochromatin domains in at least two modes, one that exchanges rapidly and one that is released slowly. The ratio between these pools ranges from approximately 8:1 in NIH/3T3 fibroblasts (Schmiedeberg *et al.*, 2004) to close to 3:1 in mouse T-cells (Festenstein *et al.*, 2003), probably depending on cell type and chromatin state. The function of the fast and the slow-exchanging HP1 subfractions is unknown. Our results show in fixed as well as in living cells that in mouse fibroblasts most HP1 proteins can be removed from DAPI-stained pericentromeric heterochromatin without a visible change in large-scale chromatin structure or a significant decrease in H3K9me. It is possible that a small fraction of the strongly bound fraction of HP1 molecules, *e.g.* the slowly exchanging fraction, remains present

in the dominant-negative experiments. Light-microscopic analysis is not sufficiently sensitive to decide this unambiguously. However, our data clearly show that most HP1 in visible pericentromeric domains is dispensable for maintaining typical heterochromatin features, including strong DAPI staining, H3K9 methylation and the heterochromatin size and shape. Our findings indicate that local accumulation of HP1α, HP1β and HP1γ is not essential for the maintenance of DAPI-stained pericentromeric heterochromatin.

Acknowledgements

We are grateful to drs. P. B. Singh and T. Jenuwein for providing us with the antibodies used in this study, dr. R.Y. Tsien (San Diego, USA) for providing the mCherry cDNA and drs. L. Schmiedeberg and P. Hemmerich (Jena, Germany) for providing EGFP-tagged HP1β. We thank dr. E. M. M. Manders and W. Takkenberg for assistance with confocal microscopy. We also thank ir. B. Hooibrink, from the Academic Medical Center in Amsterdam for cell sorting. This work was supported in part by the Netherlands Organization for Scientific Research, Earth and Life Sciences (ALW), by and ALW-PULS and ALW-VIDI grant to P. J. V. (project numbers PULS/33-98/805-4811 and VIDI 2003/03921/ALW/016.041.311).

Supplementary Figure S1. Spatial distribution of transfected truncated HP1, endogenous HP1 and DAPI-stained heterochromatin domains. Cells transfected with HP1α-Δ(2-39)-flag and HP1β-Δ(2-40)-flag were fluorescently labeled 24 hours after transfection. The anti-flag signal (first column) shows the transfected HP1α-Δ(2-39)-flag cells and the transfected HP1β-Δ(2-40)-flag cells. The distribution of endogenous HP1 is shown in the second column; HP1α after labeling with RaHP1α or with MaHP1α, HP1β after labeling with RaaHP1β or with MaHP1β and HP1γ after labeling with MaHP1γ. The DAPI staining is shown in the right column.

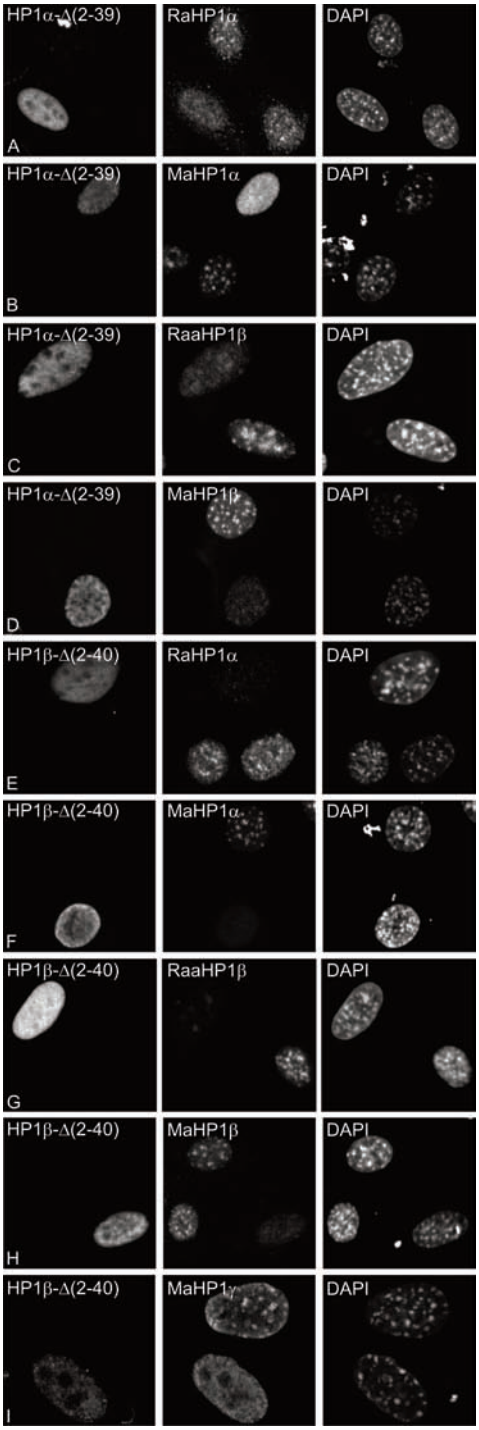

Chapter 5

A cell system to analyze epigenetic gene regulation

Maartje C. Brink, Diewertje G. E. Piebes, Hinco J. Gierman, Mireille H. Indemans, Angelique Meulemans-Rops, Giuseppina Giglia-Mari, Rogier Versteeg, Roel van Driel, Johan van der Vlag, Wim Vermeulen & Pernette J. Verschure

Adapted from patent application PCT/NL2008/050150

Abstract

Packing of the eukaryotic genome into higher-order chromatin structures is tightly related to gene expression, although the underlying molecular mechanisms are currently unclear. The lac-operator/lac-repressor system allows visualization of a specific chromatin domain as well as manipulation of such a domain by the targeting of epigenetic regulatory proteins. To systematically study the causal relationship between changes in the epigenetic state, chromatin structure and gene expression within a genomic environment, we engineered and integrated a composite targeting cassette in human cells. The cassette contains a reporter gene and two short arrays of protein-binding sites that enable targeting of fluorescent epigenetic regulatory proteins and allow manipulation of the epigenetic state and visualization of the cassette. Criteria for the functionality of the cell system are (i) single integration of the cassette at a designated site, (ii) visualization of the integrated cassette, (iii) ability to measure changes in chromatin structure and (iv) ability to measure transcriptional activity. As a proof of principle, two mono-clonal cell lines were established with a single integration using Flp recombinase in genomic environments of either high or of low gene activity. The use of fluorescent *in situ* hybridization and reverse transcription quantitative PCR enable the measurement of changes in chromatin structure and changes in gene activity, respectively. Systematic and quantitative *in vivo* measurements using this system will provide insight into causal relationships between an induced epigenetic state, changes in chromatin structure and transcriptional activity in a specific genomic environment.

Introduction

Chromatin organization plays an important role in mammalian gene regulation, although we lack clear understanding of cause-and-effect relationships (for a review, see Goetze *et al.*, 2007b). Studies indicate that silent, gene-poor chromatin is positioned more to the periphery of the nucleus, whereas active, gene-rich chromatin adopts a more central position (Finlan *et al.*, 2008; Goetze *et al.*, 2007a; Guelen *et al.*, 2008). Furthermore, chromatin condensation was seen to correlate with an epigenetic state marked by H3K9 methylation and gene repression (Verschure *et al.*, 2005). *Vice versa*, chromatin decondensation has been associated with transcriptional activity and specific H3 acetylation marks (Tumbar *et al.*, 1999). In addition, looping of genes out of their chromosome territory has been observed for several transcriptionally active genes, such as the functionally related genes of the HoxB cluster that can loop out sequentially upon induction, facilitating transcriptional co-regulation (Chambeyron and Bickmore, 2004). At the linear DNA level, clustering of functionally unrelated genes was

identified (Caron *et al.*, 2001). Specific chromosomal regions containing clusters of highly expressed gene of unrelated function were named ridges (regions of increased gene expression), and clusters of low-expressed genes anti-ridges. Integration of a GFP reporter gene in a ridge region resulted in an average four-fold higher expression of the reporter compared to expression when integrated in an anti-ridge, suggesting that the genomic environment contributes considerably to the transcriptional potential of a gene (Gierman *et al.*, 2007).

The advantage of the use of the lac operator/lac repressor system is that it provides information on the causal relationships between chromatin organization and gene activity (Robinett *et al.*, 1996). Initially, Belmont and coworkers created an artificial chromosomal domain in mammalian cells consisting of an integrated and amplified array of bacterial lactose operator (lacO) sites, flanked by a dihydrofolate (DHFR) selection marker. Binding of the lac repressor (lacR)-GFP fusion protein to the amplified chromosomal domain allowed the *in vivo* visualization of large-scale chromatin structure in mammalian cells (Robinett *et al.*, 1996). The lacO/lacR targeting system has been used in a number of studies illuminating the interplay between the higher-order packaging of chromatin and gene activity (Brink *et al.*, 2006; Tumbar *et al.*, 1999; Verschure *et al.*, 2005; and chapter 2 of this thesis). Furthermore, the targeting system has also been used to analyze the relationship between gene activity and positioning of genes in the nucleus. Tumbar and Belmont (2001) showed that after gene activation, the array was repositioned to a more central location in the nucleus. Other studies showed that targeting of the integrated lacO system to the nuclear lamina caused repression of a reporter gene and of some, but not all, of the genes near the targeting site (Finlan *et al.*, 2008; Reddy *et al.*, 2008). In a related study, it was shown that reporter gene transcription could be induced at the nuclear lamina, indicating that nuclear localization is important, but not decisive for gene regulation (Kumaran and Spector, 2008).

Although our understanding of epigenetic regulatory mechanisms has expanded considerably, we still lack insight into the effect of the local genomic environment on gene regulation. In this study we created a cell system consisting of an integrated cassette in human cells to systematically measure the causal relationship between changes in the epigenetic state, chromatin structure and gene expression in a specific genomic environment. The cassette contains a reporter gene and two short arrays of non-endogenous protein-binding DNA sites (the bacterial lactose operator (lacO) sites and the yeast Upstream Activating Sites (UAS)) that enable targeting of fluorescent epigenetic regulatory proteins, allowing induction of a specific epigenetic state and the visualization of the cassette. Criteria for the functionality of the cell system are (i) single integration of the cassette at a designated site, (ii) visualization of the integrated cassette in living cells, (iii) ability to measure changes in chromatin structure and (iv) ability to measure transcriptional activity. As a proof of principle, two mono-clonal cell lines were established with a single integration using Flp recombinase in specific

genomic sites of either high or low gene activity, *i.e.* a ridge and an anti-ridge, respectively. (Gierman *et al.*, 2007; Gronostajski and Sadowski, 1985; Sauer, 1994). The clones contain the integrated cassette in functionally different genomic regions to assess the contribution of the local chromatin environment on epigenetic gene control. We demonstrate the visualization of the lacO repeat by *in vivo* detection upon lacR-GFP binding and by fluorescent *in situ* hybridization (FISH). We provide data on gene activity of the reporter gene in the established cell lines by means of reverse transcription quantitative PCR (RT-qPCR) Our data show that when the cassette is integrated in a ridge region, reporter gene activity is two-fold higher than when integrated in an anti-ridge. We conclude that the criteria for useful functioning of the cell system are fulfilled and we discuss suggestions for additional technical improvements of the cell system. This system will be an important tool for gaining insight into the molecular mechanisms underlying epigenetic gene regulation in a controlled and systematic manner.

Materials & Methods

Cloning of plasmids

Plasmid pPS-8.4, a pUC18 derivative containing 4 copies of the lacO octamer divided by DNA spacer fragments, was used as a cloning backbone vector (Robinett *et al.*, 1996). A dsRed-MTS-IRES-hygromycin reporter cassette was constructed by inserting a pDsRed2-Mito-fragment (Clontech, USA) with *SnaBI* and filled-in *NotI* ends into *SnaBI-SmaI* sites of pIREShyg3 (Clontech, USA). The resulting reporter cassette was excised with *SalI* and inserted into the pPS-8.4 *XhoI* site. Next, the Flp Recombination Target (FRT) site (Gronostajski and Sadowski, 1985; Sauer, 1994) was synthesized with *ClaI-NruI* restriction sites 5' and *PacI-XmaI* sites 3' and subcloned into *ClaI-XmaI* of pBluescript II SK+ (Stratagene). *KpnI-MluI-SwaI* sites were added to the 5' end and *ClaI* was added to the 3' end of a 14x repeat of the UAS operator by PCR on the pZG18 plasmid (obtained from Carl Schildkraut, Department of Cell Biology, Albert Einstein college of Medicine, New York, USA). The UAS repeat was ligated into *KpnI-Cla*I of FRT-containing pBluescript. UASFRT was excised with *MluI-XmaI* and ligated into *MluI-XmaI* of p8.4dsRed, creating p32RUF (figure 1). All culturing steps involving the lacO repeat were performed at 30°C using MAX efficiency Stbl2 competent cells (Invitrogen). All products obtained by PCR or oligo synthesis were sequenced to ensure fidelity.

Cell culture, Lox and Flip-In

Cell lines H100 and H94 are human embryonal kidney (HEK293) cells containing a lentiviral construct, integrated in a ridge (HG17: position 147.192.859 in forward orientation) or anti-ridge (HG17: position 218.918.221 in reverse orientation) region, respectively (Gierman *et al.*, 2007). The lentiviral construct contained an FRT site (Flp Recombinase Target site; O'Gorman *et al.*, 1991) to promote homologous recombination at the site of integration, and a GFP reporter cassette flanked by two loxP sites. In order to insert p32RUF, the GFP reporter cassette was loxed out by transfection with Cre recombinase. Cells that had lost the GFP cassette were identified by fluorescence activated cell sorting and single cells were seeded in a 96-well plate. Next, p32RUF was inserted at the FRT integration site by Flp-In as described previously (O'Gorman *et al.*, 1991). Briefly, p32RUF was cotransfected with Flp recombinase-expressing plasmid pOG44 (Invitrogen), required for site-specific recombination at the FRT site, in a 9:1 ratio (pOG44:p32RUF) using Lipofectamine 2000 (Invitrogen) according to the manufacturer's protocol. Cells were diluted 1:10 after 24 hours and selection pressure (115 μg/ml hygromycin) was added. After 2 weeks, individual clones could be distinguished. Clones were transferred to a 12-well for further culturing and DNA isolation. Cell lines were tested for integration at the FRT site by PCR and southern blotting. VH10 and HEK cells were

cultured in Dulbecco Minimal Essential Medium (DMEM) containing 10% or 15% fetal bovine serum respectively, 1% penicillin/streptomycin and 1% glutamin at 37°C in a 10% CO_2 atmosphere. For RT-qPCR and FISH, HEK cells were transfected at 80% confluency with Lipofectamine 2000 as described by the manufacturer. After 24-48 hours, cells were either harvested for RNA isolation or transferred to poly-L-lysine coated slides in preparation for FISH.

Southern Blot
Isolation of genomic DNA was performed by overnight cell lysis at 55°C in Tris buffer (10 mM Tris pH 7.5, 2 mM EDTA, 10 mM NaCl, 0.5% SDS) supplemented with 1 mg/ml Proteinase K (Roche) and subsequent precipitation. Genomic DNA was cut overnight with *BglII* (Roche, 50 U/µl) or a combination of *ClaI* and *XhoI* (Roche, 10 and 40 U/µl, respectively), so as to cut once in the lentiviral LTR and once in the integrated p32RUF, excising a single ~5.9 and ~4 kb band, respectively. 10 µg of restricted DNA was run overnight on a 1% agarose gel and transferred to an Amersham Nylon membrane the following night. The blot was probed overnight with a ~300 bp lacO fragment, labeled with $AT^{32}P$. Washes were performed at 63°C and detection occurred with the aid of a phosphor image screen.

Reverse transcription quantitative PCR (RT-qPCR)
RNA was isolated after trypsinization from 25 cm^2 culture flasks with the Qiagen RNeasy Mini Kit according to the accompanying manual. After solution in RNAse-free H_2O, RNA was processed immediately for cDNA synthesis: 5 µg of RNA was incubated for 20 minutes with RNAse-free DNAse I (Roche) at room temperature. Next, we heated the RNA for 5 minutes at 70°C to dissociate the tertiary structure followed by immediate cooling on ice for 5 minutes. cDNA was synthesized with the Improm II kit (Promega), using oligo dT primer and incubating the reaction mix for 5 minutes at 25°C to anneal primers and 60 minutes at 42°C to allow cDNA synthesis. The reaction was inactivated for 15 minutes at 70°C and cooled on ice. Quantitative PCR reactions were performed on a 7500 Real Time Cycler (Applied Biosystems), using accompanying software and SYBR-green (Invitrogen) as a detection reagent. Relative gene expressions were calculated using the ΔΔCT method.

Three-dimensional fluorescent in situ hybridization (3D FISH)
For 3D FISH, cells were grown on poly-L-lysine coated slides and fixed in 4% paraformaldehyde for 10 minutes at 4°C. Paraformaldehyde was quenched after 3 PBS washes in 100 mM glycin for 10 minutes and cells were subsequently placed in 0.1 N HCl, washed in PBS and permeabilized in PBS containing 0.5% Triton X-100 and 0.5% Saponin for 20 minutes. After three PBS washes, slides were treated with 100 µl RNAse (100 µg/ml) at 37°C for 30 minutes. Three PBS washing steps were followed by a 5-minute incubation in 2x SSC for 5 minutes and immersion in 50% formamide in 2x SSC for up to 2 hours. For preparation of the probe 100 ng of BAC or 10 ng of lac DNA, amplified by DOP-PCR and labeled by nick translation with either biotin of digoxigenin, was dissolved in deionised formamide supplemented with 50% formamide and 10% dextrane sulfate to a final concentration of 12.5 ng probe/µl. The probe was denatured at 80°C for 10 minutes and placed on ice, followed by 1 to 2 hours of pre-annealing at 37°C. Next, the probe was added to the pre-treated slide and codenatured for 2 minutes at 80°C. Hybridization was allowed to proceed overnight in a moist chamber at 37°C. Three posthybridization washes were carried out with 2x SSC-50% formamide at 45°C, followed by three washes in 0.1x SSC at 60°C and blocking with 4x SSC containing 5% non-fat dried milk for 1 hour at room temperature. All incubations for probe detection were performed for 20 minutes at room temperature in 4x SSC containing 5% (wt/vol) non-fat dried milk, alternated by three washes in 0.05% Tween/2x SSC. Slides were finally labeled in DAPI (4', 6'-diamidino-2-phenylindole; Vector Laboratories, Burlingame, CA) and embedded in Vectashield (Brunschwig, Burlingame, CA). Slides were imaged using a Zeiss LSM 510 (Zeiss, Jena, Germany) confocal laser scanning microscope equipped with a 63x/1.4 oil immersion objective. We used multitrack scanning, employing a UV laser (364 nm), an argon laser (488 nm) and a helium-neon laser (543 nm) to excite DAPI staining and green and red fluorochromes. Emitted fluorescence was detected with BP 385-470, BP 505-550 and 560 LP filters. Three-dimensional images were scanned at 512 by 512 using 400 nm axial and 60 nm lateral sampling rates. Images were averaged 4 times.

Results and discussion

Development and single integration of the cell system

To study the *in vivo* causal relationships between local induction of an epigenetic chromatin state and the changes in chromatin structure and gene activity in a specific genomic context, we created a cell system consisting of a cassette containing two short arrays of non-endogenous protein-binding sites and a reporter gene. The cassette (p32RUF) contains 32 tandem copies of the lacO sequence (lacO repeat) and 14 tandem copies of the UAS site for targeting by lac repressor (lacR) and Gal4, respectively. In addition, the targeting cassette contains a dsRed reporter gene tagged by a mitochondrial targeting signal (MTS) to reduce fluorescent background in the nucleus, an FRT site to enable homologous recombination at defined genomic sites and a hygromycin selection marker for subsequent selection (figure 1). To test the functionality regarding visualization, ability to measure chromatin folding and gene activity, the cassette was integrated in human embryonal kidney 293 (HEK 293) cells. Integration of foreign DNA into defined genomic regions of human cells is very inefficient. We used HEK cell lines containing an FRT site promoting recombination at a defined position on chromosome 1 band q21.1 and chromosome 2 band q36.1, corresponding to a ridge and anti-ridge (Gierman *et al.*, 2007). These cell lines additionally contained a GFP reporter used for a previous study between two LoxP sites, which we removed using Cre/loxP recombinase. Next, we integrated the cassette into the FRT site with the aid of Flpase. The mono-clonally generated cell lines were screened for single integration by PCR and southern blotting. The HEK 94R99 and 100R21 clones were identified as clones having a single integration in the anti-ridge and in the ridge genomic region, respectively (figure 2).

During the multiple rounds of transfection (*i.e.* integration of an FRT and GFP reporter gene between LoxP sites, subsequent removal of the GFP reporter, integration of the composite cassette at the FRT site and the transfection with GFP-tagged lacR) the cells became increasingly difficult to culture and transfect, limiting the use of the system. The use of cell lines that enable homologous recombination, such as mouse embryonic stem cells, might be a suitable alternative to solve this issue. Moreover, the stable expression of inducible lacR targeting fusion proteins will avoid transfecting cell lines for each new experiment, while the inducibility limits continuous over-expression of lacR-tagged epigenetic regulators.

Visualization of 32 lacO sites *in vivo*

The amount of tandem copies of the non-endogenous protein-binding sites was minimized to 32 lacO sequences as the integration of large exogenous stretches of repetitive DNA may interfere with epigenetic gene regulation. To visualize the lacO repeat in the HEK cell nuclei, images were taken from nuclei with a low EGFP-lacR expression level to minimize background fluorescence (figure 3). The lacO repeat is

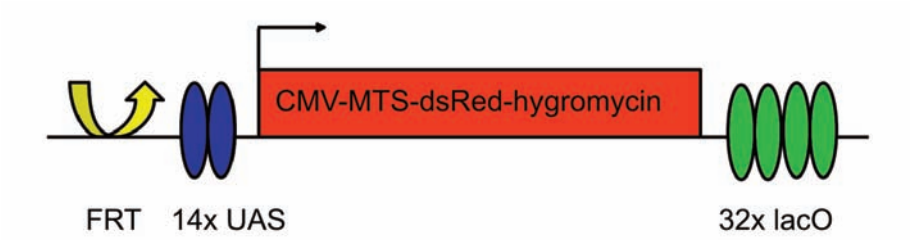

Figure 1. Schematic representation of the cassette p32RUF. The cell system consists of an integrated cassette containing a CMV-driven red fluorescent reporter with a mitochondrial targeting signal and a hygromycin selection marker separated by an IRES (internal ribosome entry site) to ensure translation initiation (red), flanked by 14 tandem copies of the non-endogenous UAS protein-binding sites (blue) upstream and 32 tandem copies of the lacO protein-binding sites (green) downstream. A Flp-recombinase targeting (FRT; yellow) site enables homologous recombination.

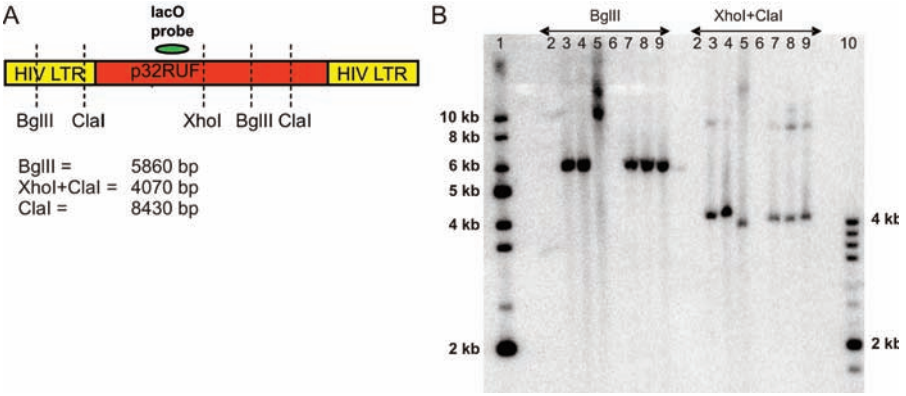

Figure 2. Southern blot analysis to verify the single integration of the p32RUF cassette. (A) Schematic representation of the position of the lacO probe (green) relative to restriction sites in the p32RUF cassette (red) that has been flipped into the virally integrated FRT, which is flanked by viral long terminal repeats (LTR; yellow). Expected fragment lengths for *BglII*, *XhoI*+*ClaI* and *ClaI* are given. (B) Genomic DNA of 6 cell lines with potential integration of p32RUF in an anti-ridge (lanes 3-5) or ridge (lanes 7-9) was digested overnight with *BglII* (first half of blot) or a combination of *XhoI* and *ClaI* (second half of blot). DNA fragments were separated by gel electrophoresis, transferred to a nylon membrane and probed for the lacO with an AT^{32}P-labeled probe. Lanes numbered 1 and 10 contain a DNA marker, lanes 2 and 6 contain a control cell line without lacO integration. The ~8.4 kb bands in the *XhoI/ClaI*-digested lanes are due to incomplete *XhoI* digestion (data not shown). Cell lines HEK 94R99 and 100R21, chosen for further experiments, were loaded in lanes 3 and 7, respectively.

indicated by the arrow.

In vivo visualization of the 32 tandem lacO copies integrated in the HEK cell lines proved to be challenging, as opposed to the clear detectability of EGFP-lacR binding at lacO arrays spanning several mega basepairs (Belmont *et al.*, 1999; Robinett *et al.*, 1996; Tumbar *et al.*, 1999). The lacR has a high affinity for the bacterial lacO sequence with a K_D between 10^{-11} and 10^{-13} M (Chen and Matthews, 1992; Riggs *et al.*, 1970). However, the lacR also binds non-specifically to DNA with dissociation constants

differing an estimated 6-8 orders of magnitude compared to specific binding (Lin and Riggs, 1975). The occupancy of a binding site depends on the affinity of the lacR for that site, the concentration of lacR molecules and on the number of binding sites. Given the relatively high amount of non-specific compared to specific binding sites, the absolute number of lacR molecules bound to non-specific DNA will be very high, thereby creating considerable background noise. We conclude that under optimal imaging conditions 32 tandem copies of the lacO site can be visualized in HEK cells if the concentration of the lacR-GFP protein is sufficiently low. To increase visibility, a higher amount of lacO sites may be used. Previously, it was shown that, in principle, a minimal amount of a 128 lacO sequences is detectable in yeast and mammalian cells (Brickner and Walter, 2004; Chubb *et al.*, 2002). Alternatively, the concentration of lacR molecules can be significantly lowered, such that only several tens of lacR molecules, which will mainly occupy lacO sites, are available in each cell (Elf *et al.*, 2007).

Chromatin structure visualized by FISH

Measurements on the distance between two positions on a single chromosome provide information on how chromatin is folded locally. Changes in the distance between these two positions after targeting epigenetic regulatory proteins are indicative of changes in chromatin folding due to the actions of these regulators. We therefore set out to detect the integrated cassette and a genomic reference site at a defined distance from the integrated region on the same chromosome by 3D FISH. We used a plasmid probe to detect the cassette and a specific BAC probe to recognize the reference site. Figure 4 illustrates the visualization of a ~100 kb BAC probe and a ~9 kb probe of the integrated plasmid. Results indicate that the 3D FISH method allows distance measurements between the lacO repeat and a genomic region nearby, recognized by a BAC probe, generating information on chromatin compaction (Mateos-Langerak *et al.*, 2009, PNAS, in press). Ultimately, measuring distances between the loci labeled by lacR and Gal4 may generate information about the *in vivo* compaction of the chromatin fiber without using the FISH method. However, the non-endogenous protein-binding sites in our current pilot system are only ~4 kb apart at linear distance, which is not sufficient to measure physical distances using standard light microscopy techniques.

The transcriptional activity of a dsRed reporter gene is influenced by its genomic context

To quantify gene activity, we have measured the fluorescence intensity of the mitochondrial dsRed reporter by fluorescence activated cell sorting (FACS) analysis. For this purpose, a mouse fibroblast cell line (VH10) was established containing multiple random, stable integrations of the lacO repeat next to the dsRed-MTS reporter. We transfected the cells with EGFP-lacR-VP16, or EGFP-lacR as a control, and

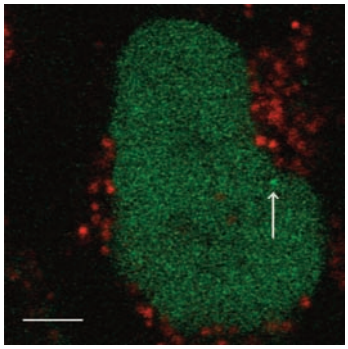

Figure 3. Living cell analysis of the integrated cassette. HEK cells with the p32RUF cassette flipped into the FRT site situated in a ridge, were transfected with EGFP-lacR. DsRed is expressed in the mitochondria. 3D images were recorded of nuclei with low EGFP-lacR expression with the pinhole set at 2.00 airy units to allow a maximal number of fluorescent proteins to be detected and averaged 8 times to reduce Poisson noise. The green signal represents EGFP-lacR. The arrow indicates the position of the lacO repeats targeted by EGFP-lacR. The image shown represents an individual optical section. Bar represents 2 µm.

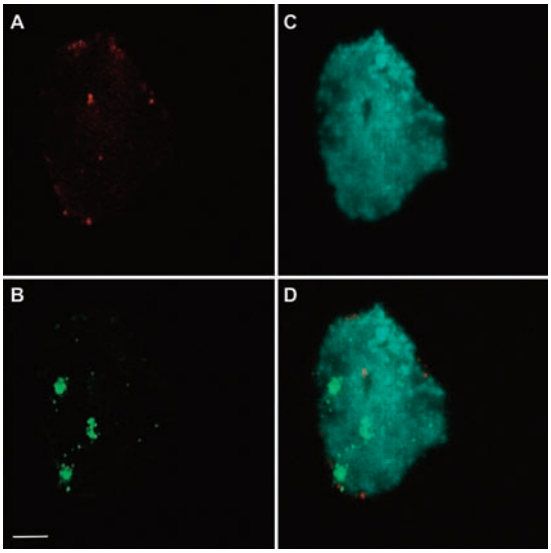

Figure 4. Fluorescent *in situ* hybridization. HEK cells with the p32RUF cassette flipped into the FRT site situated in an anti-ridge on chromosome 2 were FISH labeled. Probes containing p32RUF or nick-translated DNA from BAC RP11-465F2 (chromosome 11, q-arm), were labeled with biotin (A) or digoxigenin (B) respectively, and were hybridized to fixed and permeabilized cells. Antibody detection was achieved through Strep-Cy3 (Jackson, 1:1000) enhanced by goat anti-Strep-bio (Vector, 1:250) and Strep-Cy3 for biotin (A) and mouse anti-Dig (Boehringer, 1:250) followed by rabbit anti-mouse-FITC (Sigma, 1:1000) and goat anti-rabbit-Alexa488 (Molecular Probes, 1:200) for digoxigenin (B). 3D images were recorded in separate channels. The red signal represents the FISH labeled p32RUF probe recognized by anti-biotin antibodies, the green signal represents the FISH-labeled BAC probe recognized by anti-Dig antibodies and the blue signal represents DAPI staining. Part (D) portrays the merged image. Bar represents 2 µm.

A

epigenetic regulator	mean intensity of fluorescence	normalized intensity of fluorescence
EGFPlacR	7025	1.0
VP16	13775	2.0
HP1	6308	0.9
MeCP2	5249	0.8

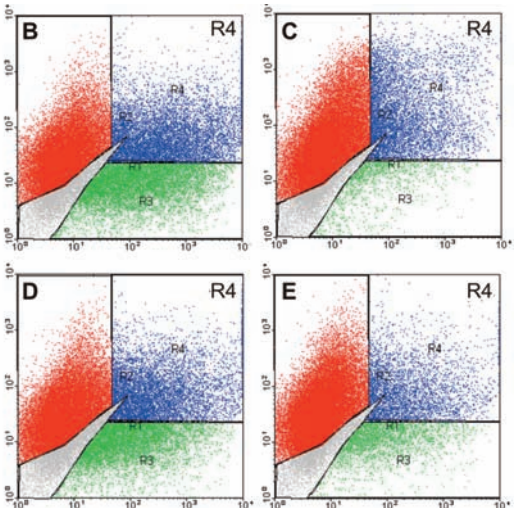

Figure 5. FACS analysis of dsRed reporter-expressing cells upon targeting. A VH10 cell line containing random integrations of 32 lacO repeats directly downstream of a dsRed reporter cassette was transiently transfected with EGFP-lacR control and EGFP-lacR-tagged VP16, HP1β and MeCP2. Fluorescence intensity was measured by FACS analysis; threshold values were set according to measurements in cells devoid of fluorescent proteins or expressing only dsRed or EGFP. (A) Table represents dsRed fluorescence intensities in EGFP-transfected cells. (B, C, D, E) Scatter plots of cells transfected with lacR (B), lacR-VP16 (C), lacR-HP1β (D) and lacR-MeCP2 (E) respectively. Green fluorescence is depicted along the *x*-axis and red fluorescence along the *y*-axis. Fluorescence intensities were measured in the R4-gated cells (blue).

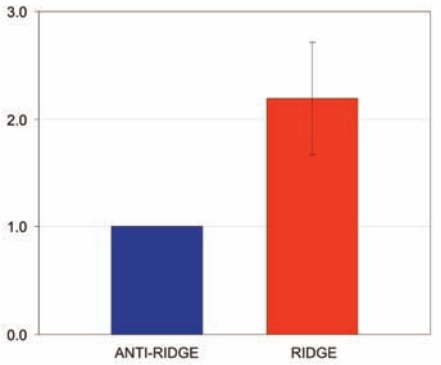

Figure 6. Relative reporter gene expression in the ridge versus anti-ridge region by RT-qPCR. RNA isolated from HEK 94R99 and 100R21 was reverse transcribed into cDNA with oligo dT primers. Relative dsRed expression from 4 different samples was determined by qPCR in a total of 23 experiments. Samples were normalized to RP L13A expression. DsRed expression in the anti-ridge region was set to 1.

analyzed dsRed expression of EGFP-expressing cells, 60 hours after transfection. The mean intensity of the dsRed fluorescence increased considerably in the VP16-expressing cells, going up to 13775 fluorescence units compared to 7205 units in the EGFP-lacR targeted control (figure 5). Next, we measured gene repression of the dsRed reporter by transiently transfecting the clones with EGFP-lacR-HP1β or EGFP-lacR-MeCP2. However, we were unable to detect an appreciable decrease in the expression levels of the reporter gene, measuring 6308 units for the HP1β-targeted and 5249 units for the MeCP2-targeted cells (EGFP-lacR = 7205 units, figure 5). The high expression and slow turnover of the dsRed protein (half life of ~5 days, Verkhusha *et al.*, 2003) prevents faithful detection of a decrease in the transcriptional activity of

the reporter gene. Therefore, we propose the use of an unstable reporter protein for future cell-system developments, for instance by fusion to a degradation signal (Lindsten *et al.*, 2003). Taken together, we conclude that in the current system fluorescence intensity of the dsRed reporter gene is an efficient read-out for gene activation, but not for gene repression.

To assess the influence of the local chromatin environment on gene expression, we measured RNA levels of the CMV-driven dsRed reporter after integration into HEK cell lines in two distinct genomic loci: a high and low expressing region, *i.e.* a ridge and anti-ridge, respectively. Reverse transcription quantitative PCR (RT-qPCR) was performed on HEK clones 94R99 and 100R21 for the dsRed gene, normalizing expression levels to ribosomal protein L13A (RPL13A; Pombo-Suarez *et al.*, 2008). We observed an approximately two-fold higher gene expression level of the dsRed protein when integrated in a ridge (chromosome 1 band q21.1) compared to an anti-ridge (chromosome 2 band q36.1; figure 6). These findings correspond to published data showing that expression levels of a GFP reporter gene driven by the PGK promoter are similarly affected by their integration into ridge or anti-ridge domains (Gierman *et al.*, 2007). It is interesting to note that the chromatin integration site of genes with a strong viral promoter (*i.e.* CMV) influences their expression to almost the same extent as a gene driven from the relatively weak PGK promoter (~three-fold difference when integrated in identical locations; H. Gierman, personal communication). These data support a model in which the transcriptional potential of a gene is partially determined by the chromatin environment in which it is embedded.

A drawback of determining RNA levels by biochemical bulk methods, such as RT-qPCR and northern blot analysis, is that they do not allow the detection of cell-to-cell variation. As an alternative, a recent advance has been made with the use of MS2 repeats, which form an RNA hairpin that is recognized by the MS2 coat protein, enabling single cell *in vivo* quantification of the expression level of a reporter gene by binding the fluorescently-tagged MS2 protein (Chubb *et al.*, 2006; Finlan *et al.*, 2008; Janicki *et al.*, 2004).

In conclusion, we have created a novel chromatin manipulation system in human cells consisting of a cassette that is integrated in a defined genomic background. We show preliminary data on the engineered cassette, integrated in single copy in a ridge and an anti-ridge region in human cell lines. We are able to (i) visualize the integrated cassette, (ii) determine the 3D position of the integrated cassette in relation to a nearby genomic reference region enabling measurement of the local chromatin compaction, (iii) measure changes in reporter gene activity by FACS analysis (gene activation) and RT-qPCR (gene activation and repression). We conclude that this cell system can be an important tool for studying molecular mechanisms of epigenetic gene regulation in living cells.

Acknowledgements

We would like to thank dr. M. J. Moné (VU, Amsterdam, The Netherlands) for expert assistance on the *in vivo* confocal imaging, ir. B. Hooijbrink (AMC, Amsterdam, The Netherlands) for performance of the FACS analysis, dr. M. S. Luijsterburg for critical reading of the manuscript and Ing. R. Bader and R. Charaffedine for technical assistance. This work was supported by the Netherlands Organisation for Scientific Research (NWO; project number VIDI2003/03921/ALW/016.041.311).

Chapter 6

Towards hierarchical eukaryotic gene network representations: a perspective

Maartje C. Brink, Roeland Merks, Pernette J. Verschure & Roel van Driel

In preparation

Gene network representations in eukaryotes

A gene network consists of a set of genes that, directly or indirectly, affect each other's activity. The combination of regulatory proteins and non-coding RNAs (ncRNAs) in the cell are the key determinant of the functional state of the network, thereby defining, in principle, the properties of the cell. Hence, understanding gene networks is essential to achieving a basic understanding of cell function. Currently, the representation of gene networks is often in the form of graphs, which can have a simple (Friedman *et al.*, 2000) or a more sophisticated format (such as CellDesigner, Cytoscape and BioTapestry; Kitano *et al.*, 2005; Longabaugh *et al.*, 2005; Shannon *et al.*, 2003). These representations are oversimplifications, ignoring most of the molecular complexity of the system, such as system dynamics and the multiple processes implicated by the edges of the graph. These edges include, even in the most simple gene-gene interaction mechanism; transcription, transcript maturation and packaging, nuclear export, translation of RNA to protein, posttranslational modification, nuclear import and assembly of an active transcription initiation complex. In this sense, gene networks are fundamentally different from metabolic networks, which mostly refer to metabolites, enzyme-catalyzed chemical conversions and protein-protein interactions (Schilling *et al.*, 1999).

Here we address the question of how eukaryotic gene network models should be shaped and which components and processes may be incorporated, including those acting at the epigenetic level of gene regulation. The rapidly increasing knowledge of genome-wide gene regulation creates a promising basis to expand gene network models in order to present a comprehensive system, allowing an in-depth understanding of gene regulation. Here, we explore what information should be incorporated in eukaryotic gene network models to make them more realistic and informative, augmenting their predictive value and insight into the logic of gene networks. Amongst others we indicate what components and variables constitute a eukaryotic gene network and how epigenetic regulatory interactions can be integrated.

Limitations of present representations of eukaryotic genetic networks

At present, most gene network representations depict genes as nodes in classical graphs. However, such representations ignore many aspects of eukaryotic gene regulation. In particular, the edges connecting the nodes are often ill-defined and may represent a wide variety of interactions, including highly indirect interactions involving for instance signal transduction pathways or processing through multi-step metabolic pathways (Schilling *et al.*, 1999). Some types of gene network representations compensate for this to some extent. For instance, the BioTapestry format annotates nodes by using different colours, signifying the type of interaction (Longabaugh *et al.*, 2005). A major challenge is to develop a gene network format that incorporates all essential aspects of the system. A key component in gene regulation that has been ignored in all eukaryotic gene network models so far is the epigenetic regulation of

gene expression, despite its impact on gene expression (Jenuwein and Allis, 2001; Turner, 2007). Additionally, the role of regulatory ncRNAs, probably being equally important to gene control at all levels as proteins, should be incorporated (Goodrich and Kugel, 2006). Inevitably, new concepts have to be developed for eukaryotic gene network models to incorporate these aspects.

Two hierarchical levels of gene regulation

Gene regulation in eukaryotes comprises at least two levels of gene regulation, *i.e.* the classic gene level, acting on individual genes, and the epigenetic level, controlling genomic loci that often contain multiple genes (Bruggeman *et al.*, 2008; de Wit and van Steensel, 2008). Gene-level and epigenetic regulation are both under control of transcription factors (TFs) and possibly ncRNAs (Mattick and Makunin, 2006), defined here as factors that recognize specific DNA sequences. These factors decide, often in a combinatorial way, exactly where in the genome a change in gene activity and/or chromatin state is induced. Subsequently, they initiate the assembly of a chromatin-associated protein or protein-ncRNA complex to execute transcription.

Epigenetic gene regulation changes the chromatin state of defined genomic loci. Locus switching may for instance be accompanied by a transition between facultative heterochromatin and euchromatin (Goetze *et al.*, 2007). Changes in the chromatin state are potentially controlled by locus control region (LCR)-like genomic sequence elements, which are different from promoters and enhancers (Noordermeer *et al.*, 2008). Epigenetic loci range from tens of kbs (*e.g.* the β-globin locus) up to several Mbs (*e.g.* the MHC locus). Locus boundaries are defined by so called boundary elements or insulators (Wei *et al.*, 2005). Epigenetic switching of chromatin states is induced by (i) changes in DNA methylation, (ii) various (but not all) histone modifications, and (iii) the exchange of canonical histones by variant histones (Bird, 2002; Henikoff *et al.*, 2004; Turner, 2007). The epigenetically controlled chromatin state is stably transmitted during cell division, *e.g.* in imprinting phenomena where one of the parental alleles is expressed while the other is repressed (Bartolomei *et al.*, 1991; Edwards and Ferguson-Smith, 2007). Epigenetic regulation is thought to play a key role in cell differentiation (Bird, 2002; Ng and Gurdon, 2008). An example of the role of epigenetics in deciding cell fate is the presence of 'bivalent domains' in the developmental regulatory genes in pluripotent ES cells (Azuara *et al.*, 2006; Bernstein *et al.*, 2006). A single bivalent domain in the undifferentiated cell contains both activating and repressive histone modifications, only one of which remains upon cell differentiation (Bernstein *et al.*, 2006). Epigenetic mechanisms are an integral part of gene regulatory systems in eukaryotes and should therefore be incorporated in gene networks.

How can we integrate the epigenetic regulatory level in gene networks?

To incorporate epigenetic regulation into eukaryotic gene networks, we propose a

simple set of rules. The epigenetically controlled genomic locus is demarcated at both sides by an insulator or boundary element. The locus can occur in two epigenetic states.

1) The non-permissive state. In the epigenetically silent state all genes of the locus are inactive, irrespective of the presence or absence of TFs that may or may not bind to the regulatory sequences of the constituent genes.

2) The permissive state. In the epigenetically permissive state the genes of a locus can be switched on and off individually by the binding of TFs to their promoter and enhancer sequences.

A well-studied example of epigenetic regulation is the β-globin locus. In non-haemopoietic cells, the β-globin locus is epigenetically non-permissive, blocking transcription of all of its genes. On the other hand, in haemopoietic cells the locus is in a permissive state, allowing regulation of its individual genes (Brown *et al.*, 2001; Higgs *et al.*, 2006). More examples of epigenetically controlled multi-gene loci are known, indicating a potentially important role for gene clustering (Sproul *et al.*, 2005). Gene clusters may contain functionally related genes or genes that are not related in an obvious way except that they have to be available for transcription under the same physiological condition.

Consequently, we identify three possible states for any gene, characterized by the state of the locus and the state of the individual gene. The three states are (epigenetic state/ genetic state): off/off, on/off, on/on. In the epigenetic 'off' state, all genes are switched off, independent of the presence of relevant TFs. On the other hand, when the epigenetic locus is 'on', the individual genes can be activated or inactivated, depending on the availability of the required TFs. This simple set of rules allows the formal, hierarchical integration of the epigenetic control level in gene regulatory networks.

What are the relevant components and variables for eukaryotic gene networks?
Gene networks in higher eukaryotes can be defined by the components and variables described below, accompanying genome-wide detection techniques are listed in table 1.

System components

1. Genes: defined as genomic sequences coding for proteins or for functional ncRNAs.
2. Transcripton factors (TFs): proteins and regulatory ncRNAs that recognize genomic sequence elements that play a role in gene-level or epigenetic regulation.
3. TF binding sites: key regulatory sequences at the epigenetic level and the individual gene level. At the gene level, TF binding sites include promoters, enhancers and enhancer blockers. At the epigenetic level they include locus control regions and boundary elements.
4. Epigenetic units: genomic domains (often gene clusters) that can be

switched between a permissive and a non-permissive state. Presently, only a limited number of epigenetic units have been thoroughly characterized, the β-globin cluster being a paradigm. The difficulty in identifying epigenetic units is that our knowledge of epigenetics is still insufficient to recognize them on the basis of genome-wide measured epigenetic markers. However, this will change rapidly with the development of highly efficient ChIP-seq technologies (Barski *et al.*, 2007; Mikkelsen *et al.*, 2007).

5. Boundary elements, insulators and enhancer blockers: boundary elements mark the two borders of epigenetic units. So far, only a limited number of boundary elements (or insulators) has been identified (van der Vlag *et al.*, 2000). Enhancer blockers act as regulatory elements that control enhancer-promoter interations. Insulator is a term used for both of these two types of elements, as we often cannot discriminate between their function at present.

System variables

1. Activity of genes: the activity level of a gene is often represented by a Boolean parameter, *i.e.* on or off, whereas in reality gene activity is a continuous variable. Currently, we have no simple and accurate method for quantifying gene activity. Most networks up to now are based on microarray data, which measure levels of RNA, rather than rates of RNA synthesis (Harbers and Carninci, 2005).
2. Activity state of TFs: the activity state of TFs depends on regulation by post-translational modifications of the TF and/or translocation between the nucleus and the cytoplasm.
3. Occupation of TF binding sites: this variable controls the activity state of genes and epigenetic units. It should be noted that gene activity and the epigenetic chromatin state often rely on the combined binding of multiple TFs to regulatory regions in the genome.
4. on/off state of epigenetic units: the epigenetic state is likely to be related to chromatin structure and can be inferred from the presence of histone modifications, DNA methylation and the incorporation of variant histones (Bird, 2002; Henikoff *et al.*, 2004; Turner, 2007). Not all histone modifications relate to the epigenetic state, some modifications are pertinent to the individual gene state. For instance, H3K9 di- and trimethylation generally mark epigenetically non-permissive loci, whereas H3K4 trimethylation and acetylation of histones H3 and H4 are components of regulatory systems that act on individual genes (Turner, 2007).
5. Activity state of boundary elements/enhancer blockers: the activity of boundary elements and enhancer blockers may be regulated as well. An example for the differential activity of enhancer blockers is best illustrated by the well-described Igf2/H19 imprinting locus (Schoenherr *et al.*, 2003). In

this locus, the LCR functions as an enhancer blocker to either the Igf2 or the H19 gene, dependent on its DNA methylation status and subsequent binding of the CCCTC-binding factor (CTCF) protein (Bell and Felsenfeld, 2000; Hark *et al.*, 2000; Szabo *et al.*, 2000). Similarly, binding by factors such as CTCF and non-coding RNAs potentially activate boundary elements (Guelen *et al.*, 2008; Rinn *et al.*, 2007).

These network components define the eukaryotic gene networks, whereas the values of the variables define the state of the network. Switching between network states may be achieved by changing intracellular or extracellular cues, such as cell-cycle signals or hormones, respectively.

Additional levels of gene control

The systematic enumeration of all components and variables does not necessarily add up to a comprehensive eukaryotic gene network. Additional factors and regulatory levels may exist that have an impact on gene regulation. For instance, the spatial folding of the genome inside the cell nucleus (at nuclear, chromosomal and subchromosomal level) may have implications for gene activity (reviewed by Goetze *et al.*, 2007) possibly resulting in chromatin-chromatin interactions at different genomic length scales. For instance, multiple transcription factor-mediated chromatin interactions have been identified at the β-globin locus by 3C and 5C (Chromosome Conformation Capture (Carbon Copy)) techniques between the LCR and the β-globin genes (Dostie *et al.*, 2006; Drissen *et al.*, 2004; Vakoc *et al.*, 2005). Another example is the possible formation of transcription factories, bringing together genes that are far apart on the linear genome (Osborne *et al.*, 2004). The functional significance of these and other chromatin-chromatin interactions remains to be clarified.

The black box

By their very nature, gene-gene interactions are indirect and involve many steps in a variety of cellular subsystems. The most direct type of gene-gene interaction is that of a gene coding for a TF, which binds to a regulatory sequence of another gene. Such an interaction is often depicted by a simple edge in a graph, but in reality includes many steps. These include pre-mRNA synthesis, RNA processing, RNA transport to the cytoplasm, interaction with ribosomes, protein synthesis, protein import into the nucleus, (frequently) posttranslational modification and binding to its regulatory site in a promoter or enhancer. Often, gene-gene interactions are much more complex, involving signal transduction or metabolic networks. These multi-step processes are not stated explicitly in gene networks and are treated as black boxes. The use of black boxes is acceptable if all components and interactions inside the black box are constitutively present and active, *i.e.* when their quantity and activity is not regulated. Obviously, this is almost never the case in gene-gene interactions. Currently, in most

Table 1. Overview of commonly used, mostly high-throughput techniques used to determine factors critical to genome-wide regulation.

system component or variable	genome-scale technique	reference
Genomic sequence elements, *e.g.* genes, TF binding sites, insulators	high throughput sequencing, computational comparative sequence analysis	reviewed in Mardis, 2008
Binding sites for TFs and regulatory proteins	Dam-ID	van Steensel and Henikoff, 2000
Regulatory sites on the basis of nucleosome depletion	DNAseI sensitivity and FAIRE	Crawford *et al.*, 2006a; Crawford *et al.*, 2006b; Giresi *et al.*, 2007; Lee *et al.*, 2004; van Steensel and Henikoff, 2000
TF proteins and their activity state	proteomics	Conrotto and Souchelnytskyi, 2008; Graham *et al.*, 2005; Patterson and Aebersold, 2003
TF binding kinetics	light microscopy: FLIP, FRAP, FRET	Hoogstraten *et al.*, 2002; Houtsmuller *et al.*, 1999; Matyus, 1992; Phair and Misteli, 2000
Occupation of TF protein-binding sites	ChIP-chip, ChIP-seq	Barski *et al.*, 2007; Blat and Kleckner, 1999; Mikkelsen *et al.*, 2007; Ren *et al.*, 2000
Binding of regulatory RNAs	no methods yet	
on/off state of genes	micro-array, RNA-seq	reviewed in Rando, 2007; Wang *et al.*, 2009
epigenetic state of chromatin	ChIP-Seq and quantitative ChIP methods: SACO (Serial Analysis of Chromatin Occupancy) and G-MAT (Genome-wide MApping Technique), bisulfite sequencing, meDIP	reviewed in Callinan and Feinberg, 2006; Rando, 2007; Schones and Zhao, 2008
chromatin compaction	4C and 5C techniques	Dostie *et al.*, 2006; Simonis *et al.*, 2006

cases it is not possible to integrate all relevant steps in gene-gene interactions. This problem should be addressed in any type of gene network. Solving this problem is essentially equivalent to integrating metabolic and signal transduction networks, as well as cell-cell signaling systems, in gene-gene networks. Difficult as this may be, there is no way around it.

Modeling epigenetic units in eukaryotic gene networks

Once epigenetic regulation units have been incorporated into a computational representation of genetic regulatory networks, the next step is to study the dynamics and to analyze its structure. In the absence of detailed descriptions of hierarchical regulation levels in real systems, a first approach is to study theoretical models. Continuous and stochastic modeling approaches have yielded detailed insights into the workings of small natural gene networks (Chabot *et al.*, 2007; Suel *et al.*, 2006; van Hoek and Hogeweg, 2006; van Zon *et al.*, 2007) and synthetic gene networks (Elowitz and Leibler, 2000; Kobayashi *et al.*, 2004; Stricker *et al.*, 2008). However, for larger natural networks this approach becomes unfeasible, because the required parameters (*e.g.*transcription rates, TF-DNA binding constants, TF-TF binding constants) are currently unknown at the large scale. Boolean approaches only consider 'on' or 'off' states of genes and can give us better insight into the switching logic of gene networks. Boolean approaches were introduced in the pioneering work of Kauffman, Thomas and Glass in the late sixties and early seventies (Glass and Kauffman, 1973; Kauffman, 1969; Thomas, 1973). Related approaches are still widely used today (for recent examples see Istrail and Davidson, 2005; Li *et al.*, 2006; Mendoza *et al.*, 1999; Shmulevich *et al.*, 2005). These 'logical' gene network analyses represent genetic regulatory circuits using networks of genes and regulatory units that assume an 'on' or an 'off' state, while the edges represent TFs produced by the other genes in the networks. Boolean functions (*e.g.* 'AND' or 'OR') determine whether the TFs act as an activator or as an inhibitor of gene expression. For example, assuming two TFs can bind to each promoter, the 'AND' function would indicate that both TFs are required for transcription to proceed, while an 'OR' function would indicate that either one of them would suffice. Other Boolean functions express more complicated inhibitory and activating interactions between the TFs and the promoter.

Although hierarchical regulation levels are currently lacking from datasets of biological regulatory networks, we can already explore the role of hierarchical regulation in dynamic models of random regulatory networks. Figure 1 illustrates how we might incorporate epigenetic regulation into Kauffman's Boolean network formalism. Figure 1A shows a standard, randomly connected, 'flat' Boolean network of 8 nodes and two TFs regulating each node, with Boolean functions chosen at random. After randomly putting each of the nodes in an 'on' or 'off' state, we iteratively update the state of each node in parallel. In this example, after an initial transition the network alternates between two expression patterns, called a state cycle.

This is typical behavior for Boolean networks: the system can reach one out several steady states or state cycles, depending on its initial pattern. These steady states or state cycles, called *attractors*, are often considered models of cell types, while the initial transitory phases—or the transition to a different attractor after an external perturbation—might resemble differentiation (Kauffman, 1969; Shmulevich *et al.*, 2005).

In panel B we add a hierarchical level of description. We insert an insulator into the network, creating two regions of hierarchical regulation. For simplicity, we assume the region assumes a 'permissive' state (*i.e.* the state in which it is accessible for

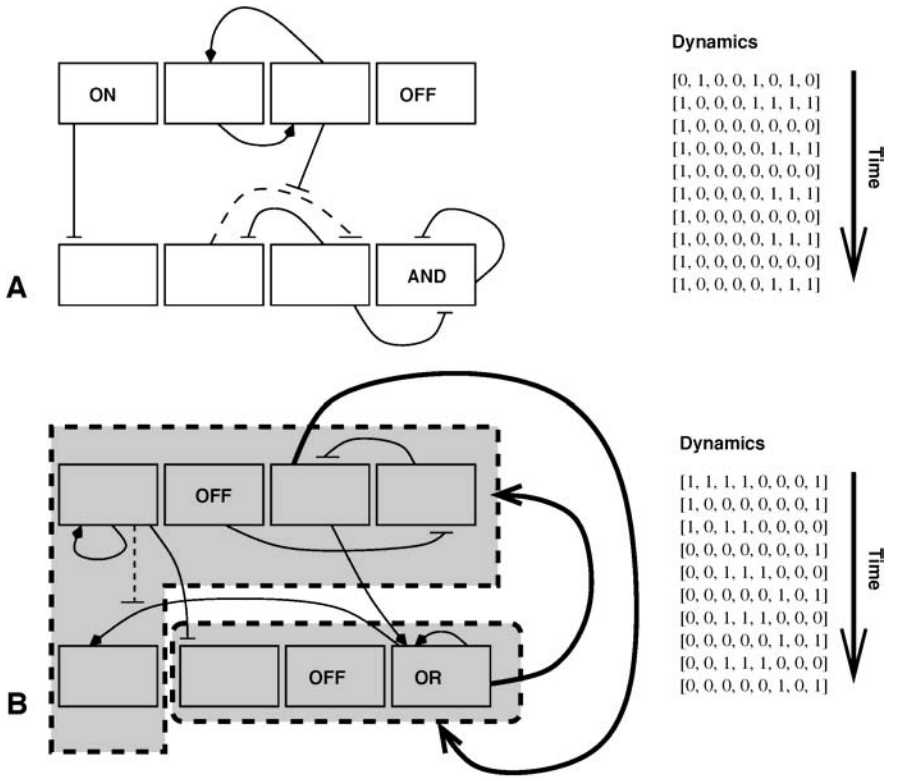

Figure 1. Boolean networks, with 8 genes receiving input from two transcription factors. Non-functional inputs were removed to improve graphical representation. Activating interactions shown with arrow heads, inhibitory interactions shown with flat arrow heads. Boolean functions indicate combinatory dependence on inputs; OR: either input, or both, can be present for their effect on transcription; AND: both inputs must be present; OFF: gene is never transcribed; ON: gene is always transcribed. Dynamics with synchroneous updating shown on the right with random initial conditions and time pointing downwards. A) Standard Boolean network. B) Boolean network with two hierarchically regulated regions shown as grey regions, regulated by genes 3 and 8 respectively. Regions are in the permissive state if the regulator is switched on.

transcription) if its regulator (chosen at random) is in the 'on' state. Here, after an initial transition state, the two subnetworks alternate between a permissive and a closed, non-permissive state.

We are currently systematically exploring the behaviour of larger Boolean networks with several insulators. Interestingly, our first results indicate that the hierarchical regulation level tends to reduce both the number and length of the attractors found in Boolean networks. Thus we may speculate that, apart from the perhaps obvious role of hierarchical regulation in compartmentalizing functionality required in only a subset of cell types, hierarchical regulation might stabilize and structure regulatory networks. The insights gained using these theoretical explorations will help to interpret the role of hierarchical regulation in biological networks once detailed datasets of eukaryotic networks, including the hierarchical regulation units, have become available.

Acknowledgements

We thank dr. Jana Rudolph for valuable discussions. This work was supported by the Netherlands Organisation for Scientific Research (NWO; project number VIDI2003/03921/ALW/016.041.311).

Bibliography

Aasland, R. and Stewart, A.F. (1995) The chrome shadow domain, a second chrome domain in heterochromatin-binding protein 1, HP1. Nucleic Acids Research, 23, 3168-3173.

Agarwal, N., Hardt, T., Brero, A., Nowak, D., Rothbauer, U., Becker, A., Leonhardt, H. and Cardoso, M.C. (2007) MeCP2 interacts with HP1 and modulates its heterochromatin association during myogenic differentiation. Nucleic Acids Res, 35, 5402-5408.

Amir, R.E., Van den Veyver, I.B., Wan, M., Tran, C.Q., Francke, U. and Zoghbi, H.Y. (1999) Rett syndrome is caused by mutations in X-linked MECP2, encoding methyl-CpG-binding protein 2. Nat Genet, 23, 185-188.

Azuara, V., Perry, P., Sauer, S., Spivakov, M., Jorgensen, H.F., John, R.M., Gouti, M., Casanova, M., Warnes, G., Merkenschlager, M. and Fisher, A.G. (2006) Chromatin signatures of pluripotent cell lines. Nat Cell Biol, 8, 532-538.

Ballestar, E., Yusufzai, T.M. and Wolffe, A.P. (2000) Effects of Rett syndrome mutations of the methyl-CpG binding domain of the transcriptional repressor MeCP2 on selectivity for association with methylated DNA. Biochemistry, 39, 7100-7106.

Bannister, A.J., Zegerman, P., Partridge, J.F., Miska, E.A., Thomas, J.O., Allshire, R.C. and Kouzarides, T. (2001) Selective recognition of methylated lysine 9 on histone H3 by the HP1 chromo domain. Nature, 410, 120-124.

Barski, A., Cuddapah, S., Cui, K., Roh, T.Y., Schones, D.E., Wang, Z., Wei, G., Chepelev, I. and Zhao, K. (2007) High-resolution profiling of histone methylations in the human genome. Cell, 129, 823-837.

Bartolomei, M.S., Zemel, S. and Tilghman, S.M. (1991) Parental imprinting of the mouse H19 gene. Nature, 351, 153-155.

Bell, A.C. and Felsenfeld, G. (2000) Methylation of a CTCF-dependent boundary controls imprinted expression of the Igf2 gene. Nature, 405, 482-485.

Belmont, A.S., Li, G., Sudlow, G. and Robinett, C. (1999) Visualization of large-scale chromatin structure and dynamics using the lac operator/lac repressor reporter system. Methods Cell Biol, 58, 203-222.

Bernstein, B.E., Mikkelsen, T.S., Xie, X., Kamal, M., Huebert, D.J., Cuff, J., Fry, B., Meissner, A., Wernig, M., Plath, K., Jaenisch, R., Wagschal, A., Feil, R., Schreiber, S.L. and Lander, E.S. (2006) A bivalent chromatin structure marks key developmental genes in embryonic stem cells. Cell, 125, 315-326.

Bird, A. (2002) DNA methylation patterns and epigenetic memory. Genes Dev, 16, 6-21.

Blat, Y. and Kleckner, N. (1999) Cohesins bind to preferential sites along yeast chromosome III, with differential regulation along arms versus the centric region. Cell, 98, 249-259.

Bolzer, A., Kreth, G., Solovei, I., Koehler, D., Saracoglu, K., Fauth, C., Muller, S., Eils, R., Cremer, C., Speicher, M.R. and Cremer, T. (2005) Three-dimensional maps of all chromosomes in human male fibroblast nuclei and prometaphase rosettes. PLoS Biol, 3, e157.

Branco, M.R. and Pombo, A. (2006) Intermingling of chromosome territories in interphase suggests role in translocations and transcription-dependent associations. PLoS Biol, 4, e138.

Brasher, S.V., Smith, B.O., Fogh, R.H., Nietlispach, D., Thiru, A., Nielsen, P.R., Broadhurst, R.W., Ball, L.J., Murzina, N.V. and Laue, E.D. (2000) The structure of mouse HP1 suggests a unique mode of single peptide recognition by the shadow chromo domain dimer. EMBO J, 19, 1587-1597.

Brero, A., Easwaran, H.P., Nowak, D., Grunewald, I., Cremer, T., Leonhardt, H. and Cardoso, M.C. (2005) Methyl CpG-binding proteins induce large-scale chromatin reorganization during terminal differentiation. J Cell Biol, 169, 733-743.

Brickner, J.H. and Walter, P. (2004) Gene recruitment of the activated INO1 locus to the nuclear membrane. PLoS Biol, 2, e342.

Brink, M.C., van der Velden, Y., de Leeuw, W., Mateos-Langerak, J., Belmont, A.S., van Driel, R. and Verschure, P.J. (2006) Truncated HP1 lacking a functional chromodomain induces heterochromatinization upon *in vivo* targeting. Histochem Cell Biol, 125, 53-61.

Brown, K.E., Amoils, S., Horn, J.M., Buckle, V.J., Higgs, D.R., Merkenschlager, M. and Fisher, A.G. (2001) Expression of alpha- and beta-globin genes occurs within different nuclear domains in

haemopoietic cells. Nat Cell Biol, 3, 602-606.
Bruggeman, F.J., Oancea, I. and van Driel, R. (2008) Exploring the behavior of small eukaryotic gene networks. J Theor Biol, 252, 482-487.
Bunker, C.A. and Kingston, R.E. (1996) Activation domain-mediated enhancement of activator binding to chromatin in mammalian cells. Proc Natl Acad Sci USA, 93, 10820-10825.
Buschdorf, J.P. and Stratling, W.H. (2004) A WW domain binding region in methyl-CpG-binding protein MeCP2: impact on Rett syndrome. J Mol Med, 82, 135-143.
Callinan, P.A. and Feinberg, A.P. (2006) The emerging science of epigenomics. Hum Mol Genet, 15 Spec No 1, R95-101.
Caron, H., van Schaik, B., van der Mee, M., Baas, F., Riggins, G., van Sluis, P., Hermus, M.C., van Asperen, R., Boon, K., Voute, P.A., Heisterkamp, S., van Kampen, A. and Versteeg, R. (2001) The human transcriptome map: clustering of highly expressed genes in chromosomal domains. Science, 291, 1289-1292.
Carter, C.W., Jr. (1978) Histone packing in the nucleosome core particle of chromatin. Proc Natl Acad Sci USA, 75, 3649-3653.
Chabot, J.R., Pedraza, J.M., Luitel, P. and van Oudenaarden, A. (2007) Stochastic gene expression out-of-steady-state in the cyanobacterial circadian clock. Nature, 450, 1249-1252.
Chahrour, M., Jung, S.Y., Shaw, C., Zhou, X., Wong, S.T., Qin, J. and Zoghbi, H.Y. (2008) MeCP2, a Key Contributor to Neurological Disease, Activates and Represses Transcription. Science, 320, 1224-1229.
Chambeyron, S. and Bickmore, W.A. (2004) Chromatin decondensation and nuclear reorganization of the HoxB locus upon induction of transcription. Genes Dev, 18, 1119-1130.
Chen, J. and Matthews, K.S. (1992) Deletion of lactose repressor carboxyl-terminal domain affects tetramer formation. J Biol Chem, 267, 13843-13850.
Cheutin, T., McNairn, A.J., Jenuwein, T., Gilbert, D.M., Singh, P.B. and Misteli, T. (2003) Maintenance of stable heterochromatin domains by dynamic HP1 binding. Science, 299, 721-725.
Chubb, J.R., Boyle, S., Perry, P. and Bickmore, W.A. (2002) Chromatin motion is constrained by association with nuclear compartments in human cells. Curr Biol, 12, 439-445.
Chubb, J.R., Trcek, T., Shenoy, S.M. and Singer, R.H. (2006) Transcriptional pulsing of a developmental gene. Curr Biol, 16, 1018-1025.
Conrotto, P. and Souchelnytskyi, S. (2008) Proteomic approaches in biological and medical sciences: principles and applications. Exp Oncol, 30, 171-180.
Cowell, I.G., Aucott, R., Mahadevaiah, S.K., Burgoyne, P.S., Huskisson, N., Bongiorni, S., Prantera, G., Fanti, L., Pimpinelli, S., Wu, R., Gilbert, D.M., Shi, W., Fundele, R., Morrison, H., Jeppesen, P. and Singh, P.B. (2002) Heterochromatin, HP1 and methylation at lysine 9 of histone H3 in animals. Chromosoma, 111, 22-36.
Crawford, G.E., Davis, S., Scacheri, P.C., Renaud, G., Halawi, M.J., Erdos, M.R., Green, R., Meltzer, P.S., Wolfsberg, T.G. and Collins, F.S. (2006a) DNase-chip: a high-resolution method to i dentify DNase I hypersensitive sites using tiled microarrays. Nat Methods, 3, 503-509.
Crawford, G.E., Holt, I.E., Whittle, J., Webb, B.D., Tai, D., Davis, S., Margulies, E.H., Chen, Y., Bernat, J.A., Ginsburg, D., Zhou, D., Luo, S., Vasicek, T.J., Daly, M.J., Wolfsberg, T.G. and Collins, F.S. (2006b) Genome-wide mapping of DNase hypersensitive sites using massively parallel signature sequencing (MPSS). Genome Res, 16, 123-131.
Cremer, M., von Hase, J., Volm, T., Brero, A., Kreth, G., Walter, J., Fischer, C., Solovei, I., Cremer, C. and Cremer, T. (2001) Non-random radial higher-order chromatin arrangements in nuclei of diploid human cells. Chromosome Res, 9, 541-567.
Cremer, T. and Cremer, C. (2001) Chromosome territories, nuclear architecture and gene regulation in mammalian cells. Nat Rev Genet 2, 292-301.
Cremer, T., Kupper, K., Dietzel, S. and Fakan, S. (2004) Higher order chromatin architecture in the cell nucleus: on the way from structure to function. Biol Cell, 96, 555-567.
Cremer, T., Kurz, A., Zirbel, R., Dietzel, S., Rinke, B., Schrock, E., Speicher, M.R., Mathieu, U., Jauch, A., Emmerich, P., Scherthan, H., Ried, T., Cremer, C. and Lichter, P. (1993) Role of chromosome territories in the functional compartmentalization of the cell nucleus. Cold Spring Harb Symp Quant Biol, 58, 777-792.
Croft, J.A., Bridger, J.M., Boyle, S., Perry, P., Teague, P. and Bickmore, W.A. (1999) Differences in

the localization and morphology of chromosomes in the human nucleus. J Cell Biol, 145, 1119-1131.
de Leeuw, W., Verschure, P.J. and van Liere, R. (2006) Isualization and analysis of large data collections: a case study applied to confocal microscopy data. IEEE Trans Vis Comput Graph, 12, 1251-1258.
de Wit, E., Greil, F. and van Steensel, B. (2007) High-resolution mapping reveals links of HP1 with active and inactive chromatin components. PLoS Genet, 3, e38.
de Wit, E. and van Steensel, B. (2008) Chromatin domains in higher eukaryotes: insights from genome-wide mapping studies. Chromosoma.
Dialynas, G.K., Terjung, S., Brown, J.P., Aucott, R.L., Baron-Luhr, B., Singh, P.B. and Georgatos, S.D. (2007) Plasticity of HP1 proteins in mammalian cells. J Cell Sci, 120, 3415-3424.
Dillon, N. (2004) Heterochromatin structure and function. Bio Cell, 96, 631-637.
Dinant, C., de Jager, M., Essers, J., van Cappellen, W.A., Kanaar, R., Houtsmuller, A.B. and Vermeulen, W. (2007) Activation of multiple DNA repair pathways by sub-nuclear damage induction methods. J Cell Sci, 120, 2731-2740.
Dostie, J., Richmond, T.A., Arnaout, R.A., Selzer, R.R., Lee, W.L., Honan, T.A., Rubio, E.D., Krumm, A., Lamb, J., Nusbaum, C., Green, R.D. and Dekker, J. (2006) Chromosome Conformation Capture Carbon Copy (5C): a massively parallel solution for mapping interactions between genomic elements. Genome Res, 16, 1299-1309.
Drissen, R., Palstra, R.J., Gillemans, N., Splinter, E., Grosveld, F., Philipsen, S. and de Laat, W. (2004) The active spatial organization of the beta-globin locus requires the transcription factor EKLF. Genes Dev, 18, 2485-2490.
Edwards, C.A. and Ferguson-Smith, A.C. (2007) Mechanisms regulating imprinted genes in clusters. Curr Opin Cell Biol, 19, 281-289.
Eissenberg, J.C., James, T.C., Foster-Hartnett, D.M., Hartnett, T., Ngan, V. and Elgin, S.C. (1990) Mutation in a heterochromatin-specific chromosomal protein is associated with suppression of position-effect variegation in Drosophila melanogaster. Proc Natl Acad Sci USA, 87, 9923-9927.
Elf, J., Li, G.W. and Xie, X.S. (2007) Probing transcription factor dynamics at the single-molecule level in a living cell. Science, 316, 1191-1194.
Elowitz, M.B. and Leibler, S. (2000) A synthetic oscillatory network of transcriptional regulators. Nature, 403, 335-338.
Fakan, S. (1994) Perichromatin fibrils are *in situ* forms of nascent transcripts. Trends Cell Biol, 4, 86-90.
Fakan, S. and van Driel, R. (2007) The perichromatin region: a functional compartment in the nucleus that determines large-scale chromatin folding. Semin Cell Dev Biol, 18, 676-681.
Felsenfeld, G. and Groudine, M. (2003) Controlling the double helix. Nature, 421, 448-453.
Festenstein, R., Pagakis, S.N., Hiragami, K., Lyon, D., Verreault, A., Sekkali, B. and Kioussis, D. (2003) Modulation of heterochromatin protein 1 dynamics in primary mammalian cells. Science, 299, 719-721.
Festenstein, R., SharghiNamini, S., Fox, M., Roderick, K., Tolaini, M., Norton, T., Saveliev, A., Kioussis, D. and Singh, P. (1999) Heterochromatin protein 1 modifies mammalian PEV in a dose- and chromosomal-context-dependent manner. Nature Genetics, 23, 457-461.
Finch, J.T., Lutter, L.C., Rhodes, D., Brown, R.S., Rushton, B., Levitt, M. and Klug, A. (1977) Structure of nucleosome core particles of chromatin. Nature, 269, 29-36.
Finlan, L.E., Sproul, D., Thomson, I., Boyle, S., Kerr, E., Perry, P., Ylstra, B., Chubb, J.R. and Bickmore, W.A. (2008) Recruitment to the nuclear periphery can alter expression of genes in human cells. PLoS Genet, 4, e1000039.
Friedman, N., Linial, M., Nachman, I. and Pe'er, D. (2000) Using Bayesian networks to analyze expression data. J Comput Biol, 7, 601-620.
Fu, X.D. and Maniatis, T. (1990) Factor required for mammalian spliceosome assembly is localized to discrete regions in the nucleus. Nature, 343, 437-441.
Georgel, P.T., Horowitz-Scherer, R.A., Adkins, N., Woodcock, C.L., Wade, P.A. and Hansen, J.C. (2003) Chromatin compaction by human MeCP2. Assembly of novel secondary chromatin structures in the absence of DNA methylation. J Biol Chem, 278, 32181-32188.
Gierman, H.J., Indemans, M.H., Koster, J., Goetze, S., Seppen, J., Geerts, D., van Driel, R. and Versteeg, R. (2007) Domain-wide regulation of gene expression in the human genome. Genome Res, 17, 1286-1295.
Gilbert, N., Boyle, S., Fiegler, H., Woodfine, K., Carter, N.P. and Bickmore, W.A. (2004) Chromatin

architecture of the human genome: gene-rich domains are enriched in open chromatin fibers. Cell, 118, 555-566.

Gilbert, N., Boyle, S., Sutherland, H., deLasHeras, J., Allan, J., Jenuwein, T. and Bickmore, W.A. (2003) Formation of facultative heterochromatin in the absence of HP1. EMBO J, 22, 5540-5550.

Gilbert, N., Thomson, I., Boyle, S., Allan, J., Ramsahoye, B. and Bickmore, W.A. (2007) DNA methylation affects nuclear organization, histone modifications, and linker histone binding but not chromatin compaction. J Cell Biol, 177, 401-411.

Giresi, P.G., Kim, J., McDaniell, R.M., Iyer, V.R. and Lieb, J.D. (2007) FAIRE (Formaldehyde-Assisted Isolation of Regulatory Elements) isolates active regulatory elements from human chromatin. Genome Res, 17, 877-885.

Glass, L. and Kauffman, S.A. (1973) The logical analysis of continuous, non-linear biochemical control networks. J Theor Biol, 39, 103-129.

Goetze, S., Mateos-Langerak, J., Gierman, H.J., de Leeuw, W., Giromus, O., Indemans, M.H., Koster, J., Ondrej, V., Versteeg, R. and van Driel, R. (2007a) The three-dimensional structure of human interphase chromosomes is related to the transcriptome map. Mol Cell Biol, 27, 4475-4487.

Goetze, S., Mateos-Langerak, J. and van Driel, R. (2007b) Three-dimensional genome organization in interphase and its relation to genome function. Semin Cell Dev Biol, 18, 707-714.

Goodrich, J.A. and Kugel, J.F. (2006) Non-coding-RNA regulators of RNA polymerase II transcription. Nat Rev Mol Cell Biol, 7, 612-616.

Gossen, M. and Bujard, H. (1992) Tight control of gene expression in mammalian cells by tetracycline-responsive promoters. Proc Natl Acad Sci USA, 89, 5547-5551.

Graham, D.R., Elliott, S.T. and Van Eyk, J.E. (2005) Broad-based proteomic strategies: a practical guide to proteomics and functional screening. J Physiol, 563, 1-9.

Gronostajski, R.M. and Sadowski, P.D. (1985) Determination of DNA sequences essential for FLP-mediated recombination by a novel method. J Biol Chem, 260, 12320-12327.

Guelen, L., Pagie, L., Brasset, E., Meuleman, W., Faza, M.B., Talhout, W., Eussen, B.H., de Klein, A., Wessels, L., de Laat, W. and van Steensel, B. (2008) Domain organization of human chromosomes revealed by mapping of nuclear lamina interactions. Nature, 453, 948-951.

Hamer, K.M., Sewalt, R.G., den Blaauwen, J.L., Hendrix, T., Satijn, D.P. and Otte, A.P. (2002) A panel of monoclonal antibodies against human polycomb group proteins. Hybrid Hybridomics, 21, 245-252.

Harbers, M. and Carninci, P. (2005) Tag-based approaches for transcriptome research and genome annotation. Nat Methods, 2, 495-502.

Harikrishnan, K.N., Chow, M.Z., Baker, E.K., Pal, S., Bassal, S., Brasacchio, D., Wang, L., Craig, J.M., Jones, P.L., Sif, S. and El-Osta, A. (2005) Brahma links the SWI/SNF chromatin-remodeling complex with MeCP2-dependent transcriptional silencing. Nat Genet, 37, 254-264.

Hark, A.T., Schoenherr, C.J., Katz, D.J., Ingram, R.S., Levorse, J.M. and Tilghman, S.M. (2000) CTCF mediates methylation-sensitive enhancer-blocking activity at the H19/Igf2 locus. Nature, 405, 486-489.

Hediger, F. and Gasser, S.M. (2006) Heterochromatin protein 1: don't judge the book by its cover! Curr Opin Genet Develop, 16, 143-150.

Henikoff, S., Furuyama, T. and Ahmad, K. (2004) Histone variants, nucleosome assembly and epigenetic inheritance. Trends Genet, 20, 320-326.

Higgs, D.R., Vernimmen, D., De Gobbi, M., Anguita, E., Hughes, J., Buckle, V., Iborra, F., Garrick, D. and Wood, W.G. (2006) How transcriptional and epigenetic programmes are played out on an individual mammalian gene cluster during lineage commitment and differentiation. Biochem Soc Symp, 11-22.

Hiragami, K. and Festenstein, R. (2005) Heterochromatin protein 1: a pervasive controlling influence. Cell Mol Life Sci, 62, 2711-2726.

Hoogstraten, D., Nigg, A.L., Heath, H., Mullenders, L.H., van Driel, R., Hoeijmakers, J.H., Vermeulen, W. and Houtsmuller, A.B. (2002) Rapid switching of TFIIH between RNA polymerase I and II transcription and DNA repair *in vivo*. Mol Cell, 10, 1163-1174.

Horn, P.J. and Peterson, C.L. (2002) Molecular biology: Chromatin higher order folding: Wrapping up transcription. Science, 297, 1824-1827.

Horsley, D., Hutchings, A., Butcher, G.W. and Singh, P.B. (1996) M32, a murine homologue of Drosophila heterochromatin protein 1 (HP1), localises to euchromatin within interphase nuclei and is

largely excluded from constitutive heterochromatin. Cytogenetics and Cell Genetics, 73, 308-311.
Houtsmuller, A.B., Rademakers, S., Nigg, A.L., Hoogstraten, D., Hoeijmakers, J.H. and Vermeulen, W. (1999) Action of DNA repair endonuclease ERCC1/XPF in living cells. Science, 284, 958-961.
Hu, K., Nan, X., Bird, A. and Wang, W. (2006) Testing for association between MeCP2 and the brahma-associated SWI/SNF chromatin-remodeling complex. Nat Genet, 38, 962-964; author reply 964-967.
Istrail, S. and Davidson, E.H. (2005) Logic functions of the genomic cis-regulatory code. Proc Natl Acad Sci USA, 102, 4954-4959.
Jacobs, S.A. and Khorasanizadeh, S. (2002) Structure of HP1 chromodomain bound to a lysine 9-methylated histone H3 tail. Science, 295, 2080-2083.
Jacobs, S.A., Taverna, S.D., Zhang, Y., Briggs, S.D., Li, J., Eissenberg, J.C., Allis, C.D. and Khorasanizadeh, S. (2001) Specificity of the HP1 chromo domain for the methylated N-terminus of histone H3. EMBO J, 20, 5232-5241.
James, T.C. and Elgin, S.C.R. (1986) Identification of a nonhistone chromosomal protein associated with heterochromatin in Drosophila melanogaster and its gene. Molecular and Cellular Biology, 6, 3862-3872.
Janicki, S.M., Tsukamoto, T., Salghetti, S.E., Tansey, W.P., Sachidanandam, R., Prasanth, K.V., Ried, T., Shav-Tal, Y., Bertrand, E., Singer, R.H. and Spector, D.L. (2004) From silencing to gene expression: real-time analysis in single cells. Cell, 116, 683-698.
Jenuwein, T. (2001) Re-SET-ting heterochromatin by histone methyltransferases. Tr Cell Biol, 11, 266-273.
Jenuwein, T. and Allis, C.D. (2001) Translating the histone code. Science, 293, 1074-1080.
Kaludov, N.K. and Wolffe, A.P. (2000) MeCP2 driven transcriptional repression *in vitro*: selectivity for methylated DNA, action at a distance and contacts with the basal transcription machinery. Nucleic Acids Res, 28, 1921-1928.
Kauffman, S.A. (1969) Metabolic stability and epigenesis in randomly constructed genetic nets. J Theor Biol, 22, 437-467.
Kitano, H., Funahashi, A., Matsuoka, Y. and Oda, K. (2005) Using process diagrams for the graphical representation of biological networks. Nat Biotechnol, 23, 961-966.
Kobayashi, H., Kaern, M., Araki, M., Chung, K., Gardner, T.S., Cantor, C.R. and Collins, J.J. (2004) Programmable cells: interfacing natural and engineered gene networks. Proc Natl Acad Sci USA, 101, 8414-8419.
Kornberg, R.D. (1977) Structure of chromatin. Annu Rev Biochem, 46, 931-954.
Kourmouli, N., Theodoropoulos, P.A., Dialynas, G., Bakou, A., Politou, A.S., Cowell, I.G., Singh, P.B. and Georgatos, S.D. (2000) Dynamic associations of heterochromatin protein 1 with the nuclear envelope. EMBO J, 19, 6558-6568.
Kouzarides, T. (2007) Chromatin modifications and their function. Cell, 128, 693-705.
Kumaran, R.I. and Spector, D.L. (2008) A genetic locus targeted to the nuclear periphery in living cells maintains its transcriptional competence. J Cell Biol, 180, 51-65.
Lachner, M. and Jenuwein, T. (2002) The many faces of histone lysine methylation. Curr Opin Cell Biol, 14, 286-298.
Lachner, M., O'Carroll, D., Rea, S., Mechtler, K. and Jenuwein, T. (2001) Methylation of histone H3 lysine 9 creates a binding site for HP1 proteins. Nature, 410, 116-120.
Lamond, A.I. and Spector, D.L. (2003) Nuclear speckles: a model for nuclear organelles. Nat Rev Mol Cell Biol, 4, 605-612.
Lechner, M.S., Schultz, D.C., Negorev, D., Maul, G.G. and Rauscher, F.J. (2005) The mammalian heterochromatin protein 1 binds diverse nuclear proteins through a common motif that targets the chromoshadow domain. Biochem Biophys Res Commun, 331, 929-937.
Lee, C.K., Shibata, Y., Rao, B., Strahl, B.D. and Lieb, J.D. (2004) Evidence for nucleosome depletion at active regulatory regions genome-wide. Nat Genet, 36, 900-905.
Leonhardt, H., Rahn, H.P., Weinzierl, P., Sporbert, A., Cremer, T., Zink, D. and Cardoso, M.C. (2000) Dynamics of DNA replication factories in living cells. J Cell Biol, 149, 271-280.
Lercher, M.J., Urrutia, A.O. and Hurst, L.D. (2002) Clustering of housekeeping genes provides a unified model of gene order in the human genome. Nat Genet, 31, 180-183.
Lewis, J.D., Meehan, R.R., Henzel, W.J., Maurer-Fogy, I., Jeppesen, P., Klein, F. and Bird, A. (1992)

Purification, sequence, and cellular localization of a novel chromosomal protein that binds to methylated DNA. Cell, 69, 905-914.

Li, G., Sudlow, G. and Belmont, A.S. (1998) Interphase cell cycle dynamics of a late-replicating, heterochromatic homogeneously staining region: precise choreography of condensation/decondensation and nuclear positioning. J Cell Biol, 140, 975-989.

Li, S., Assmann, S.M. and Albert, R. (2006) Predicting essential components of signal transduction networks: a dynamic model of guard cell abscisic acid signaling. PLoS Biol, 4, e312.

Li, Y.H., Danzer, J.R., Alvarez, P., Belmont, A.S. and Wallrath, L.L. (2003) Effects of tethering HP1 to euchromatic regions of the Drosophila genome. Development, 130, 1817-1824.

Li, Y.H., Kirschmann, D.A. and Wallrath, L.L. (2002) Does heterochromatin protein 1 always follow code? Proc Natl Acad Sci USA, 99, 16462-16469.

Lin, S. and Riggs, A.D. (1975) The general affinity of lac repressor for E. coli DNA: implications for gene regulation in procaryotes and eucaryotes. Cell, 4, 107-111.

Lindsten, K., Menendez-Benito, V., Masucci, M.G. and Dantuma, N.P. (2003) A transgenic mouse model of the ubiquitin/proteasome system. Nat Biotechnol, 21, 897-902.

Longabaugh, W.J., Davidson, E.H. and Bolouri, H. (2005) Computational representation of developmental genetic regulatory networks. Dev Biol, 283, 1-16.

Luger, K., Mader, A.W., Richmond, R.K., Sargent, D.F. and Richmond, T.J. (1997) Crystal structure of the nucleosome core particle at 2.8 A resolution. Nature, 389, 251-260.

Luijsterburg, M.S., Goedhart, J., Moser, J., Kool, H., Geverts, B., Houtsmuller, A.B., Mullenders, L.H., Vermeulen, W. and van Driel, R. (2007) Dynamic *in vivo* interaction of DDB2 E3 ubiquitin ligase with UV-damaged DNA is independent of damage-recognition protein XPC. J Cell Sci, 120, 2706-2716.

Mahy, N.L., Perry, P.E. and Bickmore, W.A. (2002a) Gene density and transcription influence the localization of chromatin outside of chromosome territories detectable by FISH. J Cell Biol, 159, 753-763.

Mahy, N.L., Perry, P.E., Gilchrist, S., Baldock, R.A. and Bickmore, W.A. (2002b) Spatial organization of active and inactive genes and noncoding DNA within chromosome territories. J Cell Biol, 157, 579-589.

Maison, C. and Almouzni, G. (2004) HP1 and the dynamics of heterochromatin maintenance. Nat Rev Mol Cell Biol, 5, 296-304.

Maison, C., Bailly, D., Peters, A.H.F.M., Quivy, J.P., Roche, D., Taddei, A., Lachner, M., Jenuwein, T. and Almouzni, G. (2002) Higher-order structure in pericentric heterochromatin involves a distinct pattern of histone modification and an RNA component. Nat Genet, 30, 329-334.

Mardis, E.R. (2008) Next-generation DNA sequencing methods. Annu Rev Genomics Hum Genet, 9, 387-402.

Mateos-Langerak, J., Brink, M.C., Luijsterburg, M.S., van der Kraan, I., van Driel, R. and Verschure, P.J. (2007) Pericentromeric heterochromatin domains are maintained without accumulation of HP1. Mol Biol Cell, 18, 1464-1471.

Mattick, J.S. and Makunin, I.V. (2006) Non-coding RNA. Hum Mol Genet, 15 Spec No 1, R17-29.

Matyus, L. (1992) Fluorescence resonance energy transfer measurements on cell surfaces. A spectroscopic tool for determining protein interactions. J Photochem Photobiol B, 12, 323-337.

Meehan, R.R., Kao, C.F. and Pennings, S. (2003) HP1 binding to native chromatin *in vitro* is determined by the hinge region and not by the chromodomain. EMBO J, 22, 3164-3174.

Meehan, R.R., Lewis, J.D. and Bird, A.P. (1992) Characterization of MeCP2, a vertebrate DNA binding protein with affinity for methylated DNA. Nucleic Acids Res, 20, 5085-5092.

Mendoza, L., Thieffry, D. and Alvarez-Buylla, E.R. (1999) Genetic control of flower morphogenesis in Arabidopsis thaliana: a logical analysis. Bioinformatics, 15, 593-606.

Mikkelsen, T.S., Ku, M., Jaffe, D.B., Issac, B., Lieberman, E., Giannoukos, G., Alvarez, P., Brockman, W., Kim, T.K., Koche, R.P., Lee, W., Mendenhall, E., O'Donovan, A., Presser, A., Russ, C., Xie, X., Meissner, A., Wernig, M., Jaenisch, R., Nusbaum, C., Lander, E.S. and Bernstein, B.E. (2007) Genome-wide maps of chromatin state in pluripotent and lineage-committed cells. Nature, 448, 553-560.

Minc, E., Allory, V., Worman, H.J., Courvalin, J.C. and Buendia, B. (1999) Localization and phosphorylation of HP1 proteins during the cell cycle in mammalian cells. Chromosoma, 108, 220-234.

Minc, E., Courvalin, J.C. and Buendia, B. (2000) HP1 gamma associates with euchromatin and heterochromatin in mammalian nuclei and chromosomes. Cytogenet Cell Genet, 90, 279-284.

Muchardt, C., Guilleme, M., Seeler, J.S., Trouche, D., Dejean, A. and Yaniv, M. (2002) Coordinated methyl and RNA binding is required for heterochromatin localization of mammalian HP1 alpha. EMBO Rep, 3, 975-981.

Nakayama, J., Rice, J.C., Strahl, B.D., Allis, C.D. and Grewal, S.I. (2001) Role of histone H3 lysine 9 methylation in epigenetic control of heterochromatin assembly. Science, 292, 110-113.

Nan, X., Campoy, F.J. and Bird, A. (1997) MeCP2 is a transcriptional repressor with abundant binding sites in genomic chromatin. Cell, 88, 471-481.

Nan, X., Cross, S. and Bird, A. (1998a) Gene silencing by methyl-CpG-binding proteins. Novartis Found Symp, 214, 6-16; discussion 16-21, 46-50.

Nan, X., Meehan, R.R. and Bird, A. (1993) Dissection of the methyl-CpG binding domain from the chromosomal protein MeCP2. Nucleic Acids Res, 21, 4886-4892.

Nan, X., Ng, H.H., Johnson, C.A., Laherty, C.D., Turner, B.M., Eisenman, R.N. and Bird, A. (1998b) Transcriptional repression by the methyl-CpG-binding protein MeCP2 involves a histone deacetylase complex. Nature, 393, 386-389.

Ng, R.K. and Gurdon, J.B. (2008) Epigenetic inheritance of cell differentiation status. Cell Cycle, 7, 1173-1177.

Nielsen, A.L., Ortiz, J.A., You, J., OuladAbdelghani, M., Khechumian, R., Gansmuller, A., Chambon, P. and Losson, R. (1999) Interaction with members of the heterochromatin protein 1 (HP1) family and histone deacetylation are differentially involved in transcriptional silencing by members of the TIF1 family. EMBO J, 18, 6385-6395.

Nielsen, A.L., OuladAbdelghani, M., Ortiz, J.A., Remboutsika, E., Chambon, P. and Losson, R. (2001) Heterochromatin formation in mammalian cells: Interaction between histones and HP1 proteins. Mol Cell, 7, 729-739.

Nielsen, P.R., Nietlispach, D., Mott, H.R., Callaghan, J., Bannister, A., Kouzarides, T., Murzin, A.G., Murzina, N.V. and Laue, E.D. (2002) Structure of the HP1 chromodomain bound to histone H3 methylated at lysine 9. Nature, 416, 103-107.

Nikitina, T., Ghosh, R.P., Horowitz-Scherer, R.A., Hansen, J.C., Grigoryev, S.A. and Woodcock, C.L. (2007a) MeCP2-chromatin interactions include the formation of chromatosome-like structures and are altered in mutations causing Rett syndrome. J Biol Chem, 282, 28237-28245.

Nikitina, T., Shi, X., Ghosh, R.P., Horowitz-Scherer, R.A., Hansen, J.C. and Woodcock, C.L. (2007b) Multiple modes of interaction between the methylated DNA binding protein MeCP2 and chromatin. Mol Cell Biol, 27, 864-877.

Noordermeer, D., Branco, M.R., Splinter, E., Klous, P., van Ijcken, W., Swagemakers, S., Koutsourakis, M., van der Spek, P., Pombo, A. and de Laat, W. (2008) Transcription and chromatin organization of a housekeeping gene cluster containing an integrated beta-globin locus control region. PLoS Genet, 4, e1000016.

Nye, A.C., Rajendran, R.R., Stenoien, D.L., Mancini, M.A., Katzenellenbogen, B.S. and Belmont, A.S. (2002) Alteration of large-scale chromatin structure by estrogen receptor. Mol Cell Biol, 22, 3437-3449.

O'Gorman, S., Fox, D.T. and Wahl, G.M. (1991) Recombinase-mediated gene activation and site-specific integration in mammalian cells. Science, 251, 1351-1355.

Osborne, C.S., Chakalova, L., Brown, K.E., Carter, D., Horton, A., Debrand, E., Goyenechea, B., Mitchell, J.A., Lopes, S., Reik, W. and Fraser, P. (2004) Active genes dynamically colocalize to shared sites of ongoing transcription. Nat Genet, 36, 1065-1071.

Patterson, S.D. and Aebersold, R.H. (2003) Proteomics: the first decade and beyond. Nat Genet, 33 Suppl, 311-323.

Perez-Burgos, L., Peters, A.H., Opravil, S., Kauer, M., Mechtler, K. and Jenuwein, T. (2004) Generation and characterization of methyl-lysine histone antibodies. Methods Enzymol, 376, 234-254.

Peters, A.H., O'Carroll, D., Scherthan, H., Mechtler, K., Sauer, S., Schofer, C., Weipoltshammer, K., Pagani, M., Lachner, M., Kohlmaier, A., Opravil, S., Doyle, M., Sibilia, M. and Jenuwein, T. (2001) Loss of the suv39h histone methyltransferases impairs Mammalian heterochromatin and genome stability. Cell, 107, 323-337.

Phair, R.D. and Misteli, T. (2000) High mobility of proteins in the mammalian cell nucleus. Nature, 404,

604-609.
Platero, J.S., Hartnett, T. and Eissenberg, J.C. (1995) Functional analysis of the chromo domain of HP1. EMBO J, 14, 3977-3986.
Pombo-Suarez, M., Calaza, M., Gomez-Reino, J.J. and Gonzalez, A. (2008) Reference genes for normalization of gene expression studies in human osteoarthritic articular cartilage. BMC Mol Biol, 9, 17.
Rando, O.J. (2007) Chromatin structure in the genomics era. Trends Genet, 23, 67-73.
Reddy, K.L., Zullo, J.M., Bertolino, E. and Singh, H. (2008) Transcriptional repression mediated by repositioning of genes to the nuclear lamina. Nature, 452, 243-247.
Ren, B., Robert, F., Wyrick, J.J., Aparicio, O., Jennings, E.G., Simon, I., Zeitlinger, J., Schreiber, J., Hannett, N., Kanin, E., Volkert, T.L., Wilson, C.J., Bell, S.P. and Young, R.A. (2000) Genome-wide location and function of DNA binding proteins. Science, 290, 2306-2309.
Riggs, A.D., Suzuki, H. and Bourgeois, S. (1970) Lac repressor-operator interaction. I. Equilibrium studies. J Mol Biol, 48, 67-83.
Rinn, J.L., Kertesz, M., Wang, J.K., Squazzo, S.L., Xu, X., Brugmann, S.A., Goodnough, L.H., Helms, J.A., Farnham, P.J., Segal, E. and Chang, H.Y. (2007) Functional demarcation of active and silent chromatin domains in human HOX loci by noncoding RNAs. Cell, 129, 1311-1323.
Robinett, C.C., Straight, A., Li, G., Willhelm, C., Sudlow, G., Murray, A. and Belmont, A.S. (1996) In vivo localization of DNA sequences and visualization of large-scale chromatin organization using lac operator/repressor recognition. J Cell Biol, 135, 1685-1700.
Sauer, B. (1994) Site-specific recombination: developments and applications. Curr Opin Biotechnol, 5, 521-527.
Schilling, C.H., Schuster, S., Palsson, B.O. and Heinrich, R. (1999) Metabolic pathway analysis: basic concepts and scientific applications in the post-genomic era. Biotechnol Prog, 15, 296-303.
Schmiedeberg, L., Weisshart, K., Diekmann, S., Meyer Zu Hoerste, G. and Hemmerich, P. (2004) High- and low-mobility populations of HP1 in heterochromatin of mammalian cells. Mol Biol Cell, 15, 2819-2833.
Schoenherr, C.J., Levorse, J.M. and Tilghman, S.M. (2003) CTCF maintains differential methylation at the Igf2/H19 locus. Nat Genet, 33, 66-69.
Schones, D.E. and Zhao, K. (2008) Genome-wide approaches to studying chromatin modifications. Nat Rev Genet, 9, 179-191.
Schultz, D.C., Ayyanathan, K., Negorev, D., Maul, G.G. and Rauscher, F.J., 3rd. (2002) SETDB1: a novel KAP-1-associated histone H3, lysine 9-specific methyltransferase that contributes to HP1-mediated silencing of euchromatic genes by KRAB zinc-finger proteins. Genes Dev, 16, 919-932.
Shaner, N.C., Campbell, R.E., Steinbach, P.A., Giepmans, B.N., Palmer, A.E. and Tsien, R.Y. (2004) Improved monomeric red, orange and yellow fluorescent proteins derived from Discosoma sp. red fluorescent protein. Nat Biotechnol, 22, 1567-1572.
Shannon, P., Markiel, A., Ozier, O., Baliga, N.S., Wang, J.T., Ramage, D., Amin, N., Schwikowski, B. and Ideker, T. (2003) Cytoscape: a software environment for integrated models of biomolecular interaction networks. Genome Res, 13, 2498-2504.
Shmulevich, I., Kauffman, S.A. and Aldana, M. (2005) Eukaryotic cells are dynamically ordered or critical but not chaotic. Proc Natl Acad Sci USA, 102, 13439-13444.
Simonis, M., Klous, P., Splinter, E., Moshkin, Y., Willemsen, R., de Wit, E., van Steensel, B. and de Laat, W. (2006) Nuclear organization of active and inactive chromatin domains uncovered by chromosome conformation capture-on-chip (4C). Nat Genet, 38, 1348-1354.
Sims, R.J., Nishioka, K. and Reinberg, D. (2003) Histone lysine methylation: a signature for chromatin function. Trends Genet, 19, 629-639.
Singh, P.B. and Georgatos, S.D. (2002) HP1: Facts, open questions, and speculation. J Struct Biol, 140, 10-16.
Smothers, J.F. and Henikoff, S. (2000) The HP1 chromo shadow domain binds a consensus peptide pentamer. Current Biology, 10, 27-30.
Smothers, J.F. and Henikoff, S. (2001) The hinge and chrome shadow domain impart distinct targeting of HP1- like proteins. Mol Cell Biol, 21, 2555-2569.
Sproul, D., Gilbert, N. and Bickmore, W.A. (2005) The role of chromatin structure in regulating the expression of clustered genes. Nat Rev Genet, 6, 775-781.
Stewart, M.D., Li, J.W. and Wong, J.M. (2005) Relationship between histone H3 lysine 9 methylation,

transcription repression, and heterochromatin protein 1 recruitment. Mol Cell Biol, 25, 2525-2538.
Stricker, J., Cookson, S., Bennett, M.R., Mather, W.H., Tsimring, L.S. and Hasty, J. (2008) A fast, robust and tunable synthetic gene oscillator. Nature, 456, 516-519.
Suel, G.M., Garcia-Ojalvo, J., Liberman, L.M. and Elowitz, M.B. (2006) An excitable gene regulatory circuit induces transient cellular differentiation. Nature, 440, 545-550.
Szabo, P., Tang, S.H., Rentsendorj, A., Pfeifer, G.P. and Mann, J.R. (2000) Maternal-specific footprints at putative CTCF sites in the H19 imprinting control region give evidence for insulator function. Curr Biol, 10, 607-610.
Taverna, S.D., Li, H., Ruthenburg, A.J., Allis, C.D. and Patel, D.J. (2007) How chromatin-binding modules interpret histone modifications: lessons from professional pocket pickers. Nat Struct Mol Biol, 14, 1025-1040.
Thiru, A., Nietlispach, D., Mott, H.R., Okuwaki, M., Lyon, D., Nielsen, P.R., Hirshberg, M., Verreault, A., Murzina, N.V. and Laue, E.D. (2004) Structural basis of HP1/PXVXL motif peptide interactions and HP1 localisation to heterochromatin. EMBO J, 23, 489-499.
Thomas, R. (1973) Boolean formalization of genetic control circuits. J Theor Biol, 42, 563-585.
Tolhuis, B., Palstra, R.J., Splinter, E., Grosveld, F. and de Laat, W. (2002) Looping and interaction between hypersensitive sites in the active beta-globin locus. Mol Cell, 10, 1453-1465.
Tsukamoto, T., Hashiguchi, N., Janicki, S.M., Tumbar, T., Belmont, A.S. and Spector, D.L. (2000) Visualization of gene activity in living cells. Nat Cell Biol, 2, 871-878.
Tumbar, T. and Belmont, A.S. (2001) Interphase movements of a DNA chromosome region modulated by VP16 transcriptional activator. Nat Cell Biol, 3, 134-139.
Tumbar, T., Sudlow, G. and Belmont, A.S. (1999) Large-scale chromatin unfolding and remodeling induced by VP16 acidic activation domain. J Cell Biol, 145, 1341-1354.
Turner, B.M. (2007) Defining an epigenetic code. Nat Cell Biol, 9, 2-6.
Vakoc, C.R., Letting, D.L., Gheldof, N., Sawado, T., Bender, M.A., Groudine, M., Weiss, M.J., Dekker, J. and Blobel, G.A. (2005a) Proximity among distant regulatory elements at the beta-globin locus requires GATA-1 and FOG-1. Mol Cell, 17, 453-462.
Vakoc, C.R., Mandat, S.A., Olenchock, B.A. and Blobel, G.A. (2005b) Histone H3 lysine 9 methylation and HP1gamma are associated with transcription elongation through mammalian chromatin. Mol Cell, 19, 381-391.
van der Vlag, J., den Blaauwen, J.L., Sewalt, R.G., van Driel, R. and Otte, A.P. (2000) Transcriptional repression mediated by polycomb group proteins and other chromatin-associated repressors is selectively blocked by insulators. J Biol Chem, 275, 697-704.
van Hoek, M.J. and Hogeweg, P. (2006) In silico evolved lac operons exhibit bistability for artificial inducers, but not for lactose. Biophys J, 91, 2833-2843.
van Royen, M.E., Cunha, S.M., Brink, M.C., Mattern, K.A., Nigg, A.L., Dubbink, H.J., Verschure, P.J., Trapman, J. and Houtsmuller, A.B. (2007) Compartmentalization of androgen receptor protein-protein interactions in living cells. J Cell Biol, 177, 63-72.
van Steensel, B. and Henikoff, S. (2000) Identification of *in vivo* DNA targets of chromatin proteins using tethered dam methyltransferase. Nat Biotechnol, 18, 424-428.
van Zon, J.S., Lubensky, D.K., Altena, P.R. and ten Wolde, P.R. (2007) An allosteric model of circadian KaiC phosphorylation. Proc Natl Acad Sci USA, 104, 7420-7425.
Verkhusha, V.V., Kuznetsova, I.M., Stepanenko, O.V., Zaraisky, A.G., Shavlovsky, M.M., Turoverov, K.K. and Uversky, V.N. (2003) High stability of Discosoma DsRed as compared to Aequorea EGFP. Biochemistry, 42, 7879-7884.
Verschure, P.J., van der Kraan, I., de Leeuw, W., van der Vlag, J., Carpenter, A.E., Belmont, A.S. and van Driel, R. (2005) In vivo HP1 targeting causes large-scale chromatin condensation and enhanced histone lysine methylation. Mol Cell Biol, 25, 4552-4564.
Verschure, P.J., Van Der Kraan, I., Enserink, J.M., Mone, M.J., Manders, E.M. and Van Driel, R. (2002) Large-scale chromatin organization and the localization of proteins involved in gene expression in human cells. J Histochem Cytochem, 50, 1303-1312.
Verschure, P.J., van der Kraan, I., Manders, E.M. and van Driel, R. (1999) Spatial relationship between transcription sites and chromosome territories. J Cell Biol, 147, 13-24.
Versteeg, R., van Schaik, B.D., van Batenburg, M.F., Roos, M., Monajemi, R., Caron, H., Bussemaker, H.J. and van Kampen, A.H. (2003) The human transcriptome map reveals extremes in gene density, intron length, GC content, and repeat pattern for domains of highly and weakly

expressed genes. Genome Res, 13, 1998-2004.
Vicent, G.P., Ballare, C., Nacht, A.S., Clausell, J., Subtil-Rodriguez, A., Quiles, I., Jordan, A. and Beato, M. (2008) Convergence on chromatin of non-genomic and genomic pathways of hormone signaling. J Steroid Biochem Mol Biol, 109, 344-349.
Volpi, E.V., Chevret, E., Jones, T., Vatcheva, R., Williamson, J., Beck, S., Campbell, R.D., Goldsworthy, M., Powis, S.H., Ragoussis, J., Trowsdale, J. and Sheer, D. (2000) Large-scale chromatin organization of the major histocompatibility complex and other regions of human chromosome 6 and its response to interferon in interphase nuclei. J Cell Sci, 113 (Pt 9), 1565-1576.
Wang, W. (2003) The SWI/SNF family of ATP-dependent chromatin remodelers: similar mechanisms for diverse functions. Curr Top Microbiol Immunol, 274, 143-169.
Wang, Z., Gerstein, M. and Snyder, M. (2009) RNA-Seq: a revolutionary tool for transcriptomics. Nat Rev Genet, 10, 57-63.
Wansink, D.G., Schul, W., van der Kraan, I., van Steensel, B., van Driel, R. and de Jong, L. (1993) Fluorescent labeling of nascent RNA reveals transcription by RNA polymerase II in domains scattered throughout the nucleus. J Cell Biol, 122, 283-293.
Wei, G.H., Liu, D.P. and Liang, C.C. (2005) Chromatin domain boundaries: insulators and beyond. Cell Res, 15, 292-300.
Wreggett, K.A., Hill, F., James, P.S., Hutchings, A., Butcher, G.W. and Singh, P.B. (1994) A Mammalian Homologue of Drosophila Heterochromatin Protein 1 (Hp1) Is a Component of Constitutive Heterochromatin. Cytogenetics and Cell Genetics, 66, 99-103.
Yasui, D.H., Peddada, S., Bieda, M.C., Vallero, R.O., Hogart, A., Nagarajan, R.P., Thatcher, K.N., Farnham, P.J. and Lasalle, J.M. (2007) Integrated epigenomic analyses of neuronal MeCP2 reveal a role for long-range interaction with active genes. Proc Natl Acad Sci USA, 104, 19416-19421.
Yusufzai, T.M. and Wolffe, A.P. (2000) Functional consequences of Rett syndrome mutations on human MeCP2. Nucleic Acids Res, 28, 4172-4179.

Summary

Chapter 1 is an introductory chapter, presenting the current view of eukaryotic gene control with respect to the spatial organization of the genome within the cell nucleus. Eukaryotic gene regulation is achieved at several levels. For instance, at the genetic level or linear DNA-sequence level, genes with a similar activity level can occur in clusters, suggesting that the genomic environment can contribute to transcriptional activity. Furthermore, at the chromatin level, active genes often seem to loop away from their chromosome territory, demonstrating a correlation between chromatin organization and transcription. Finally, the radial organization of the genome within the nucleus likely exerts regulatory influences. A more peripheral position can have a silencing effect on genes, as opposed to a more central nuclear position.

In **chapter 2** we utilized Chinese Hamster Ovary cells containing an amplified lac operator array to examine how MeCP2, a protein embedded in the DNA methylation pathway, influences epigenetic regulation. We demonstrated that the *in vivo* targeting of MeCP2 caused extensive chromatin decondensation requiring the C-terminal part of MeCP2. MeCP2-induced chromatin decondensation occurred throughout interphase in the absence of transcriptional activation or changes in CpG methylation. We demonstrate an intricate interplay between MeCP2 and HP1 proteins by showing that MeCP2 promotes eviction of HP1γ from chromatin, but not of HP1α or HP1β. We propose that MeCP2-induced chromatin decondensation reflects a poised status, preparing chromatin for further transcriptional regulation.

In **chapter 3** we studied whether HP1 that lacks a functional chromodomain (CD), normally mediating binding to chromatin via histone H3 tri-methylated at lysine 9, is able to induce heterochromatinization. After targeting of CD-less HP1 we observe chromatin compaction, locally enhanced H3K9me3 levels and recruitment of endogenous HP1α and HP1β to the targeted region. These results suggest that recruitment of factors by the chromoshadow and hinge domain of HP1 is sufficient to induce heterochromatinization.

In **chapter 4** we present the effects on chromatin structure of the depletion of endogenous HP1 from mouse chromocenters. We used a dominant-negative approach by expressing truncated HP1 lacking a functional CD in mouse fibroblasts, resulting in a reduction of the accumulation of endogenous HP1 in pericentromeric heterochromatin domains. The expression levels of HP1 did not change. The displacement of HP1 from pericentromeric heterochromatin domains did not result in visible structural changes as visualized by DAPI staining and H3K9me3 labeling. Our data indicate that accumulation of HP1 at pericentromeric heterochromatin domains is not required to maintain such domains.

In **chapter 5** we describe the creation of an engineered targeting system in human cells and discuss its benefits and points for improvement. The distinguishing feature of this targeting system is its single-copy integration into two cell lines in a predefined well-characterized genomic location exhibiting opposing characteristics. This system enables us to study the effect of the endogenous genomic environment on gene expression and chromatin structure. Furthermore, two small targeting sites incorporated in the engineered construct can be targeted simultaneously by different epigenetic factors that will provide information on factor interactions and cross-talk. These targeting sites have been limited in size to reduce potential artifacts that can arise from the integration of exogenous DNA. Pilot studies demonstrate the potential of our novel targeting system.

Chapter 6 is a perspective in which we discuss eukaryotic gene network models and their use in gaining insight into the gene regulatory system. We offer insight into the role of epigenetics in biological systems, including a proposal for the integration of the epigenetic layer in gene network models.

Chromatine-organisatie en de regulatie van genexpressie: een samenvatting voor iedereen.

Jij, ik, Barack Obama, de hond van de buurvrouw; wij bestaan allemaal uit miljarden cellen. Iedere cel heeft haar eigen taken en samen vormen de cellen één werkend levend wezen. Maar hoe weten de cellen nou wat ze moeten doen? Netjes opgeborgen in die cellen zitten de chromosomen. Dit zijn hele lange moleculen, samengesteld uit DNA en eiwitten. Tezamen noemen we al deze moleculen ook wel 'chromatine'. Het DNA is het erfelijk materiaal van de cel en bevat de informatie die de cel nodig heeft om haar taken uit te voeren. Je zou dit kunnen vergelijken met bladmuziek: het samenraapsel aan lijntjes, noten en rusten vormt als het ware een code die alleen door een muzikant gelezen en gespeeld kan worden. De zwarte tekentjes worden door de muzikant vertaald naar een klinkende melodie. Zo bevat het DNA (bladmuziek) een code, die door speciale moleculen in de cel (muzikanten) vertaald kan worden tot eiwitten die alle processen in de cel te laten verlopen (de muziek). Elk stukje DNA dat de code voor één eiwit bevat noemen we een gen; het vertalen van het gen tot een eiwit noemen we genexpressie.

Frappant genoeg is in elke cel hetzelfde DNA, dus precies dezelfde informatie aanwezig, ongeacht of we nu naar een spiercel, een levercel of een huidcel kijken. Toch hebben al deze cellen heel verschillende functies en zien ze er heel anders uit. Blijkbaar komt niet al het DNA tegelijk en in alle cellen tot expressie. Stel, je neemt een groot symfonie-orkest en je zet ze dezelfde partituur van bijvoorbeeld de 5e symfonie van Beethoven voor. Als alle muzikanten nu tegelijk hun eigen stukje zouden gaan spelen zou het een chaos worden. Beethoven zou zich omdraaien in zijn graf! De symfonie wordt pas muziek wanneer de juiste muzikanten alleen hun muziek spelen op het moment dat de dirigent hen een teken geeft. Net zoals elke muzikant alleen op het juiste moment moet spelen, moet ook elk gen in een bepaalde cel op het juiste moment tot expressie worden gebracht. Dit noemen we het reguleren van genexpressie. Naast de genetische code (het DNA), is er dus nog een tweede code nodig die bepaalt welke genen tot expressie komen. We noemen dit de epigenetische code, naar het Griekse 'επι' dat 'bij' betekent.

De epigenetische code neemt verschillende vormen aan (zie ook **hoofdstuk 1** van dit proefschrift). Soms hangen er kleine moleculen aan het DNA of aan chromatine, die functioneren als vlaggetjes of markeringen om het DNA wel of niet te laten vertalen. Een andere belangrijke vorm van epigenetische informatie vinden we in de vorm en ruimtelijke verdeling, oftewel de "organisatie" van chromatine. Misschien kun je je daar iets bij voorstellen als je weer denkt aan het voorbeeld van het orkest. Wanneer het orkest een symfonie speelt staat het in een heel andere opstelling dan wanneer het een jazz-stuk uitvoert. Er worden andere solisten naar voren gehaald en bepaalde instrumentgroepen verdwijnen zelfs naar de kleedkamers. Zo lijkt er ook binnen de cel een duidelijke organisatie van chromatine te zijn. Chromatine dat tot expressie

komt wordt meestal naar het centrum van de cel gehaald. Ook zien we vaak dat chromatine zich ontrolt van een compacte structuur tot een wollige kluwen. Omgekeerd wordt chromatine dat niet tot expressie komt vaak stevig opgerold en aan de kant gezet.

Voor dit proefschrift hebben we onderzoek gedaan naar het effect van bepaalde eiwitten op die ruimtelijke verdeling en vouwing van het chromatine en vervolgens op de expressie van genen. Eén van de ontdekkingen die we hierbij hebben gedaan is dat niet alle eiwitten die genen uitzetten het chromatine netjes oprollen. Sterker nog, één specifiek eiwit (MeCP2) zet genexpressie uit, maar ontrolt het chromatine toch tot een gigantische kluwen (**hoofdstuk 2**). Dit zou je kunnen vergelijken met het concertgebouworkest dat in vol ornaat onder de schijnwerpers gaat zitten, strijkstokken heft...maar niet gaat spelen. Wellicht zijn er dus bepaalde eiwitten die chromatine wel voorbereiden op genexpressie, zonder de genen ook daadwerkelijk aan te zetten. In **hoofdstuk 3** en **4** doen we proeven met een eiwit (HP1) dat vaak onderdeel vormt van chromatine, helpt bij het strak oprollen daarvan en ook bij het uitzetten van de genen. Het blijkt dat dit eiwit alleen maar in eerste instantie nodig is: nadat we HP1 weghalen blijft het chromatine toch opgerold. Dit soort resultaten laat zien dat er nog veel kennis binnen de epigenetica ontbreekt of tegenstrijdig is, wat het ook tot zo'n spannend onderzoeksgebied maakt binnen de biologie.

Om duidelijke, causale verbanden tussen chromatine-organisatie, eiwitten en genexpressie te kunnen aantonen ontwikkelden we een nieuw, genetisch gemodificeerd, DNA-systeem (**hoofdstuk 5**). Op dit systeem rust nu een patent-aanvraag. Tot slot bediscussiëren we in **hoofdstuk 6** hoe we het concept epigenetische regulatie kunnen digitaliseren zodat we er de miljarden interacties tussen eiwitten en genen die een cel omvat mee kunnen beschrijven in plaats van slechts één enkele interactie. Door het opstellen van computermodellen hopen we op den duur het gedrag van cellen nauwkeurig te kunnen voorspellen. Naast fundamentele kennis zal dit ons ook inzicht over epigenetische aandoeningen, zoals sommige vormen van kanker en diabetes, opleveren. Hiermee en met behulp van het DNA-systeem uit **hoofdstuk 5** hopen wij bij te dragen aan de bestrijding van epigenetische aandoeningen.